USING AIRBORNE LIDAR TO DIFFERENTIATE COTTONWOOD TREES IN A RIPARIAN AREA AND REFINE RIPARIAN WATER USE ESTIMATES

by

Alireza Faridhosseini

A Dissertation Submitted to the Faculty of the

DEPARTMENT OF HYDROLOGY AND WATER RESOURCES

In Partial Fulfillment of the Requirements
For the Degree of

DOCTOR OF PHILOSOPHY
WITH A MAJOR IN HYDROLOGY

In the Graduate College

THE UNIVERSITY OF ARIZONA

2 0 0 6

THE UNIVERSITY OF ARIZONA
GRADUATE COLLEGE

As members of the Dissertation Committee, we certify that we have read the dissertation prepared by Alireza Faridhosseini entitled "Using Airborne Lidar to Differentiate Cottonwood Trees in a Riparian Area and Refine Riparian Water Use Estimates" and recommend that it be accepted as fulfilling the dissertation requirement for the

Degree of Doctor of Philosophy with a Major in Hydrology

Dr. David C. Goodrich	5/24/06 Date
Dr. Jim Shuttleworth	5/24/06 Date
Dr. Soroosh Sorooshian	5/24/06 Date
Dr. Stuart E. Marsh	5/24/06 Date
Dr. Kurtis J. Thome	5/24/06 Date

Final approval and acceptance of this dissertation is contingent upon the candidate's submission of the final copies of the dissertation to the Graduate College.

I hereby certify that I have read this dissertation prepared under my direction and recommend that it be accepted as fulfilling the dissertation requirement.

Co-Dissertation Director: Dr. David C. Goodrich	5/24/06 Date
Co-Dissertation Director: Dr. Jim Shuttleworth	5/24/06 Date

STATEMENT BY AUTHOR

This dissertation has been submitted in partial fulfillment of the requirements for an advanced degree at The University of Arizona and is deposited in the University Library to be made available to borrowers under rules of the Library.

Brief quotations from this dissertation are allowable without special permission, provided that accurate acknowledgement of source is made. Requests for permission for extended quotation from or reproduction of this manuscript in whole or in part may be granted by the head of the major department of the Dean of the Graduate College when in his or her judgment the proposed use of the material is in the interests of scholarship. In all other instances, however, permission must be obtained from the author.

SIGNED: Alireza Faridhosseini

ACKNOWLEDGMENTS

I would like to thank my major advisor, Dr. David Goodrich, for giving me the opportunity to work on this fascinating topic. I acknowledge his invaluable contribution to this study and his insightful academic advising throughout my study.

I am particularly thankful to Dr. Soroosh Sorooshian, Dr. David Thoma, Doug Rautenkranz, Ross Bryant, Catlow Shipek and Michael Sartori from the University of Florida for their help on my research work. Especially Dr. Sorooshian is much appreciated for being a great co-advisor. He always left me motivated and excited about my work with his positive affirmation and enthusiasm.

Thanks are also extended to Drs. Stuart Marsh, Kurtis Thome, and Jim Shuttleworth for serving on my examination committee. The lessons I have learned from Dr. Marsh were fundamental throughout my study. I thank him for being a great teacher and for his assistance whenever I was looking for advice.

I am thankful for the financial support from SAHRA (Sustainability of semi-Arid Hydrology and Riparian Areas) under the STC Program of the National Science Foundation, grant EAR-9876800. Among the SAHRA administrators and staff, I want to express my special appreciation to Drs. Soroosh Sorooshian, Jim Shuttleworth, and James Washburne, who gave me the freedom to pursue my ideas, and to Mary Nett for her editorial assistance.

I wish to thank my friends and colleagues, SoniYatheendradas, Wolfgang Schmid, Yang Hong, Felipe Ip, Kevin Dressler, Julio Canon Barriga, Gustavo De Goncalves, and Sam Najmaii, who helped me to grow with the challenges of my Ph.D. study.

I would not have completed this Ph.D. without the encouragement and support of my family. A particular thanks goes to my parents, who always believed in me when I didn't. Thanks, Dad, for being my manager at the "home front." But most importantly, I would like to thank my wife Sherma for her love and understanding, and all the sacrifices she had to endure. Thanks for being there when I needed you, and thanks for your patience during the many weekends I spent on my research instead of with you.

TABLE OF CONTENTS

TABLE OF CONTENTS - *continued*

LIST OF ILLUSTRATIONS

LIST OF ILLUSTRATIONS - *continued*

LIST OF TABLES

ABSTRACT

Airborne lidar (**li**ght **d**etecting **a**nd **r**anging) is a useful tool for probing the structure of forest canopies. Such information is not readily available from other remote sensing methods and is essential for modern forest inventories. In this study, small-footprint lidar data were used to estimate biophysical properties of young, mature, and old cottonwood trees in the Upper San Pedro River Basin, Arizona, USA. The lidar data were acquired in June 2003 and 2004, using Optech's 1233 ALTM (Optech Incorporated, Toronto, Canada). Canopy height, crown diameter, stem diameter at breast height (dbh), canopy cover, and mean intensity of return laser pulses from the canopy surface are estimated for the cottonwood trees from lidar data. The lidar estimates show a good degree of correlation with ground-based measurements. This study also demonstrates that other parameters of young, mature, and old cottonwood trees such as height and canopy cover, when derived from lidar, are significantly different ($p < 0.05$). These lidar-derived canopy metrics provided the basis for a supervised image classification of cottonwood age categories, using a maximum likelihood algorithm. The results of classification illustrate the potential of airborne lidar data to differentiate age classes of cottonwood trees for riparian areas quickly and quantitatively.

In addition, four metrics (tree height, height of median energy, ground return ratio, and canopy return ratio) were derived by synthetically constructing a large footprint lidar waveform from small-footprint lidar data (we summed up a series of Gaussian pulses that vertically stacked at the elevations produced by the small-footprint elevation data to create a modeled large-footprint return waveform and compared the synthetic waveforms

with ground-based Intelligent Laser Ranging and Imaging System (ILRIS) scanner images in cottonwood trees). These four metrics were incorporated into a stepwise regression procedure to predict field-derived LAI for different age classes of cottonwoods.

Additionally, this study applied the Penman-Monteith model to estimate transpiration of the cottonwood clusters using lidar-derived canopy metrics, such as height and LAI, and compared it with transpiration measured by sap flow, so that improved riparian water use estimates could be made.

CHAPTER 1

INTRODUCTION

1.1 Research Motivation

Vegetation patterns and associated canopy structure influence landscape functions such as water use, biomass production, and energy cycles. The properties of vegetation and canopy must be quantified in order to understand their roles in landscapes and before management plans can be developed for the purpose of conserving natural resources.

Vegetation patterns can be mapped from ground-based inventory techniques, or by using aerial photography or satellite imagery. If sampling is sufficiently intense, ground-based techniques alone can produce accurate results. However, determining the physical properties of canopy architecture and structure (i.e. height, density, timber volume) with conventional ground-based technology is difficult, labor intensive, costly, and usually very limited for assessing large scale or landscape characteristics. Resource managers are always interested in developing and utilizing alternative sources of information that are more cost effective or offer opportunities to manage resources more efficiently.

The primary purpose of this research was to use a small-footprint lidar to estimate biophysical variables in cottonwood trees in the San Pedro Riparian National Conservation Area (SPRNCA) in southeastern Arizona, USA. The secondary objective of this study was to differentiate different age classes of cottonwood trees by using small-footprint lidar and consequently improve riparian cottonwood water use estimates.

The SPRNCA is a globally important migratory bird route. Its cottonwood riparian forest supports a great diversity of species and is widely recognized as a regionally and globally important ecosystem (World Rivers Review, 1997). Additionally, lidar studies published to this point have shown success in several forest types with large-footprint lidar, but applications of small-footprint lidar to forestry have not progressed as far (Means, 2000), being limited mainly to measuring even-aged conifer stands. Thus, the performance of lidar in cottonwood riparian forests remains untested and any related analytical and processing issues are yet to be identified.

The main objective of this study was to estimate Leaf Area Index (LAI) from various laser height metrics and synthetic large footprint lidar waveform for different age classes of cottonwood trees. Additionally, this study applied the Penman-Monteith model (Monteith and Unsworth, 1990) to estimate cottonwood transpiration using lidar-derived canopy metrics, compared with transpiration measured by sap flow. Riparian cottonwood trees use water in proportion to their age and leaf area (Schaeffer et al., 2000), and are especially large users of water in flood plains along rivers in semi-arid environments. More accurate quantification of riparian water use is required to manage basin water resources to maintain the economic, social, and ecological viability of these areas and ensure water for a growing human population in the basin. Cottonwoods of different age cannot be distinguished by multi-spectral methods. However, the older cottonwoods exhibit a canopy that is more crowned in shape than the younger trees, thus differences in tree shape as a function of tree age led us to investigate the use of lidar to identify and classify cottonwoods of different age classes. Another important reason for determining

the age and canopy characteristics of cottonwood is to discern the recruitment and establishment of cottonwood seedlings in riparian corridors. Because of regulation of streamflow by dams and reservoirs in many western rivers, the occurrence of significant floods which are essential for the recruitment of young cottonwoods, has been greatly reduced. The capability of rapidly quantifying the age distribution of cottonwoods from lidar in a riparian corridor would provide a useful indicator of cottonwood regeneration capacity of a given corridor.

1.2 Research Objectives

The specific goals of this study were:

(1) Derive various geometric measures for different age classes of cottonwoods from lidar data and determine the relationships between cottonwood biophysical properties with ground-based measurements.

(2) Use lidar derived-metrics to differentiate different age classes of cottonwood trees.

(3) Model a laser altimeter return waveform as the sum of reflections within a laser small footprint and compare the results with ground-based Intelligent Laser Ranging and Imaging System (ILRIS) scanner images in cottonwood trees.

(4) Derive various laser height metrics (maximum laser height, mean laser height, and canopy height) from the small footprint lidar data and determine how well they can estimate LAI for different age classes of cottonwoods.

(5) Derive four metrics (canopy height, height of median energy, ground return ratio, and canopy return ratio) from synthetic lidar full-waveform. These four metrics incorporate

into a stepwise regression procedure to predict field-derived LAI for different age classes of cottonwood trees.

(6) Apply the Penman-Monteith model to estimate transpiration of the cottonwood clusters using lidar-derived canopy metrics, such as height and LAI, and compare the results with transpiration measured by sap flow, so improved riparian water use estimates can be made.

1.3 Literature Review

Remote sensing has facilitated extraordinary advances in the modeling, mapping, and understanding of ecosystems. Typical applications of remote sensing involve either images from passive optical systems, such as aerial photography and Landsat Thematic Mapper (Goward and Williams, 1997), or to a lesser degree, active radar sensors such as RADARSAT (Waring et al., 1995). These types of sensors have proven to be satisfactory for many ecological applications, such as mapping land cover into broad classes and, in some biomes, estimating aboveground biomass and LAI. Moreover, they enable researchers to analyze the spatial pattern of these images. However, conventional sensors have significant limitations for ecological applications. The sensitivity and accuracy of these devices have repeatedly been shown to fall with increasing aboveground biomass and LAI (Waring et al., 1995). They are also limited in their ability to represent spatial patterns: They produce only two-dimensional (x and y) images, which cannot fully represent the three-dimensional structure of, for instance, an old-growth forest canopy. Yet ecologists have long understood that the presence of specific organisms, and the

overall richness of wildlife communities, can be highly dependent on the three-dimensional spatial pattern of vegetation (MacArthur and MacArthur, 1961), especially in systems where biomass accumulation is significant (Hansen and Rotella, 2000). Individual bird species, in particular, are often associated with specific three-dimensional features in forests (Carey et al., 1991). Additionally, other functional aspects of forests, such as productivity, may be related to forest canopy structure. Laser altimetry, or lidar (**li**ght **d**etecting **a**nd **r**anging), is an alternative remote sensing technology that promises to both increase the accuracy of biophysical measurements and extend spatial analysis into the third dimension (z). Lidar sensors directly measure the three-dimensional distribution of plant canopies as well as subcanopy topography, thus providing high-resolution topographic maps and highly accurate estimates of vegetation height, cover, and canopy structure. In addition, lidar has been shown to accurately estimate LAI and aboveground biomass even in those high-biomass ecosystems where passive optical and active radar sensors typically fail to do so.

1.3.1 Lidar Sensors

The basic measurement made by a lidar device is the distance between the sensor and a target surface, obtained by determining the elapsed time between the emission of a short-duration laser pulse and the arrival of the reflection of that pulse (the return signal) at the sensor's receiver. Multiplying this time interval by the speed of light results in a measurement of the round-trip distance traveled, and dividing that figure by two yields the distance between the sensor and the target (Bachman, 1979). When the vertical

distance between a sensor contained in a level-flying aircraft and the Earth's surface is repeatedly measured along a transect, the result is an outline of both the ground surface and any vegetation obscuring it. Even in areas with high vegetation cover, where most measurements will be returned from plant canopies, some measurements will be returned from the underlying ground surface, resulting in a highly accurate map of canopy height.

Key differences among lidar sensors are related to the laser's wavelength, power, pulse duration and repetition rate, beam size and divergence angle, the specifics of the scanning mechanism, and the information recorded for each reflected pulse.

Lasers for terrestrial applications generally have wavelengths in the range of 900–1064 nanometers, where vegetation reflectance is high. In the visible wavelengths, vegetation absorbance is high and only a small amount of energy would be returned to the sensor. One drawback of working in this range of wavelengths is absorption by clouds, which impedes the use of these devices during overcast conditions. Bathymetric lidar systems (used to measure elevations under shallow water bodies) make use of wavelengths near 532 nm for better penetration of water. Early lidar sensors were profiling systems, recording observations along a single narrow transect.

Later systems operate in a scanning mode, in which the orientation of the laser illumination and receiver field of view is directed from side to side by a rotating mirror, or mirrors, so that as the plane (or other platform) moves forward, the sampled points fall across a wide band or swath, which can be gridded into an image. The power of the laser and size of the receiver aperture determine the maximum flying height, which limits the width of the swath that can be collected in one pass (Wehr and Lohr, 1999). The intensity

or power of the return signal depends on several factors: the total power of the transmitted pulse, the fraction of the laser pulse that is intercepted by a surface, the reflectance of the intercepted surface at the laser's wavelength, and the fraction of reflected illumination that travels in the direction of the sensor. The laser pulse returned after intercepting a morphologically complex surface, such as a vegetation canopy, will be a complex combination of energy returned from surfaces at numerous distances, the distant surfaces represented later in the reflected signal.

The type of information collected from this return signal distinguishes two broad categories of sensors. Discrete-return (small footprint) lidar devices measure either one (single-return systems) or a small number (multiple-return systems) of heights by identifying, in the return signal, major peaks that represent discrete objects in the path of the laser illumination. The distance corresponding to the time elapsed before the leading edge of the peak(s), and sometimes the power of each peak, are typical values recorded by this type of system (Wehr and Lohr, 1999). Waveform-recording (large footprint) devices record the time-varying intensity of the returned energy from each laser pulse, providing a record of the height distribution of the surfaces illuminated by the laser pulse (Harding et al., 1994; 2001; Dubayah et al., 2000).

By analogy to chromotography, the discrete-return systems identify, while receiving the return signal, the retention times and heights of major peaks; the waveform-recording systems capture the entire signal trace for later processing. Both discrete-return and waveform sampling sensors are typically used in combination with instruments for locating the source of the return signal in three dimensions. These include Global

Positioning System (GPS) receivers to obtain the position of the platform, Inertial Navigation Systems (INS) to measure the attitude (roll, pitch, and yaw) of the lidar sensor, and angle encoders for the orientation of the scanning mirror(s). Combining this information with accurate time referencing of each source of data yields the absolute position of the reflecting surface, or surfaces, for each laser pulse.

There are advantages to both discrete-return and waveform-recording lidar sensors. For example, discrete-return systems feature high spatial resolution, made possible by the small diameter of their footprint and the high repetition rates of these systems (as high as 100,000 points per second), which together can yield dense distributions of sampled points. Thus, discrete-return systems are preferred for detailed mapping of ground and canopy surface topography (Flood and Gutelis, 1997). An additional advantage made possible by this high spatial resolution is the ability to aggregate the data over areas and scales specified during data analysis, so that specific locations on the ground, such as a particular forest inventory plot or even a single tree crown, can be characterized. Finally, discrete-return systems are readily and widely available, with ongoing and rapid development, especially for surveying and photogrammetric applications (Flood and Gutelis, 1997).

The primary users of these systems are surveyors serving public and private clients, and natural resource managers seeking a cheaper source of high-resolution topographic maps and Digital Terrain Models (DTMs). A potential drawback is that proprietary data-processing algorithms and established sensor configurations designed for commercial use may not coincide with scientific objectives. A detailed technical review of the various

sensors can be found in Wehr and Lohr (1999). Baltsavias (1999) reviews a directory of sensors and lidar remote sensing firms.

The advantages of waveform-recording lidar include an enhanced ability to characterize canopy structure, the ability to concisely describe canopy information over increasingly large areas, and the availability of global data sets. Examples of waveform-recording laser altimeters include MKII (Aldred and Bonnor, 1985) and a similar system described in Nilsson (1996), as well as a series of airborne devices developed at NASA's Goddard Space Flight Center, starting with a profiling sensor described by Bufton and colleagues (1991) and including SLICER (Scanning Lidar Imager of Canopies by Echo Recovery; Blair et al., 1994; Harding et al., 1994; 2001), SLA (Shuttle Laser Altimeter; Garvin et al., 1998), LVIS (Laser Vegetation Imaging Sensor; Blair et al., 1999), and VCL (Vegetation Canopy Lidar; Dubayah et al., 1997) satellite. One advantage of these waveform-recording lidar systems is that they record the entire time-varying power of the return signal from all illuminated surfaces and are therefore capable of collecting more information on canopy structure than all but the most spatially dense collections of small-footprint lidar. In addition, waveform-recording lidar integrates canopy structure information over a relatively large footprint and is capable of storing that information efficiently, from the perspective of both data storage and data analysis.

Finally, only waveform-recording lidar will, in the near future, be collected globally from space. Spaceborne waveform-recording lidar techniques have been successfully demonstrated by the SLA missions (Garvin et al., 1998), which were intended to collect topographic data and to test hardware and algorithm approaches from orbit. These data

were collected along a single track, using footprints of approximately 100 meters in diameter, which limits their utility for the measurement of vegetation canopy structure, especially in high-slope areas (Harding et al., 2001). The VCL mission is the first satellite specifically designed with the problem of vegetation inventory in mind. VCL is a waveform-recording system, expected to inventory, using 25-m diameter footprints, canopy height and structure over approximately 5% of the Earth's land surface between ±68° latitude during its 18-month mission (Dubayah et al., 1997).

1.3.2 Applications of Lidar Remote Sensing

Only a few areas of application for lidar remote sensing have been rigorously evaluated. Numerous other applications are generally considered feasible, but they have not yet been explored; developments in lidar remote sensing are occurring so rapidly that it is difficult to predict which applications will be dominant in the future. Currently, applications of lidar remote sensing in ecology fall into three general categories: remote sensing of ground topography, measurement of the three-dimensional structure and function of vegetation canopies, and prediction of forest stand structure attributes (such as LAI).

1.3.2.1 Topographic Applications

Mapping of topographic features is the largest and fastest growing area of application for lidar remote sensing, because of its use in commercial land surveys (Flood and Gutelis, 1997). Ecologists are also interested in topography and bathymetry, which often has a strong influence on the structure, composition, and function of ecological systems. Traditional survey and photogrammetric techniques for determining ground elevations are limited in several ways. The primary disadvantages of traditional surveying are its substantial time and labor requirements and associated costs. Photogrammetric methods for determining elevations from aerial photographs or images collected by other sensors are an established alternative to field surveys (Baltsavias, 1999). However, they are inaccurate in forested areas, where the ground is not visible, and in areas of low relief and texture, such as wetland areas and coastal dune systems. In these cases, airborne laser altimetry can be an accurate and cost-effective alternative.

Topographic applications most often use discrete-return data. When ranging information from the lidar is combined with position and pointing information, the result is a series of x, y, and z data points (triplets), describing the location of the observed surfaces in three-dimensional space. With adequate quality control, the accuracy of these points can achieve 50 cm root mean square error (RMSE) in the horizontal planes and 20 cm RMSE in the vertical. However, the elevations recorded in these triplets will be associated with myriad features, including the ground, human-made objects, clouds, vegetation, or anything else in the path of the laser pulse. To extract a topographic surface from these points, a series of filters must be applied to eliminate points not on the ground surface.

Numerous methods exist for this process, but generally they combine highly automated processes with some manual correction (Kraus and Pfeifer, 1998). Examples of topographic applications of lidar include mapping of polar ice sheets for mass balance investigations (Krabill et al., 1999), mapping of wetlands and shallow water (Irish and Lillycrop, 1999), and high-resolution mapping of topography under forest for geomorphic investigations and hydrologic modeling (Harding and Berghoff, 2000). The mapping of dynamic features such as beaches and a dune (Krabill, 2000) is one application for which lidar is proving to be particularly well suited.

1.3.2.2 Measuring Vegetation Canopy Structure and Function

In general, the single most important step in lidar mapping of topography involves the deletion of data points returned from vegetation and, in urban areas, buildings. However, for most ecological applications, it is the returns from the vegetation canopy that will be of primary interest. The simplest canopy structure measurements are of canopy height and cover. Altimetric canopy heights have been compared, with varying accuracy and strength of correlation, to maximum and mean tree height in temperate (Maclean and Krabill, 1986), tropical (Nelson et al., 1997; Drake et al., 2002), and boreal (Naesset, 1997a; Magnussen and Boudewyn, 1998; Magnussen et al., 1999; Persson et al., 2002; Holmgren et al., 2003) forests. In addition, Ritchie and colleagues (1995) found excellent agreement between lidar measurements of height in both temperate deciduous forests and desert scrub. There are two general problems in determining vegetation height using lidar data. Determining the exact elevation of the ground surface poses difficulties for both

discrete-return and waveform-recording lidar. In complex canopies, elevations returned from what appears to be the ground level in fact may be from the understory, if the understory is dense enough to substantially occlude the ground surface. In addition, each type of lidar system presents difficulties in detecting the uppermost portion of the plant canopy. With discrete-return lidar, very high footprint densities are required to ensure that the highest portion of individual tree crowns is sampled. With waveform sampling devices, a large footprint is illuminated, increasing the probability that treetops will be illuminated by the laser. However, the top portion of the crown may not be of sufficient area to register as a significant return signal and therefore may not be detected. In either case, the height of the canopy may be underestimated. Estimates of canopy cover have been made using both discrete-return and waveform-recording lidar sensors. These estimates are made using the fraction of the lidar measurements that are considered to have been returned from the ground surface (Nelson et al., 1984; Ritchie et al., 1992; 1995; 1996; Weltz et al., 1994; Lefsky, 1997), where the measurements are the number of discrete returns, or the integrated power of a waveform. In some cases, a scaling factor is needed to correct for the relative reflectance of ground and canopy surfaces at the wavelength of the laser (Lefsky, 1997; Means et al., 1999). As with the measurement of canopy height, the definition of the ground surface is a critical aspect of cover determination. Although the height and cover of the canopy surface are useful canopy structure descriptions, there are more detailed measurements that can better describe canopy function and structure. The height distribution of outer canopy surfaces, which quantifies such important features as light gaps (Watt, 1947; Canham et al., 1990; Spies

et al., 1990), has been manually mapped in several studies (Leonard and Federer, 1973; Ford, 1976; Miller and Lin, 1985). These maps were laboriously made, using devices such as plumb bobs and telescoping rods. With lidar, the process is greatly accelerated (Nelson et al., 1984; Lefsky et al., 1999b). The vertical distribution of all material within the canopy (not just the outer canopy surfaces) may be inferred, using the foliage-height profile technique (MacArthur and Horn, 1969; Aber, 1979) recently adapted for use with waveform-recording lidar as the canopy-height profile (Lefsky, 1997; Harding et al., 2001). Calculation of these height profiles relies on assumptions about the rate of occlusion of canopy surfaces that are not applicable to all forests; however, they have been shown to yield a good approximation in closed-canopy, temperate deciduous forests (Aber, 1979; Fukushima et al., 1998; Harding et al., 2001). Lidar data have been used to predict the fractional transmittance of light as a function of height, based on a series of assumptions relating the penetration of the laser light into the canopy to the penetration of natural light into the canopy. Although both the wavelength and orientation of typical laser illumination differs from that of natural illumination, a study (Parker et al., 2001) indicates that lidar can accurately estimate the rate of Photosynthetically Active Radiation (PAR) absorption and define the location and depth of the zone where the maximum rate of PAR absorption occurs (Parker, 1997). Lidar has also been used to predict the aerodynamic properties of plant canopies and landscapes. Menenti and Ritchie (1994) used a profiling laser altimeter to predict aerodynamic roughness length of complex landscapes containing a mixture of grassland, shrub, woodland areas, and found good agreement with field estimates. The techniques described so far use lidar data to

make measurements of canopy structure that had been made with technologically simpler and more time-consuming methods. Lidar's ability to rapidly measure the three-dimensional structure of canopies should stimulate the development of new systems of canopy description. One such system, the Canopy Volume Method (CVM), is the first to take advantage of the ability of a waveform-recording sensor (SLICER) to directly measure the three-dimensional distribution of canopy structure.

1.3.2.3 Prediction of Forest Stand Structure

Lidar data also have been used to predict biophysical characteristics of plant communities, most notably forests (Dubayah and Drake, 2000). Although the following studies may not by themselves constitute ecological research, they lay the groundwork for future studies that use these relationships to map biophysical variables over large extents (using data from sensors such as LVIS and VCL), making possible a new class of large-scale ecological research.

Prediction of forest stand structure using discrete return lidar had its start in the work of Maclean and Krabill (1986), who adapted a photogrammetric technique – the canopy profile cross-sectional area – to the interpretation of lidar data. The canopy profile cross-sectional area is the total area between the ground and the upper canopy surface along a transect. When species composition was taken into account, the authors were able to explain 92% of the variation in gross-merchantable timber volume (the volume of the main stem of trees, excluding the stump and top but including defective and decayed wood) in stands dominated by oaks, loblolly pine, or mixtures of the two types. Similar

methods have proved effective in a variety of forest communities. Nelson et al. (1988) successfully predicted the volume and biomass of southern pine forests using several estimates of canopy height and cover from discrete-return lidar, explaining between 53% and 65% of variance in field measurements of these variables. Later work by Nelson et al. (1997) in tropical wet forests at the La Selva biological station obtained similar results for prediction of basal area, volume, and biomass. They also developed a canopy structure model that led to greater understanding of the optimal spatial configuration of field sampling for comparison with profiling lidar data. Naesset (1997b) explained 45%–89% of variance in stand volume in stands of Norway spruce and Scots pine, using measurements of maximum and mean canopy height and cover. Hyyppä and Inkinen (2000) reported on use of small footprint lidar to detect and measure single trees in Finland. In the sparse boreal forest that they studied, more than 30% of pulses reached the ground before producing a first return, so that determining tree heights crown extents was relatively straightforward and allowed very good estimates to be made of the dimensions of individuals trees, with an R^2 of 0.97 between field measurements of tree height and tree heights derived from lidar. Aggregating the lidar measurements of individual trees produced an estimate of the stand that surpassed the accuracy of conventional field inventories, with standard errors of mean height, basal area and stem volume being 13.6%, 9.6% and 9.5% respectively.

Five published studies document the utility of waveform recording lidar in predicting forest stand structure. Nilsson (1996) adapted a bathymetric lidar system for use in forest inventory, and successfully predicted timber volume for stands of even-aged Scots pine.

He used the height and the total power of each waveform as independent variables, and explained 78% of variance. Lefsky and colleagues (1999a) used data from SLICER to predict aboveground biomass and basal area in eastern deciduous forests using indices derived from the canopy height profile. Of particular note, they found that relationships between height indices and forest structure attributes (basal area and aboveground biomass) could be generated using field estimates of the canopy height profiles, and applied directly to the lidar-estimated profiles, resulting in unbiased estimates of forest structure. Means and colleagues (1999) applied similar methods to evaluate 26 plots in forests of Douglas-fir and western hemlock at the H. J. Andrews experimental forest. They found that very accurate estimates of basal area, aboveground biomass, and foliage biomass could be made using lidar height and cover estimates.

A fourth study (Lefsky et al., 1999b) used statistics derived from the CVM to predict numerous forest structure attributes, including several not previously predicted from lidar remote sensing. Stepwise multiple regressions were performed to predict ground-based measures of stand structure from both conventional canopy structure indices (mean and maximum canopy surface height, canopy cover) and CVM indices such as filled canopy volume, open and closed gap volume, and a canopy diversity index – the average number of CVM classes per unit height. The fifth published study (Drake et al., 2002) extends the application of waveform recording lidar to a tropical wet forest in Costa Rica, where, using the LVIS sensor, data were collected near the La Selva biological station. Using a set of indices describing the vertical distribution of the raw waveforms and the fraction of total power associated with the ground returns, they were able to predict field-measured

quadratic mean stem diameter, basal area, and aboveground biomass, explaining up to 93%, 72%, and 93% of variance, respectively.

CHAPTER 2

PRESENT STUDY

This chapter summarizes and documents the conclusions from this dissertation research. The details are presented in the papers in the appendices of this dissertation.

2.1 Summary of Paper 1: Using airborne lidar to discern age classes of cottonwood trees in a riparian area. Published in the *Western Journal of Applied Forestry (A. Farid, D.C. Goodrich, S. Sorooshian).*

Airborne lidar (**li**ght **d**etecting **a**nd **r**anging) is a useful tool for probing the structure of forest canopies. Such information is not readily available from other remote sensing methods and is essential for modern forest inventories. In this study, small-footprint lidar data were used to estimate biophysical properties of young, mature, and old cottonwood trees in the San Pedro River Basin near Benson, Arizona, USA. The lidar data were acquired in June 2004, using Optech's 1233 ALTM (Optech Incorporated, Toronto, Canada), during flyovers conducted at an altitude of 600 m. Canopy height, crown diameter, stem diameter at breast height (dbh), canopy cover, and mean intensity of return laser pulses from the canopy surface were estimated for the selected cottonwood trees from the lidar data. Linear regression models were used to develop equations relating lidar-derived tree characteristics with corresponding field acquired data for each age class of cottonwoods. The lidar estimates show a good degree of correlation with ground-based measurements. This study also demonstrates that other parameters of

young, mature, and old cottonwood trees such as height and canopy cover, when derived from lidar, are significantly different ($p < 0.05$). Additionally, mean crown diameters of mature and young trees are not statistically different at the study site ($p = 0.31$). The results illustrate the potential of airborne lidar data to differentiate different age classes of cottonwood trees for riparian areas quickly and quantitatively.

The conclusions of paper 1 are presented as follows.

The results of the current study show that lidar data can be used to accurately estimate the properties of cottonwood canopies at the individual tree level. Lidar offers the possibility of rapidly deriving biophysical variables in riparian areas using automated techniques. Thus, seeing the cottonwoods in the riparian forest and more importantly measuring them with lidar brings an important contribution to concepts such as precision forest inventory and automated data processing for riparian forestry applications.

Overall, this research proved that small-footprint airborne lidar data is able to predict stand structure attributes such as height, crown diameter, and canopy cover of riparian cottonwood forests. Measurements of cottonwood canopy properties made with lidar data in the riparian area were not significantly different from measurements taken on the ground. The main objective of this research was to use lidar-derived estimates to differentiate young, mature, and old cottonwood patches. The results illustrate the potential of lidar data to differentiate different age classes of cottonwood trees for riparian areas quickly and quantitatively. Furthermore, there is value in the intensity return data for assisting in differentiating cottonwood trees, but this parameter needs further investigation in order to develop a good understanding of the factors affecting

how intensity returns are produced and recorded by the lidar sensor. Finally, the capability to rapidly quantify the age distribution of cottonwoods in a riparian area will provide an indicator of cottonwood regeneration capacity of a given area.

2.2 Summary of Paper 2: Riparian vegetation classification from airborne laser scanning data with an emphasis on cottonwood trees. Published in the *Canadian Journal of Remote Sensing (A. Farid, D. Rautenkranz, D.C. Goodrich, S.E. Marsh, S. Sorooshian).*

The high point density of airborne laser mapping systems enables achieving a detailed description of geographic objects and of the terrain. Growing experience indicates, however, that extracting useful information directly from the data can be difficult. In this study, small-footprint lidar data were used to differentiate between young, mature, and old cottonwood trees in the San Pedro River Basin near Benson, Arizona, USA. The lidar data were acquired in June 2003, using Optech's 1233 ALTM (Optech Incorporated, Toronto, Canada), during flyovers conducted at an altitude of 750 m. The lidar data was pre-processed to create a two-band image of the study site: a high accuracy canopy altitude model band and a near-infrared intensity band. These lidar-derived images provided the basis for supervised classification of cottonwood age categories, using a maximum likelihood algorithm. The results of the classification illustrate the potential of airborne lidar data to differentiate age classes of cottonwood trees for riparian areas quickly and accurately.

The conclusions of paper 2 are presented as follows.

This research employed a supervised classification technique, the maximum likelihood algorithm, for differentiating age classes of cottonwood trees in a riparian area using small-footprint airborne lidar data. We performed a maximum likelihood classification of the 2-band lidar image (altitude and intensity images), resulting in seven land-cover classes: young, mature, and old cottonwoods, mesquite, saltcedar, dry stream channel, and open ground. To validate the image classification, we performed an accuracy assessment, in which actual land-cover, as determined by field identification, was compared with classes for the corresponding areas assigned by the maximum likelihood classification. The overall classification accuracy was 78%; and the overall Kappa statistic value of classification was 0.73. Accuracy assessment of the classified land-cover map illustrates that lidar data contains information of value for image analysis. Old and mature cottonwoods were well determined on the classified image. Young cottonwoods were, for the most part, correctly classified, although some image areas actually corresponding to mesquite or mature cottonwood were incorrectly identified as young cottonwoods.

Overall, classification results illustrate the potential of airborne lidar data to differentiate age classes of cottonwood trees for riparian areas quickly and quantitatively. Thus, identifying cottonwoods in the riparian forest and, more importantly, differentiating cottonwood age classes using lidar provides an important contribution to precision forest inventory and automated data processing for riparian forestry applications.

2.3 Summary of Paper 3: Using airborne lidar to predict leaf area index in cottonwood trees and refine riparian water use estimates. Submitted to *Journal of Arid Environments (A. Farid, D.C. Goodrich, R. Bryant, S. Sorooshian).*

Quantification of riparian forest structure is important for developing a better understanding of how riparian forest ecosystems function. Additionally, estimation of riparian forest structural attributes, such as Leaf Area Index (LAI), is an important step in identifying the amount of water use in riparian forest areas. In this study, small-footprint lidar data were used to estimate biophysical properties of young, mature, and old cottonwood trees in the Upper San Pedro River Basin, Arizona, USA. The lidar data were acquired in June 2003, using Optech's 1233 ALTM (Optech Incorporated, Toronto, Canada), during flyovers conducted at an altitude of 750 m. Canopy height, maximum laser height, and mean laser height were derived for the cottonwood trees from the data. Linear regression models were used to develop equations relating lidar height metrics with corresponding field-measured LAI for each age class of cottonwoods. The lidar height metrics show a good degree of correlation with field-measured LAI. In addition, four metrics (tree height, height of median energy, ground return ratio, and canopy return ratio) were derived by synthetically constructing a large footprint lidar waveform from small-footprint lidar data (we summed up a series of Gaussian pulses that were vertically stacked by elevation band produced by the small-footprint elevation data to create a modeled large-footprint return waveform and compared the synthetic waveforms with ground-based Intelligent Laser Ranging and Imaging System (ILRIS) scanner images in cottonwood trees). These four metrics were incorporated into a stepwise regression

procedure to predict field-derived LAI for different age classes of cottonwoods. Metrics from lidar synthetic waveform are able to significantly estimate LAI, though in all cases logarithmic transformation of the dependent variable was necessary. Furthermore, this research applied the Penman-Monteith model to estimate transpiration of the cottonwood clusters using lidar-derived canopy metrics, such as height and LAI, so improved riparian water use estimates could be made.

The conclusions of paper 3 are presented as follows.

We have shown that one can synthesize the vertical structure information for cottonwood trees in a medium-large footprint laser altimeter return waveform using a small-footprint elevation data set. The similarity between modeled waveform and return waveform from ILRIS scanner was assessed using Pearson correlation. Overall, the waveforms had a good degree of correlation. Although the modeled and ILRIS waveforms identify reflecting layers at the same elevations, the relative strengths of reflections from those layers varied. In addition, cottonwood tree-age changes are likely mirrored in the shape or vertical geolocation of the waveform.

For each cottonwood tree, three laser height metrics were derived by all small-footprint lidar returns from cottonwood canopy surface. The derived h_{canopy} and Lz_{max} laser height metrics are capable of estimating LAI for different age classes of cottonwoods. Additionally, four metrics were derived from the modeled large-footprint return waveforms for different age classes of cottonwood trees in a riparian corridor. These four metrics were incorporated into a stepwise regression procedure to predict field-derived LAI. Metrics from lidar waveform are able to significantly estimate LAI for different age

classes of cottonwood trees, though in all cases logarithmic transformation of the dependent variable was necessary. Furthermore, the slightly weaker relationship between LAI and lidar metrics among young, mature, and old-growth stands is caused by the lack of significant differences in LAI between different age classes of cottonwoods that have been measured in field. We have presented the lidar-predicted versus sap flow measured cottonwood transpirations at two contrasting riparian sites. Lidar-predicted transpiration of the cottonwood cluster at two stream sites was 2-5% more than their sap flow measurements. The differences in LAI between the lidar-derived and sap flow measured account for most of the differences in the magnitude of ET. Additionally, the differences in the projected canopy area of the clusters between lidar and aerial photograph estimates caused reductions in sap flow measured transpiration at two stream sites. Overall, canopy structure, atmospheric demand, and depth to groundwater played significant roles in the fluctuations in transpiration of cottonwood trees in this riparian ecosystem. Understanding the different unique attributes and behaviors of cottonwood forests in different parts of this riparian area is important to accurately estimate the water budget of the whole riparian corridor.

The primary research conclusions of the dissertation can be summarized as follows.

(1) Measurements of cottonwood canopy properties made with airborne lidar were not significantly different from ground-based measurements.

(2) Small footprint airborne lidar system allows rapid measurements cottonwood canopy characteristics over large and inaccessible areas.

(3) The results indicate it is possible to use small footprint airborne lidar data to differentiate isolated young, mature, and old cottonwood patches.

(4) The results of the synthetic waveform approach from small footprint airborne lidar indicate that vertical tree structure information, such as LAI, can be derived.

(5) Lidar-predicted transpiration of the cottonwood cluster at two stream sites was 2-5% more than their sap flow measurements. The differences in LAI between the lidar-derived and sap flow measured account for most of the differences in the magnitude of ET. While riparian cottonwood water use is also regulated by stomata control, strategically acquired lidar data and derived spatially explicit LAI measurements, offer significant potential to improve corridor level riparian water use estimates.

REFERENCES

Aber, J.D., 1979. Foliage-height profiles and succession in northern hardwood forests. Ecology, 60: 18–23.

Aldred, A., Bonnor, G., 1985. Application of airborne lasers to forest surveys. Chalk River (Ontario, Canada): Petawawa National Forestry Institute, Canadian Forestry Service. Information Report, PI-X-51.

Bachman, C.G., 1979. Laser Radar Systems and Techniques. Norwood (MA): Artech House.

Baltsavias, E.P., 1999. Airborne laser scanning: Existing systems and firms and other resources. ISPRS Journal of Photogrammetry and Remote Sensing. 54: 164–198.

Blair, J.B., Coyle, D.B., Bufton, J.L., Harding, D.J., 1994. Optimization of an airborne laser altimeter for remote sensing of vegetation and tree canopies. Pages 939–941 in Proceedings of the International Geosciences Remote Sensing Symposium. Pasadena (CA): California Institute of Technology.

Blair, J.B., Rabine, D.L., Hofton, M.A., 1999. The Laser Vegetation Imaging Sensor (LVIS): A medium-altitude, digitization-only, airborne laser altimeter for mapping vegetation and topography. ISPRS Journal of Photogrammetry and Remote Sensing. 54: 115–122.

Bufton, J.L., Garvin, J.B., Cavanaugh, J.F., Ramos-Izquierdo, L., Clem, T.D., Krabill, W.B., 1991. Airborne lidar for profiling of surface topography. Optical Engineering, 30: 72–78.

Canham, C.D., Denslow, J.S., Platt, W.J., Runkle, J.R., Spies, T.A., White, P.S., 1990. Light regimes beneath closed canopies and tree-fall gaps in temperate and tropical forests. Canadian Journal of Forestry Research, 20: 620–631.

Carey, A.B., Hardt, M.M., Horton, S.P., Biswell, B.L., 1991. Spring bird communities in the Oregon coast range. Pages 123–142 in Wildlife and Vegetation of Unmanaged Douglas-Fir Forests. Portland (OR): USDA Forest Service, Pacific Northwest Research Station. General Technical Report PNW-GTR 285.

Drake, J.B., Dubayah, R.O., Clark, D.B., Knox, R.G., Blair, J.B., Hofton, M.A., Chazdon, R.L., Weishampel, J.F., Prince, S.D., 2002. Estimation of tropical forest structural characteristics using large-footprint lidar. Remote Sensing of Environment, 79: 305-319.

Dubayah, R.O., Blair, J.B., Bufton, J.L., Clark, D.B., JaJa, J., Knox, R., Luthcke, S.B., Prince, S., Weishampel, J., 1997. The vegetation canopy lidar mission. Pages 100–112 in Proceedings of Land Satellite Information in the Next Decade, II: Sources and Applications. Bethesda (MD): American Society of Photogrammetry and Remote Sensing.

Dubayah, R.O., Drake, J.B., 2000. Lidar remote sensing for forestry. Journal of Forestry, 98: 44–46.

Dubayah, R.O., Knox, R., Hofton, M., Blair, J.B., Drake, J., 2000. Land surface characterization using lidar remote sensing. Pages 25–38 in Hill MJ, Aspinall RJ, eds. Spatial Information for Land Use Management. Singapore: International Publishers Direct.

Flood, M., Gutelis, B., 1997. Commercial implications of topographic terrain mapping using scanning airborne laser radar. Photogrammetric Engineering and Remote Sensing, 63: 327–366.

Ford, E.D., 1976. The canopy of a Scots pine forest. Description of a surface of complex roughness. Agricultural and Forest Meteorology, 17: 9–32.

Fukushima, Y., Hiura, T., Tanabe, S., 1998. Accuracy of the MacArthur-Horn method of estimating a foliage profile. Journal of Agricultural Forest Meteorology, 92: 203–210.

Garvin, J., Bufton, J., Blair, J., Harding, D., Luthcke, S., Frawley, J., Rowlands, D., 1998. Observations of the Earth's topography from the Shuttle Laser Altimeter (SLA). Laser-pulse echo-recovery measurements of terrestrial surfaces. Physics and Chemistry of the Earth. 23: 1053–1068.

Goward, S.N., Williams, D.L., 1997. Landsat and earth system science. Development of terrestrial monitoring. Photogrammetric Engineering and Remote Sensing, 63: 887–900.

Hansen, A., Rotella, J.J., 2000. Bird responses to forest fragmentation. Pages 201–219 in Knight RL, Smith FW, Romme WH, Buskirk SW, eds. Forest Fragmentation in the Southern Rockies. Boulder: University Press of Colorado.

Harding, D.J., Blair, J.B., Garvin, J.B., Lawrence, W.T., 1994. Laser altimetry waveform measurement of vegetation canopy structure. Pages 1251–1253 in Proceedings of the International Remote Sensing Symposium 1994. Pasadena (CA): California Institute of Technology.

Harding, D.J., Berghoff, G.S., 2000. Fault scarp detection beneath dense vegetation cover. Airborne lidar mapping of the Seattle fault zone, Bainbridge Island, Washington

State. Proceedings of the American Society for Photogrammetry and Remote Sensing Annual Conference; May 2000; Washington, DC. Washington (DC): ASPRS.

Harding, D.J., Lefsky, M.A., Parker, G.G., Blair, J.B., 2001. Lidar altimeter measurements of canopy structure: Methods and validation for closed-canopy, broadleaf forests. Remote Sensing of Environment, 76: 283–297.

Holmgren, J., Nilsson, M., Olsson, H., 2003. Estimation of tree height and stem volume on plots using airborne laser scanning. Forest science, 49: 419-428.

Hyyppä, J., Inkinen, M., 2000. Detecting and estimating attributes for single trees using laser scanner. The Photogrammetric Journal of Finland, 16(2): 27-42.

Irish, J.L., Lillycrop, W.J., 1999. Scanning laser mapping of the coastal zone: The SHOALS system. ISPRS Journal of Photogrammetry and Remote Sensing, 54: 123–129.

Krabill, W., Frederick, E., Yungel, J., 1999. Rapid thinning of the southern Greenland ice sheet. Science 283: 1522.

Krabill, W.B., 2000. Airborne laser mapping of Assateague national seashore beach. Photogrammetry and Remote Sensing, 66: 65–71.

Kraus, K., Pfeifer, N., 1998. Determination of terrain models in wooded areas with airborne laser scanning. ISPRS Journal of Photogrammetry and Remote Sensing, 53: 93–203.

Lefsky, M.A., 1997. Application of Lidar Remote Sensing to the Estimation of Forest Canopy and Stand Structure. PhD dissertation. University of Virginia, Charlottesville, VA.

Lefsky, M.A., Harding, D., Cohen, W.B., Parker, G.G., 1999a. Surface lidar remote sensing of the basal area and biomass in deciduous forests of eastern Maryland, USA. Remote Sensing of Environment, 67: 83–98.

Lefsky, M.A., Cohen, W.B., Acker, S.A., Spies, T.A., Parker, G.G., Harding, D., 1999b. Lidar remote sensing of biophysical properties and canopy structure of forest of Douglas-fir and western hemlock. Remote Sensing of Environment, 70: 339–361.

Leonard, R.E., Federer, C.A., 1973. Estimated and measured roughness parameters for a pine forest. Journal of Applied Meteorology, 12: 302–307.

MacArthur, R.H., MacArthur, J.W., 1961. On bird species diversity. Ecology, 50: 594–598.

MacArthur, R.H., Horn, H.S., 1969. Foliage profile by vertical measurements. Ecology, 50: 802–804.

Maclean, G.A., Krabill, W.B., 1986. Gross-merchantable timber volume estimation using an airborne LIDAR system. Canadian Journal of Remote Sensing, 12: 7–18.

Magnussen, S., Boudewyn, P., 1998. Derivations of stand heights from airborne laser scanner data with canopy-based quantile estimators. Canadian Journal of Forestry Research, 28: 1016–1031.

Magnussen, S., Eggermont, P., LaRiccia, V.N., 1999. Recovering tree heights from airborne laser scanner data. Forest Science, 45: 407–422.

Means, J.E., Acker, S.A., Harding, D.J., Blair, J.B., Lefsky, M.A., Cohen, W.B., Harmon, M., McKee, W.A., 1999. Use of large-footprint scanning airborne lidar to estimate forest stand characteristics in the western Cascades of Oregon. Remote Sensing of Environment, 67: 298–308.

Means, J.E., 2000. Comparison of large-footprint and small-footprint lidar systems: design, capabilities, and uses, Proceedings: Second International Conference on Geospatial Information in Agriculture and Forestry, 10-12 January, Lake Buena Vista, Florida (ERIM International), 1:85-192.

Menenti, M., Ritchie, J.C., 1994. Estimation of effective aerodynamic roughness of Walnut Gulch Watershed with laser altimeter measurements. Water Resources Research. 30: 1329–1337.

Miller, D.R., Lin, J.D., 1985. Canopy architecture of a red maple edge stand measured by the point drop method. Pages 59–70 in Hutchinson BA, Hicks BB, eds. The Forest–Atmosphere Interaction. Dordrecht (Netherlands): Reidel Publishing.

Monteith, J.L., Unsworth, M.H., 1990. Principles of Environmental Physics. Edward Arnold, London.

Naesset, E., 1997a. Determination of mean tree height of forest stands using airborne laser scanner data. ISPRS Journal of Photogrammetry and Remote Sensing, 52: 49–56.

Naesset, E., 1997b. Estimating timber volume of forest stands using airborne laser scanner data. Remote Sensing of Environment, 61: 246–253.

Nelson, R.F., Krabill, W.B., Maclean, G.A., 1984. Determining forest canopy characteristics using airborne laser data: Remote Sensing of Environment. 15: 201–212.

Nelson, R.F., Krabill, W.B., Tonelli, J., 1988. Estimating forest biomass and volume using airborne laser data. Remote Sensing of Environment, 24: 247–267.

Nelson, R., Oderwald, R., Gregoire, T.G., 1997. Separating the ground and airborne laser sampling phases to estimate tropical forest basal area, volume, and biomass. Remote Sensing of Environment, 60: 311–326.

Nilsson, M., 1996. Estimation of tree heights and stand volume using an airborne lidar system. Remote Sensing of Environment, 56: 1–7.

Parker, G.G., 1997. Canopy structure and light environment of an old-growth Douglas fir/western hemlock forest. Northwest Science, 71: 261–270.

Parker, G.G., Lefsky, M.A., Harding, D.J., 2001. PAR transmittance in forest canopies determined from airborne lidar altimetry and from in-canopy quantum measurements. Remote Sensing of Environment, 76: 298–309.

Persson, A., Holmgren, J., Soderman, U., 2002. Detecting and measuring individual trees using an airborne laser scanner. Photogrammetric Engineering & Remote Sensing, 68(9): 925-932.

Ritchie, J.C., Everitt, J.H., Escobar, D.E., Jackson, T.J., Davis, M.R., 1992. Airborne laser measurements of rangeland canopy cover and distribution. Journal of Range Management, 45: 189–193.

Ritchie, J.C., Humes, K.S., Weltz, M.A., 1995. Laser altimeter measurements at Walnut Gulch watershed, Arizona: Journal of Soil and Water Conservation. 50: 440–442.

Ritchie, J.C., Menenti, M., Weltz, M.A., 1996. Measurements of land surface features using an airborne laser altimeter: The HAPEX-Sahel experiment. International Journal of Remote Sensing, 17: 3705–3724.

Schaeffer, S.M., Williams, D.G., Goodrich, D.C., 2000. Transpiration of cottonwood/willow forest estimated from sap flux. Agric. For. Meteorol., 105, 257-270.

Spies, T.A., Franklin, J.F., Klopsch, M., 1990. Canopy gaps in Douglas-fir forests of the Cascade Mountains. Canadian Journal of Forestry Research, 5: 649–658.

Waring, R.H., Way, J., Hunt, E.R., Morrissey, L., Ranson, K.J., Weishampel, J.F., Oren, R., Franklin, S.E., 1995. Imaging radar for ecosystem studies. BioScience, 45: 715–723.

Watt, A.S., 1947. Pattern and process in the plant community. Journal of Ecology, 35: 1–22.

Wehr, A., Lohr, U., 1999. Airborne laser scanning – an introduction and overview. ISPRS Journal of Photogrammetry and Remote Sensing, 54: 68–82.

Weltz, M.A., Ritchie, J.C., Fox, H.D., 1994. Comparison of laser and field-measurements of vegetation height and canopy cover. Water Resources Research, 30: 1311–1319.

World Rivers Review, 1997. Biodiversity, North America. World Rivers Review, News Briefs, Vol. 12, No. 1, February 1997. International Rivers Network. Internet document: http://www.irn.org/pubs/wrr/9701/briefs.html (last date accessed: 15 May 2004).

APPENDIX A: Using airborne lidar to discern age classes of cottonwood trees in a riparian area

A. Farid [a,*], D.C. Goodrich [b], S. Sorooshian [c]

[a] Department of Hydrology and Water Resources, University of Arizona, Tucson, AZ 85721, USA

[b] USDA-ARS-SWRC, Southwest Watershed Research Center, Tucson, AZ, USA

[c] Department of Civil and Environmental Engineering, University of California, Irvine, CA, USA

Abstract

Airborne lidar (**li**ght **d**etecting **a**nd **r**anging) is a useful tool for probing the structure of forest canopies. Such information is not readily available from other remote sensing methods and is essential for modern forest inventories. In this study, small-footprint lidar data were used to estimate biophysical properties of young, mature, and old cottonwood trees in the San Pedro River Basin near Benson, Arizona, USA. The lidar data were acquired in June 2004, using Optech's 1233 ALTM (Optech Incorporated, Toronto, Canada), during flyovers conducted at an altitude of 600 m. Canopy height, crown diameter, stem diameter at breast height (dbh), canopy cover, and mean intensity of return laser pulses from the canopy surface were estimated for the cottonwood trees from the data. Linear regression models were used to develop equations relating lidar-derived tree characteristics with corresponding field acquired data for each age class of cottonwoods. The lidar estimates show a good degree of correlation with ground-based

measurements. This study also demonstrates that other parameters of young, mature, and old cottonwood trees such as height and canopy cover, when derived from lidar, are significantly different ($p < 0.05$). Additionally, mean crown diameters of mature and young trees are not statistically different at the study site ($p = 0.31$). The results illustrate the potential of airborne lidar data to differentiate different age classes of cottonwood trees for riparian areas quickly and quantitatively.

Keywords: Lidar; Canopy; Cottonwood; Riparian; San Pedro River basin

* Corresponding author. Tel.: +1-520-891-0735; fax: +1-520-626-4479.
E-mail address: farid@hwr.arizona.edu (A. Farid).

A.1 Introduction

Vegetation patterns and associated canopy structure influence landscape functions such as water use, biomass production, and energy cycles. The properties of vegetation and canopy must be quantified in order to understand their roles in landscapes and before management plans can be developed for the purpose of conserving natural resources.

Vegetation patterns can be mapped from ground-based inventory techniques, or by using aerial photography or satellite imagery. If sampling is sufficiently intense, ground-based techniques alone can produce accurate results. However, determining the physical properties of canopy architecture and structure (i.e. height, density, timber volume) with conventional ground-based technology is difficult, labor intensive, costly, and usually very limited for assessing large scale or landscape characteristics. Resource managers have become increasingly interested in developing and utilizing alternative sources of information that are more cost effective or offer opportunities to manage resources more efficiently.

Recent progress in three-dimensional forest characterization at the stand level mainly includes digital stereophotogrammetry, synthetic aperture radar, and lidar (**li**ght **d**etecting **a**nd **r**anging). Lidar is a technique in which light at high frequencies, typically in the infrared wavelengths, is used to measure the range between a sensor and a target, based on the round trip travel time between source and target. Airborne Laser Scanning (ALS) is a measurement system in which pulses of light (most commonly produced by a laser) are emitted from an instrument mounted in an aircraft, directed to the ground in a scanning pattern. This method of recording the travel time of the returning pulse is

referred to as pulse ranging (Wehr and Lohr, 1999). The type of information collected from this returning pulse distinguishes two broad categories of lidar sensors: discrete-return (small footprint) lidar devices and full-waveform (large footprint) recording devices.

The foundations of lidar forest measurements lie with the photogrammetric techniques developed to assess tree height, canopy density, forest volume, and biomass. Airborne laser measurements were used in place of photogrammetric measurements to estimate forest heights and canopy density (Nelson et al., 1984) and forest volume or biomass (Maclean and Krabill, 1986; Nelson et al., 1988a; 1988b). For instance, Nelson et al. (1988b) predicted the volume and biomass of southern pine (*Pinus taeda, P. elliotti, P. echinata, and P. palustris)* forests using several estimates of canopy height and cover from small-footprint lidar, explaining between 53% and 65% of the variance in field measurements of these variables.

Research efforts investigated the estimation of forest stand characteristics with scanning lasers that provided lidar data with either relatively large laser footprints (Blair et al., 1999; Lefsky et al., 1999) or small footprints, but with only one laser return (Naesset, 1997a; 1997b; Magnussen et al., 1999). Small-footprint lidars are available commercially and research results on their potential for forestry applications are very promising. Despite the intense research efforts, practical applications of small-footprint lidar have not progressed as far, mainly because of the current cost of lidar data.

The height of a forest stand is a crucial forest inventory attribute for calculating timber volume, site potential, and silvicultural treatment scheduling. Tree heights have been

derived from scanning lidar data sets and have been compared with ground-based canopy height measurements (Naesset, 1997a; 1997b; Magnussen et al., 1999). Results were well correlated with ground-based data, but a high spatial density of lidar shots is required to achieve an acceptable level of accuracy.

An estimate of canopy cover has been made using discrete-return lidar devices. This estimate is produced by counting the number of measurements considered to have been returned from the canopy surface and dividing the result by the total number of measurements for the study site (Ritchie et al., 1993; Weltz et al., 1994), where the measurements are the number of discrete returns.

The primary purpose of this research was to use a small-footprint lidar to estimate biophysical variables in cottonwood trees in the San Pedro Riparian National Conservation Area (SPRNCA) in southeastern Arizona, USA. The SPRNCA is a globally important migratory bird route. Its cottonwood riparian forest supports a great diversity of species and is widely recognized as a regionally and globally important ecosystem (World Rivers Review, 1997). Additionally, lidar studies published to this point have shown success in several forest types with large-footprint lidar, but applications of small-footprint lidar to forestry have not progressed as far (Means, 2000), being limited mainly to measuring even-aged conifer stands. Thus, the performance of lidar in cottonwood riparian forests remains untested and any related analytical and processing issues are yet to be identified. The main objective of this study was to differentiate different age classes of cottonwood trees by using small-footprint lidar for riparian areas. Riparian cottonwood trees use water in proportion to their age (Schaeffer et al., 2000), and are especially large

users of water in flood plains along rivers in semi-arid environments. More accurate quantification of riparian water use is required to manage basin water resources to maintain the economic, social, and ecological viability of these areas and ensure water for a growing human population in the basin. Cottonwoods of different age cannot be distinguished by multi-spectral methods. However, the older cottonwoods exhibit a canopy that is more crowned in shape than the younger trees, thus differences in tree shape as a function of tree age led us to investigate the use of lidar to identify and classify cottonwoods of different age classes. Another important reason for determining the age and canopy characteristics of cottonwood is to discern the recruitment and establishment of cottonwood seedlings in riparian corridors. Because of regulation of streamflow by dams and reservoirs in many western rivers, the occurrence of significant floods which are essential for the recruitment of young cottonwoods, has been greatly reduced. The capability of rapidly quantifying the age distribution of cottonwoods from lidar in a riparian corridor would provide a useful indicator of cottonwood regeneration capacity of a given corridor. The specific goals of this study were:

(1) Derive various geometric measures for different age classes of cottonwoods from lidar data and determine the relationships between cottonwood biophysical properties with ground-based measurements.

(2) Use lidar derived-metrics to differentiate different age classes of cottonwood trees.

A.2 Materials and methods

A.2.1 Study area

The study was conducted along a reach of the San Pedro River (Escalante study site; 31º 51´N, 110º 13´W; 1110m elevation) within the SPRNCA in southeastern Arizona, USA (Fig. A.1). The study site is about 1.2 km long north to south and 1.4 km wide east to west and is relatively flat. The overstory is dominated by riparian forest vegetation, consisting of cottonwood (*Populus fremontii*) and mesquite (*Prosopis velutina*) as dominant and sub-dominant overstory species, respectively. The study area is populated by young-to-old dense cottonwood stands. Patches of cottonwood riparian forest are located along the stream channel. The understory consists mainly of a perennial bunchgrass (*Sporobolus wrightii*), creosote (*Larrea tridentata*), and saltcedar (*Tamarix chinensis*).

A.2.2 Ground inventory data

Ground validation data were collected from July 2004 to April 2005. Three different ages of cottonwood trees were included in the field sampling – young cottonwoods (less than 15 years), mature cottonwoods (16 to 50 years), and old cottonwoods (greater than 50 years) (Fig. A.2). Stem diameters at breast height (dbh) (diameter measured at 1.37 m above the ground) were measured with a diameter tape and recorded to the nearest mm to discriminate between young, mature, and old cottonwood patches, based on river-specific equations that relate dbh to tree age (Stromberg, 1998). Dbh values varied, from less than

25 cm for young cottonwoods, 25 to 90 cm for mature cottonwood stands, and greater than 90 cm for old cottonwoods.

A total of 84 cottonwood trees were used to determine forest mensuration. Of the 84 cottonwoods, 25 old, 30 mature, and 29 young isolated trees were selected that were at least 6 m apart. A differential global positioning system (DGPS) was used to determine the location of each individual tree within sub-meter planimetric accuracy (Trimble 5700 GPS). We measured 4 points around each tree at the edge of the tree canopy. In addition, all tree locations were determined using 60-second static measurements with a 12-channel GPS receiver. The GPS antenna height varied between 1.8 m and 3.6 m, with an average height of 2.5 m. All measurements were collected during the leaf-off season. The lack of canopy foliage and the raised antenna in the old cottonwood stands reduced the error effects of forest canopies on GPS measurements. These trees were identified in the lidar dataset by matching field DGPS locations with the georeferenced lidar data.

Within the study area, dbh, tree height, and crown widths along the major and minor axes were measured for each cottonwood tree. It was assumed that cottonwood tree crowns could be represented by an ellipsoidal geometric shape. The height and crown widths along the major and minor axes were estimated using a hand held laser distance measuring instrument (Impulse 200LR). Two measures for height were taken from different vantage points separated by 90 degrees. The mean of these two height measures for each tree was regressed on the corresponding height estimated from lidar data. The crown diameter, the average of crown widths along two perpendicular directions, was measured for each crown. Descriptive statistics of the field inventory data for young,

mature, and old cottonwoods were computed are given in Table A.1. The mean dbh was 22 cm for young cottonwoods. The mean dbh for mature and old cottonwoods was 51 cm and 106 cm, respectively. As would be expected, the young cottonwoods had the lowest height with values ranging from approximately 7 to 16 m. The lowest mean crown diameter also corresponded to the young trees with a value of 5 m. Old cottonwoods were the tallest trees with values ranging from 20 to 27 m in height with a mean crown diameter at 21 m. For mature cottonwoods, height ranged from 15 to 22 m, with a mean crown diameter of 10 m.

A.2.3 Lidar dataset and analysis

The Optech ALTM 1233 (Optech Incorporated, Toronto, Canada) was used to survey the study site on June 22, 2004. Characteristics of the ALTM 1233 include a pulse rate of 33 kHz, a scanning frequency of 28 Hz, a scan angle of ± 20º, a collection mode of first and last returns, and intensity of returns from a 1064 nm laser. The ALTM 1233 was mounted on a University of Florida plane flying at 600 m above the ground at a velocity of 60 m/s. The aircraft and ALTM 1233 configuration resulted in a cross track point spacing of 0.73 m, a forward point spacing of 2.1 m, and a footprint size of approximately 15 cm. The density of lidar point measurements is approximately 2-4 points/m²; as a result, the entire study area was covered by 8 parallel flight lines. For the entire research area, 50% overlapping flight lines were used to ensure complete coverage, which generated approximately 5 million laser returns. The lidar data were processed and classified using the Optech REALM 3.0.3d software. Three data layers were produced

from the classification: (1) ground last, (2) vegetation last and (3) vegetation first. The ground last data layer was a robust representation of the terrain. For this study, vegetation last and vegetation first data layers were merged into a single vegetation class.

To derive any type of tree height measurement, a ground reference level must be established. The point data in the ground class were interpolated using the kriging interpolation technique to produce a Digital Elevation Model (DEM) with a 0.5 m spatial resolution. Kriging is a method of interpolation, which predicts unknown values from data observed at known locations. This method uses variogram to express the spatial variation, and it minimizes the error of predicted values, which are estimated by spatial distribution of the predicted values (Oliver and Webster, 1990). The DEM was created by ordinary kriging (no drift) using the linear semivariogram model (slope = 1, anisotropy ratio = 1 and anisotropy angle = 0) and the 25 closest points at each grid node. Kriging is a powerful and flexible gridding method. This method sufficed in producing accurate elevation models in comparison with other techniques like inverse distance weighted (Cressie, 1991). Kriging interpolation also works best for known values that are not evenly scattered (Oliver and Webster, 1990). Additionally, kriging technique has the ability to provide an assessment of the interpolation error (Cressie, 1991). The point data in vegetation-classified hits were interpolated to a regular grid that corresponded to the DEM, thereby creating a canopy altitude model. The canopy altitude model was produced by ordinary kriging (no drift) using the linear semivariogram model with nugget effect (error variance = 0.05, micro variance = 1) and the 16 closest points at each grid node. Additionally, the search radius for the canopy altitude model is less than the DEM search

radius. The canopy altitude model has a grid size of 0.5 m. Fig. A.3 shows the terrain and overlaid canopy altitude model for the study site. The local maximum technique (Wulder et al., 2000) was used to discriminate cottonwoods in the canopy altitude model. The process for using the local maximum technique took place in different steps. First, four differentially corrected GPS points were acquired in the field at the corners of a square centered on each cottonwood, from which we identified each cottonwood on the canopy altitude model. Second, the algorithm reads the elevation value at each pixel in the tree's canopy altitude model and if the current pixel corresponds to the local maximum, it is flagged as a tree top. The base of the tree was taken to be the point on the DEM beneath the top of the tree. Tree height was calculated by subtracting of the elevations of the bottom from the top of the tree. Finally, successful identification of the tree crown using the local maximum technique depends on the careful selection of the filter window size. Tree crown form has been associated with different geometric shapes. Although the form of a tree crown does not follow exactly a Euclidean geometric shape, when seen from above, the tree crown can be projected most closely within a circle. Therefore, it is evident that using local maximum technique to identify individual crowns with a circular window of variable diameter is more appropriate than using a square window (Popescu et al., 2003). The derivation of the appropriate window size is based on the assumption that there is a relationship between the height of the trees and their crown width. Thus, tree height and crown width data from the field inventory were used to derive a relationship between tree height and crown width. Based on the canopy altitude model heights and the relationships between the height and crown width, the window size varied between 8 by 8

and 63 by 63 pixels, which corresponds to crown widths between 4.0 m and 31.5 m. This algorithm was implemented in IDL Version 6.0 (Research Systems, Inc., Boulder, CO).

The process for computing the lidar estimate of dbh for different age classes of cottonwoods took place in three steps: First, the relation of field measurements of tree height and dbh was incorporated into a second order polynomial regression procedure. Second, field height was replaced by lidar height in the regression analysis, with equations 1, 4, and 7 in Table A.2. Finally, lidar tree dbh was predicted from lidar tree height metric by using second-order regression equation. The lidar estimate of canopy cover was determined for each age-class of cottonwood tree, by counting the number of first returns from the canopy surface and dividing by the total number of the first and last returns. Canopy cover is estimated in percent and is related to the size of the objects (tree crowns).

Lidar crown diameter is the average of two values measured along two perpendicular directions of the same canopy altitude models. The two perpendicular directions of each tree crown are centered on the tree top. The fourth-degree polynomial allows the corresponding function to have a convex shape along the vertical profile of each direction of tree crown. The fitted function follows the vertical profile of a tree crown, and points of inflection or critical points occur on the edges of a crown profile, where the concavity of the fitted function changes. When these conditions are met, the fitted function indicates a tree crown profile; the distance between critical points was used to calculate the length of each of the two directions. The critical points of the fitted function were found based on the first and second derivatives. A similar technique was used by Popescu

et al. (2003) with lidar data to estimate crown diameter for stands of pine and deciduous trees.

A.2.3.1 Intensity of Reflected Laser Pulse

Little work has been published on the information content of lidar intensity returns for vegetation/forest analysis. For instance, Schreier et al. (1984) developed a method to discriminate broadleaf and conifer forests based on canopy heights, the power of the laser intensity return, and the variability of the power; Lim et al. (2003) derived mean laser height from filtered lidar returns, based on a threshold applied to the intensity return values for tolerant hardwood forests in Canada. The return intensity is related to surface reflectance. At lidar wavelength, young cottonwoods exhibit different reflectance than older ones because of their different leaf area index (Schaeffer et al., 2000). Thus, the return intensity could potentially assist in the discrimination of different age classes of cottonwoods. Using basic exploratory data analysis techniques, the mean of the intensity distribution of each canopy surface was calculated for all cottonwoods.

A.3 Results and discussion

A.3.1 Lidar versus ground-based estimates of canopy properties

Linear regression models were used to develop equations relating lidar-derived parameters, such as tree height and crown diameter, with corresponding field inventory data for each age class of cottonwood trees. The linear regression models that were found to be the most predictive were then cross-validated (Cressie, 1991) to define a generalization error (RMSE). Lidar forest biophysical properties such as mean height have been compared, with varying accuracy and strength of correlation, to ground measurements in temperate (Maclean and Krabill, 1986), tropical (Nelson et al., 1997), and boreal (Naesset, 1997a; Magnussen et al., 1999) forests. However, the performance of lidar in cottonwood riparian forests remained untested and any related analytical and processing issues had yet been identified. Also, in previous studies, regression models for developing equations relating lidar-derived variables with corresponding field inventory data were used to differentiate between different forest types. But in this study, these models are used to differentiate between different ages of one forest type (cottonwood). A summary of all regression models that we developed is presented in Table A.2. Fig. A.4a-c contains the scatterplots comparing lidar-derived and field-measured height for each type of cottonwood tree. In this case, the coefficient of determination for lidar versus field heights were 0.90, 0.87, and 0.81 for young, mature, and old, respectively. The lowest r^2 value was obtained for old cottonwoods. The lidar system presents difficulties in detecting the uppermost portion of old cottonwood tree canopies because of the conical nature of the tree crown. However, the top portion of the crown may not be of

sufficient area to register as a significant return signal and therefore may not be detected. In addition, determining the exact elevation of the ground surface poses difficulties for both old and mature cottonwoods because the understory is dense enough to substantially occlude the ground surface. As a result, old cottonwood tree heights were underestimated. During fieldwork, many situations arose where the top of an old tree crown was not discernible and Impulse 200LR was simply pointed at what was perceived to be the tree top. The r^2 increased from 0.81 to 0.90 when young cottonwoods were considered. The actual ground terrain detected by lidar for young trees is more accurate and precise than those estimates for old and mature trees because the area beneath the young trees is predominantly bare soil. However, even given these complications it is encouraging that the height RMSE was less than the typical vertical accuracy of small-footprint lidar (~10 cm). The scatterplots comparing lidar-derived and field-measured crown diameter for each age class of cottonwood trees are presented in Fig. A.4d-f. The coefficient of determination for lidar versus field crown diameters were 0.84, 0.81, and 0.88 for young, mature, and old, respectively. The lowest r^2 value was obtained for mature cottonwoods because some of the crowns of mature cottonwoods overlap, while the algorithm for calculating crown diameter on the lidar canopy altitude model applies best to measuring non-overlapping crowns. The field measurements considered crowns to their full extent and therefore measured overlapping crown diameters. The r^2 improved from 0.81 to 0.88 when old cottonwoods were examined. The crowns of these old cottonwoods are isolated from each other, and therefore lidar distinguished them easily and more accurately. Also, there is a large difference between the elevations of each tree

crown and its surrounding understory vegetation, allowing easier discrimination between their pixels on the lidar canopy altitude model. Part of the unexplained variance for crown diameter can also be attributed to errors of co-registration between lidar and the ground location of trees, influenced by both lidar positioning accuracy and DGPS errors for locating trees.

The scatterplots comparing lidar-derived and field-measured dbh for each age class of cottonwoods are shown in Fig. A.4g-i. Results from regressing dbh on all age classes of cottonwoods did not produce r^2 values greater than 0.70. The relatively poor regression relationship is likely because dbh derived indirectly from the relation of field tree height to field measured dbh, and therefore lidar dbh accuracy, is directly related to the accuracy of the height estimate from lidar. The highest r^2 was found for young trees, because the relative accuracy of young tree height estimates from lidar data is the highest of the three tree age groups. Meanwhile, the RMSE for all age classes of tree dbh (Table A.2) is the highest.

The results of comparison of tree height between lidar and the field measurement for old, mature, and young cottonwood trees are presented in Fig. A.5a-c. The range of differences of tree height between lidar and the field measurements for all types of cottonwoods is 10~200 cm, reflecting a relatively good correlation overall. Lidar heights tend to be somewhat lower than field measurements (Fig. A.5a). However, in some of the young trees (Fig. A.5c), tree height calculated by lidar is higher than field measurements. This may have occurred due to lidar returns reflected from the canopy top of taller trees in close proximity to the field-measured tree.

A.3.2 Differences among age classes of cottonwood trees

In contrast to Lefsky et al. (1999), which explained differences in canopy structure between four age classes of Douglas-fir and western hemlock forests using full-waveform lidar, we differentiated different age classes of cottonwoods using various lidar metrics such as height based on statistical analysis. Comparing lidar-derived mean heights for age classes indicates, as expected, that tree height is correlated to age (Fig. A.6a), and is statistically significant by age class. The old cottonwoods had the highest mean height estimate. An independent samples t-test showed the difference between young and mature means of height was significant ($p < 0.001$). Also, mean heights of young and old trees differed significantly ($p < 0.001$). The old and mature trees were taller and lidar showed this difference quite well. Similarly, Figs. A.6b and A.6c compare the mean of crown diameter and canopy cover. As expected, the young cottonwoods had the lowest mean crown diameter. The highest mean crown diameter was estimated for old cottonwoods. The mean crown diameter of old trees was higher than young ($p = 0.0001$) because old cottonwoods had cone or cylinder shaped crowns, whereas young cottonwoods had narrow and upright crowns. Some of the crowns of mature trees overlapped. Since the algorithm for calculating crown diameter on the lidar canopy altitude model best suited to measure the non-overlapping portion of crowns, the lidar-estimated crown diameter is lower than field determined size. Thus, mean crown diameters of mature and young trees were not statistically different at the study site ($p = 0.31$).

The mean canopy cover was significantly different for young and old cottonwoods with young canopy cover less than old ($p = 0.0003$). The young cottonwoods have columnar shaped crowns and thus their crown size is much smaller than for old trees, which have conical and flat-topped crowns. Mean canopy covers of mature and young also differed significantly ($p < 0.05$) at the study site. The lidar estimate of canopy cover is directly related to the number of laser returns from a crown, and because of the gaps in young canopies, a number of the laser pulses were able to penetrate the canopy, generating lower values for canopy cover.

Mean lidar intensities were least for old and greatest for young canopies (Fig. A.6d). The return intensity is related to surface reflectance. At 1064nm wavelength, young cottonwoods exhibit higher reflectance than older ones because of their higher leaf area index (Schaeffer et al., 2000) and different leaf architecture, such as less drooping and less micro gaps between leaves. Mean intensity of mature trees did not differ significantly ($p = 0.16$) from young ones. The reflectance of mature and young canopies is similar due to their leaves and branches having almost the same color and brightness, as seen in Fig. A.2. It is evident from this discussion that more study is required focusing on the information content of intensity return data and the factors that influence how much energy is reflected from a surface back to a lidar sensor. Furthermore, lidar-derived canopy metrics from this study and the return intensity data will be incorporated into supervised image classification algorithms, using a maximum likelihood technique, to differentiate age classes of cottonwood trees.

A.4 Conclusions

The results of the current study show that lidar data can be used to accurately estimate the properties of cottonwood canopies at the individual tree level. Lidar offers the possibility of rapidly deriving biophysical variables in riparian areas using automated techniques. Thus, seeing the cottonwoods in the riparian forest and more importantly measuring them with lidar brings an important contribution to concepts such as precision forest inventory and automated data processing for riparian forestry applications.

Overall, this research proved that small-footprint airborne lidar data is able to predict stand structure attributes such as height, crown diameter, and canopy cover of riparian cottonwood forests. Measurements of cottonwood canopy properties made with lidar data in the riparian area were not significantly different from measurements taken on the ground. The main objective of this research was to use lidar-derived estimates to differentiate young, mature, and old cottonwood patches. The results illustrate the potential of lidar data to differentiate different age classes of cottonwood trees for riparian areas quickly and quantitatively. Furthermore, there is value in the intensity return data for assisting in differentiating cottonwood trees, but this parameter needs further investigation in order to develop a good understanding of the factors affecting how intensity returns are produced and recorded by the lidar sensor.

Future research will apply the well-known P-M model (Monteith and Unsworth, 1990) to model age classes of cottonwood transpiration using lidar-derived canopy metrics, such as height and Leaf Area Index (LAI), so improved riparian water use estimates can be made. The LAI will be derived by synthetically constructing a large footprint lidar

waveform from the airborne small-footprint lidar data. In addition, the capability to rapidly quantify the age distribution of cottonwoods in a riparian area will provide an indicator of cottonwood regeneration capacity of a given area.

Acknowledgements

This study is based upon work supported by SAHRA (Sustainability of semi-Arid Hydrology and Riparian Areas) under the STC Program of the National Science Foundation, Agreement No. EAR-9876800. Special thanks to Sherma Zibadi who was involved in the collection of the field data. We are indebted to the following people who assisted us in various aspects of this work: Michael Sartori and Catlow Shipek. In addition, we wish to acknowledge the staff at the USDA-ARS Southwest Watershed Research Center, Tucson, Arizona.

A.5 References

Blair, J.B., Rabine, D.L., Hofton, M.A., 1999. The Laser Vegetation Imaging Sensor (LVIS): a medium-altitude, digitization-only, airborne laser altimeter for mapping vegetation and topography. ISPRS Journal of Photogrammetry & Remote Sensing, 54, 115-122.

Cressie, N.A., 1991. Statistics for spatial data. New York: Wiley, 900 p.

Lefsky, M.A., Cohen, W.B., Acker, S.A., Spies, T.A., Parker, G.G., Harding, D., 1999. Lidar remote sensing of biophysical properties and canopy structure of forest of Douglas-fir and western hemlock. Remote Sensing of Environment, 70, 339-361.

Lim, K., Treitz, P., Baldwin, K., Morrison, I., Green, J., 2003. Lidar remote sensing of biophysical properties of tolerant northern hardwood forests. Can. J. Remote Sensing, 29, 658-678.

Maclean, G.A., Krabill, W.B., 1986. Gross-merchantable timber volume estimation using an airborne LIDAR system. Can. J. Remote Sensing, 12, 7-18.

Magnussen, S., Eggermont, P., LaRiccia, V.N., 1999. Recovering tree heights from airborne laser scanner data. Forest Science, 45, 407-422.

Means, J.E., 2000. Comparison of large-footprint and small-footprint lidar systems: design, capabilities, and uses, Proceedings: Second International Conference on Geospatial Information in Agriculture and Forestry, 10-12 January, Lake Buena Vista, Florida (ERIM International), 1:85-192.

Monteith, J.L., Unsworth, M.H., 1990. Principles of Environmental Physics. Edward Arnold, London.

Naesset, E., 1997a. Determination of mean tree height of forest stands using airborne laser scanner data. ISPRS Journal of Photogrammetry and Remote Sensing, 52: 49-56.

Naesset, E., 1997b. Estimating timber volume of forest stands using airborne laser scanner data. Remote Sensing of Environment, 61, 246-253.

Nelson, R.F., Krabill, W.B., Maclean, G.A., 1984. Determining forest canopy characteristics using airborne laser data. Remote Sensing of Environment, 15, 201-212.

Nelson, R.F., Swift, R., Krabill, W.B., 1988a. Using airborne lasers to estimate forest canopy and stand characteristics. Journal of Forestry, 86, 31-38.

Nelson, R.F., Krabill, W.B., Tonelli, J., 1988b. Estimating forest biomass and volume using airborne laser data. Remote Sensing of Environment, 24, 247-267.

Nelson, R.F., Oderwald, R., Gregoire, T.G., 1997. Separating the ground and airborne laser sampling phases to estimate tropical forest basal area, volume, and biomass. Remote Sensing of Environment, 60, 311-326.

Oliver, M.A., Webster, R., 1990. Kriging: a method of interpolation for geographical information system. INT. J. Geographical Information Systems, Vol. 4, No. 3, 313-332.

Popescu, S.C., Wynne, R.H., Nelson, R.F., 2003. Measuring individual tree crown diameter with lidar and assessing its influence on estimating forest volume and biomass. Can. J. Remote Sensing, 29, 564-577.

Ritchie, J.C., Evans, D.L., Jacobs, D., Everitt, J.H., Weltz, M.A., 1993. Measuring canopy structure with an airborne laser altimeter. Transactions of the ASAE, Vol. 36, 1235-1238.

Schaeffer, S.M., Williams, D.G., Goodrich, D.C., 2000. Transpiration of cottonwood/willow forest estimated from sap flux. Agric. For. Meteorol., 105, 257-270.

Schreier, H., Lougheed, J., Gibson, J.R., Russell, J., 1984. Calibrating an airborne laser profiling system. Photogrammetric Engineering & Remote Sensing, 50(11): 1591-1598.

Stromberg, J.C., 1998. Dynamics of Fremont cottonwood (*Populus fremontii*) and saltcedar (*Tamarix chinensis*) populations along the San Pedro River, Arizona. Journal of Arid Environments, 40, 133-155.

Wehr, A., Lohr, U., 1999. Airborne laser scanning-an introduction and overview. ISPRS Journal of Photogrammetry and Remote Sensing, 54, 68-82.

Weltz, M.A., Ritchie, J.C., Fox, H.D., 1994. Comparison of laser and field measurements of vegetation height and canopy cover. Water Resources Research, 30: 1311-1319.

World Rivers Review, 1997. Biodiversity, North America. World Rivers Review, News Briefs, Vol. 12, No. 1, February 1997. International Rivers Network. Internet document: http://www.irn.org/pubs/wrr/9701/briefs.html (last date accessed: 15 May 2004).

Wulder, M., Niemann, K.O., Goodenough, D.G., 2000. Local maximum filtering for the extraction of tree locations and basal area from high spatial resolution imagery. Remote Sensing of Environment, 73, 103-114.

Table A.1 Descriptive statistics of the field inventory data for young, mature, and old cottonwoods

Statistic	dbh (cm)	Height (m)	Crown diameter (m)
Young (*n* = 29)			
Mean	22	12	5
Min.	10	7	4
Max.	29	16	9
SD	6	3	1
Mature (*n* = 30)			
Mean	51	19	10
Min.	27	15	6
Max.	73	22	15
SD	15	3	3
Old (*n* = 25)			
Mean	106	24	21
Min.	93	20	11
Max.	131	27	32
SD	12	2	7

Note: SD, standard deviation.

Table A.2 Regression equations and statistics for cottonwood forest structural characteristics

Forest structural characteristic	Equation	R^2*	RMSE
Young			
Height (m)	(1) Fieldht = 1.16 + 0.90 × Lidarht	0.90	0.74
Crown diameter (m)	(2) Fieldcd = -1.13 + 1.17 × Lidarcd	0.84	1.58
dbh (cm)	(3) Fielddbh = 0.02 + 1.03 × Lidardbh	0.67	3.27
Mature			
Height (m)	(4) Fieldht = 1.03 + 0.97 × Lidarht	0.87	0.97
Crown diameter (m)	(5) Fieldcd = 3.32 + 0.76 × Lidarcd	0.81	1.77
dbh (cm)	(6) Fielddbh = -2.46 + 1.03 × Lidardbh	0.64	8.85
Old			
Height (m)	(7) Fieldht = 4.26 + 0.89 × Lidarht	0.81	1.97
Crown diameter (m)	(8) Fieldcd = 0.20 + 1.02 × Lidarcd	0.88	1.23
dbh (cm)	(9) Fielddbh = 38.27 + 0.64 × Lidardbh	0.59	9.42

* All values significant (P<0.01).

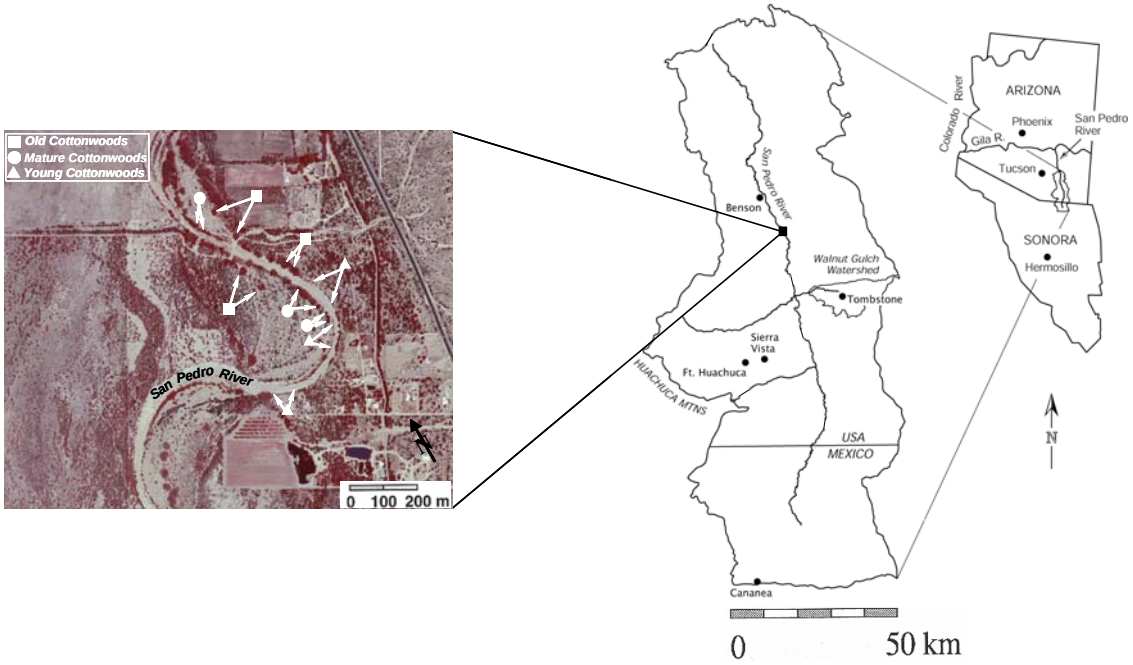

Figure A.1. Location map and color infrared aerial photograph of the Escalante study site in the San Pedro River Basin, Arizona.

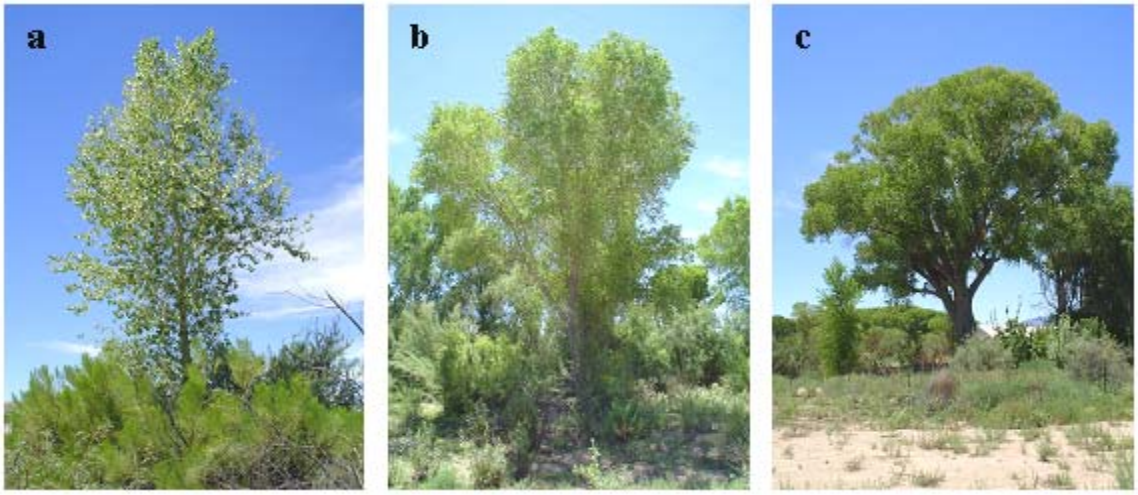

Figure A.2. Photos depicting (**a**) young, (**b**) mature, and (**c**) old cottonwood trees.

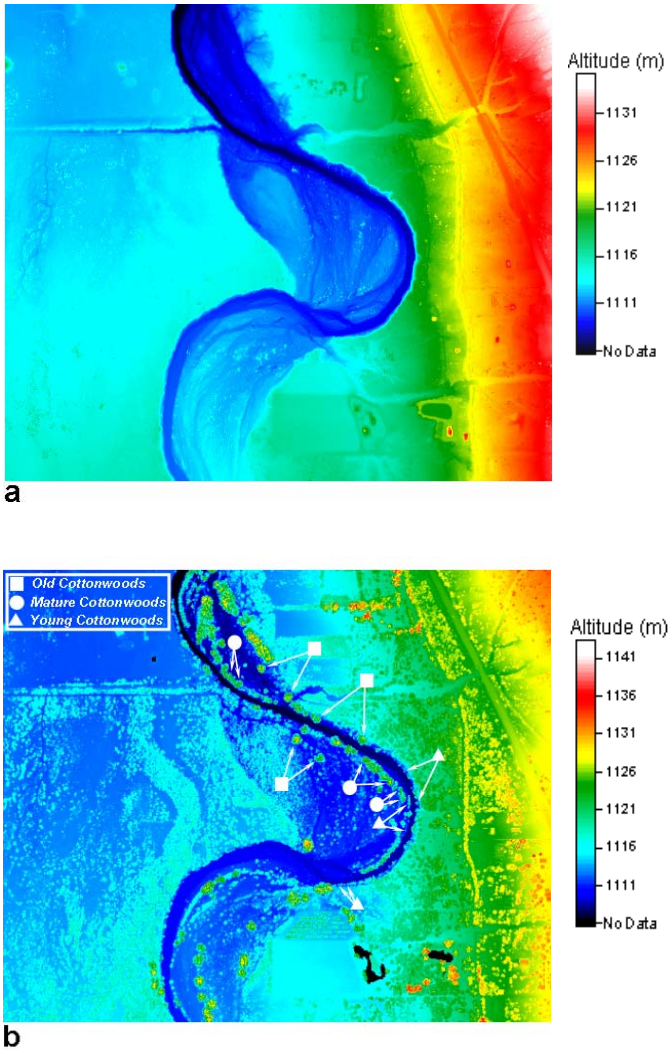

Figure A.3. Spatial pattern of DEMs (a) bare ground model and (b) canopy altitude model for the study site.

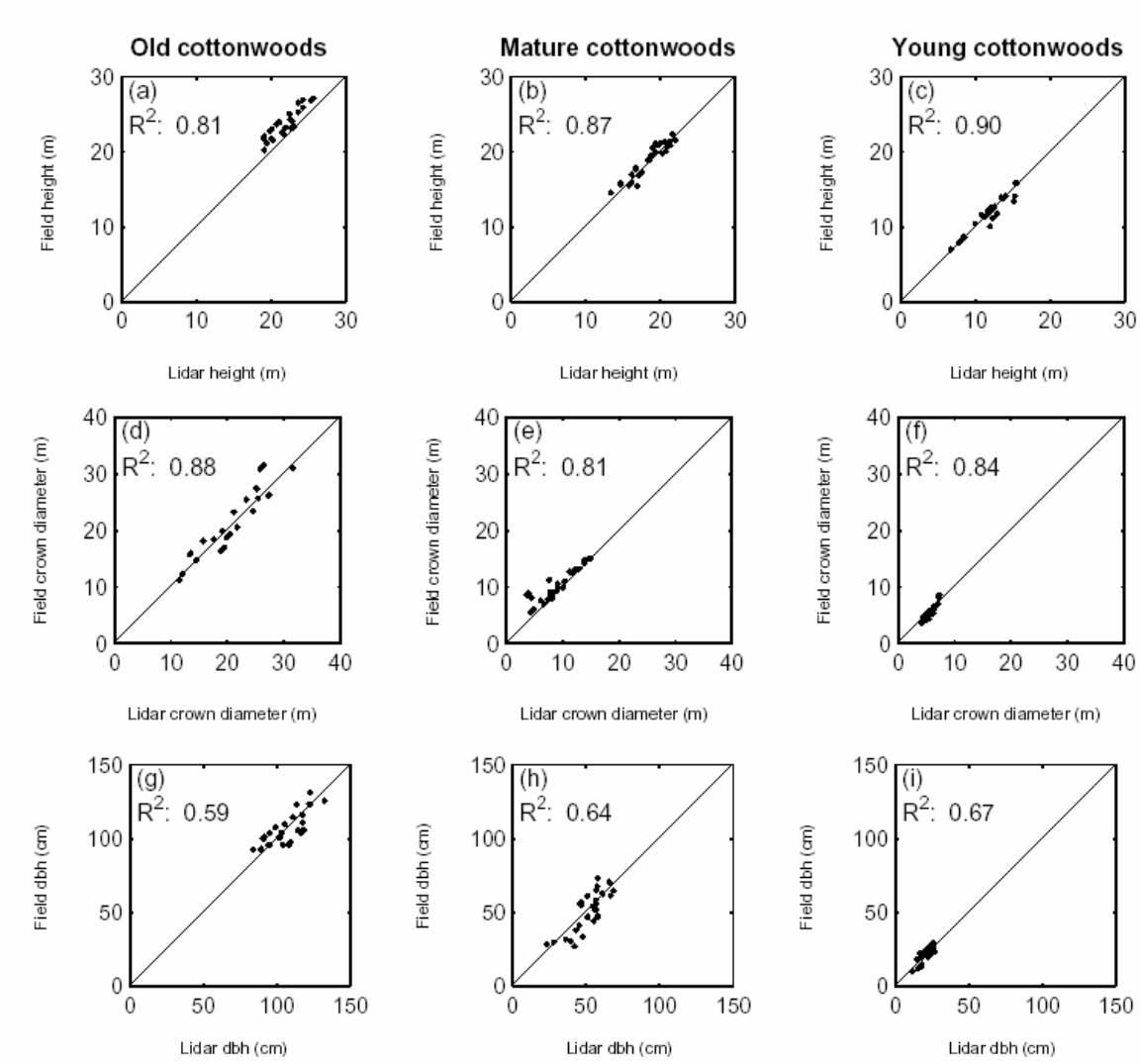

Figure A.4. Scatterplots comparing lidar-derived and field-measured height, crown diameter, and dbh for each type of cottonwood tree on the study region.

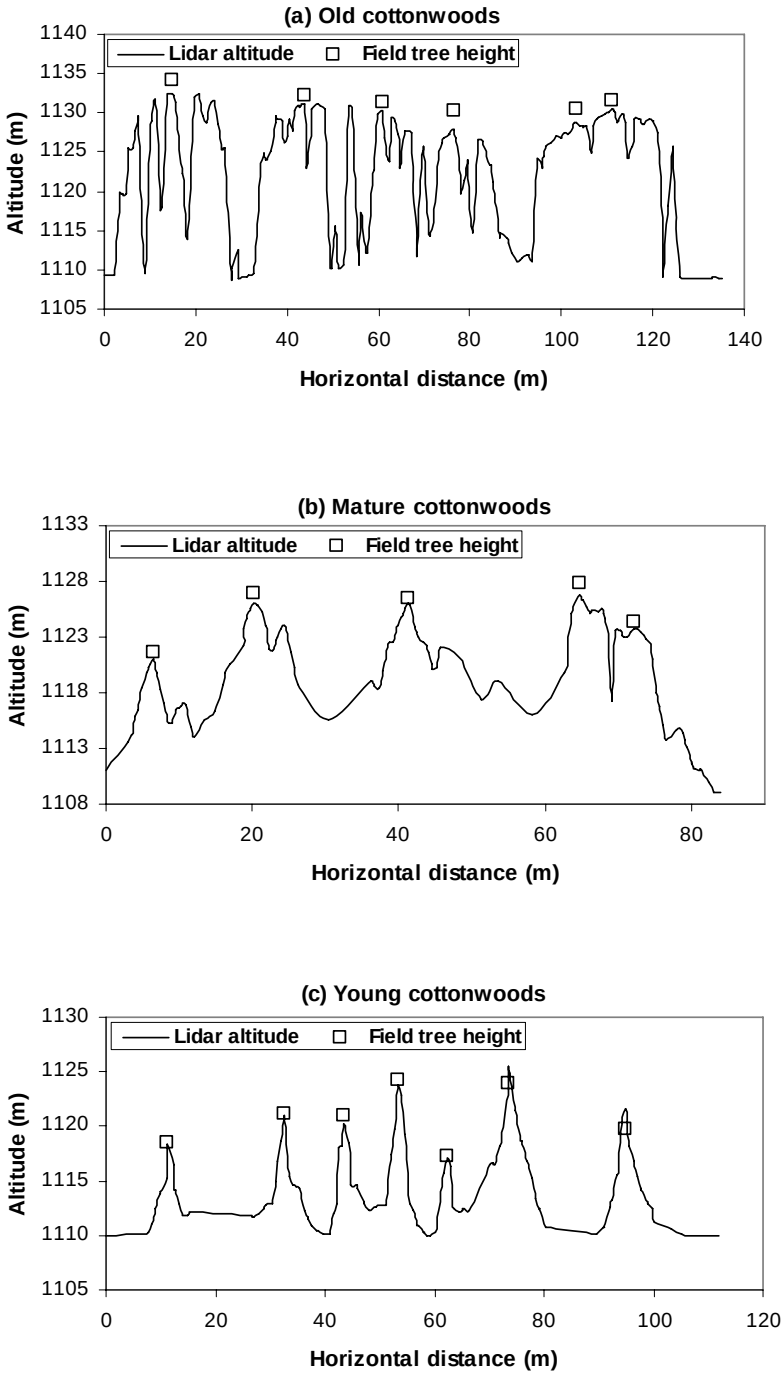

Figure A.5. Comparison of height (cross-section) for old (a), mature (b), and young (c) cottonwood trees.

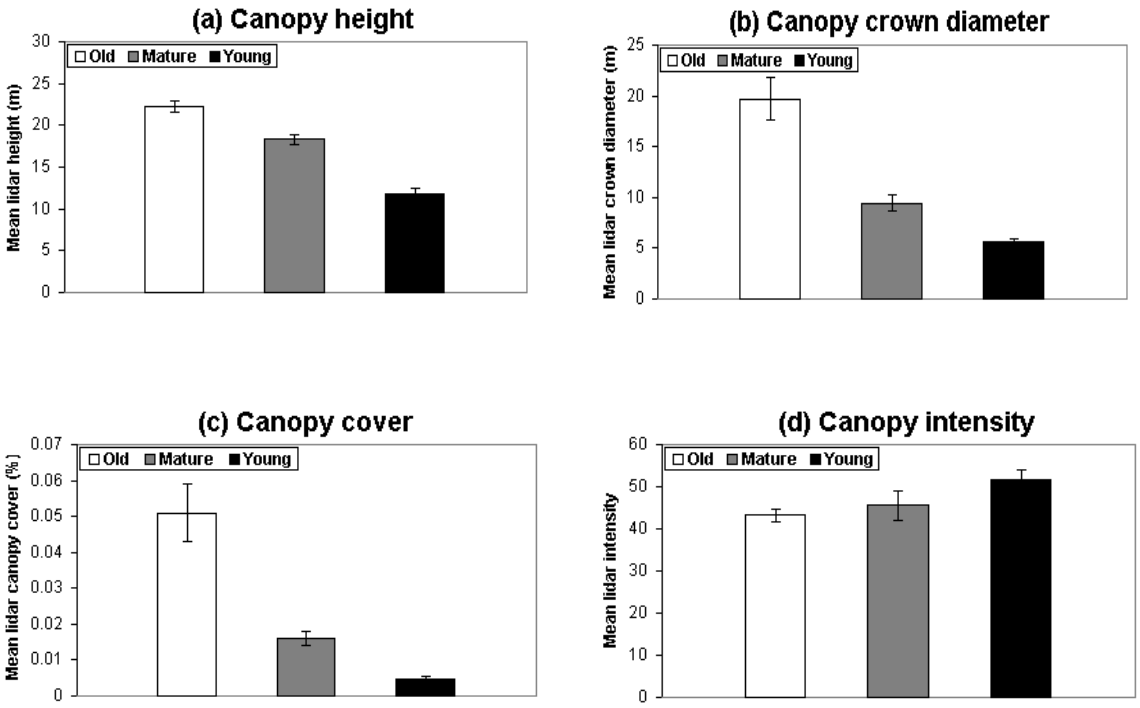

Figure A.6. T-test analyses comparing the means of height (a), crown diameter (b), canopy cover (c), and canopy intensity (d) derived from lidar data for different age classes of cottonwood trees.

A.6 Appendix I: Specifics of intensity data from airborne laser scanning (ALS) system

A.6.1 Intensity of reflected laser pulse

The ALS systems with intensity returns enable the user to simultaneously see the features, like black and white photography, and gives visual help to understand surveyed areas.

Intensity is the relative reflectance value between transmitted and received power. Let us assume that the laser footprint completely covers the entire target area which reflects the beam back to the source and the reflected power radiates uniformly into a hemisphere.

Based on the equations by Baltsavias (1999) for the relation between transmitted and received laser pulse, the total power reflected from the target is:

$$P_{refl} = \frac{\rho}{\pi} \Phi_{tar} A_{tar} = \rho \frac{M P_T D_{tar}^2}{\pi (D + R\gamma)^2} \qquad \text{(A.6-1)}$$

Where

ρ = reflectivity of target,

$\boldsymbol{A_{tar}}$ (m^2) = target area,

$\Phi \mathbf{t_{ar}}$ = power density within an illuminated target,

$\boldsymbol{P_T}$ = Transmitted power,

M =Atmospheric transmission,

$\boldsymbol{D_{tar}}$ = diameter of target object,

R = range (distance between sensor and object),

γ (mrad) = laser beam divergence (IFOV).

The power reflected from the target, P_{refl} that is collected by the receiver optics, with M the atmospheric transmission and A_r the receiver area, is the power collected by the receiver, P_r :

$$P_r = P_{refl} M \frac{A_r}{R^2} \tag{A.6-2}$$

$$A_r = \frac{\pi D^2 r}{4} \tag{A.6-3}$$

Where ***D*r** = Diameter of receiving optics. Combining the above equation yields: (with assuming $A_I = A_{tar}$)

$$P_r = \rho \frac{M^2 A_r}{\pi R^2} P_T \tag{A.6-4}$$

The above equation can also be used with the transmitted and received energy per pulse instead of the power. In the pulse laser 1064 nm wavelength of the ALS system, intensity can be expressed in the form shown in Equation A.6-5.

$$Intensity \cong \rho_{1064} \frac{M^2 A_r}{\pi R^2} P_T \tag{A.6-5}$$

This is an approximation by Baltsavias (1999) since there are additional losses, due to the optical transmission of the transmitter and receiver optics, and the narrow band pass filter at the receiver which exclude background radiation.

The returning intensity depends on the reflectance of the surface. At 1064nm wavelength, sand, water, concrete, and vegetation exhibit high reflectance. Dark surfaces, such as asphalt, wet surfaces, and mud have much lower reflectivity. The intensity is also affected by the surface texture, the distance from the aircraft to the surface, and the orientation of the surface to the receiver.

A.6.2 Correlation between ALS intensity and target reflectance

When discussing laser wavelength, one should also consider the backscattering properties of the target on object surface. For instance, Figure A.6.1 is a digital color image taken by the UF ADP system. It is a coastal scene near St. Augustine, Florida, which includes grasses, concrete sidewalks, asphalt roads, sand, and ocean. In Figure A.6.2, we show the ALS laser data of the same area. The ALS points were manually divided into six land-cover groups, as shown in Table A.6-1.

Since the ALS data has height and intensity information at each X and Y coordinate, some ground objects can be classified using the correlation between height and intensity. In Figure A.6.3, we show the correlation between the ALS intensity and height. Examination of Figure A.6.3 shows that for this scene, buildings, asphalt, and ocean areas

Figure A.6.1. Test area for checking reflectance of the wavelength of the ALS laser intensity.

Table A.6-1 Classification of ALS data group. Table adapted from Park et al. (2002).

Raw ALSM data group	Classification
A	Ocean
B	Asphalt
C	Building1
D	Concrete building
E	Concrete + Grass
F	Grass + Sand

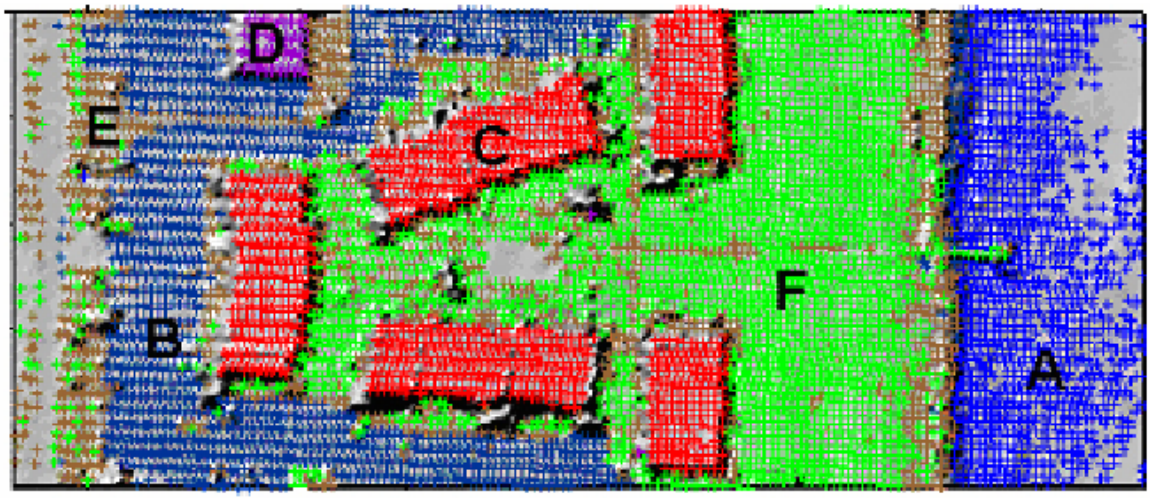

Figure A.6.2. Classification by correlation of ALS elevation and intensity. Figure adapted from Park et al. (2002).

can be easily classified, but groups E and F, which consist of mixtures of concrete and grass, and grass and sand, could not be separated to one class.

To check reflectance of the 1064nm wavelength of the ALS laser intensity, the AVIRIS hyperspectral data for sand, asphalt, grass and concrete are shown at Figure A.6.4. Although asphalt has low reflectance, just as it has a lower intensity value, the reflectance of grass, sand, and concrete is too close to distinguish each object using just reflectance.

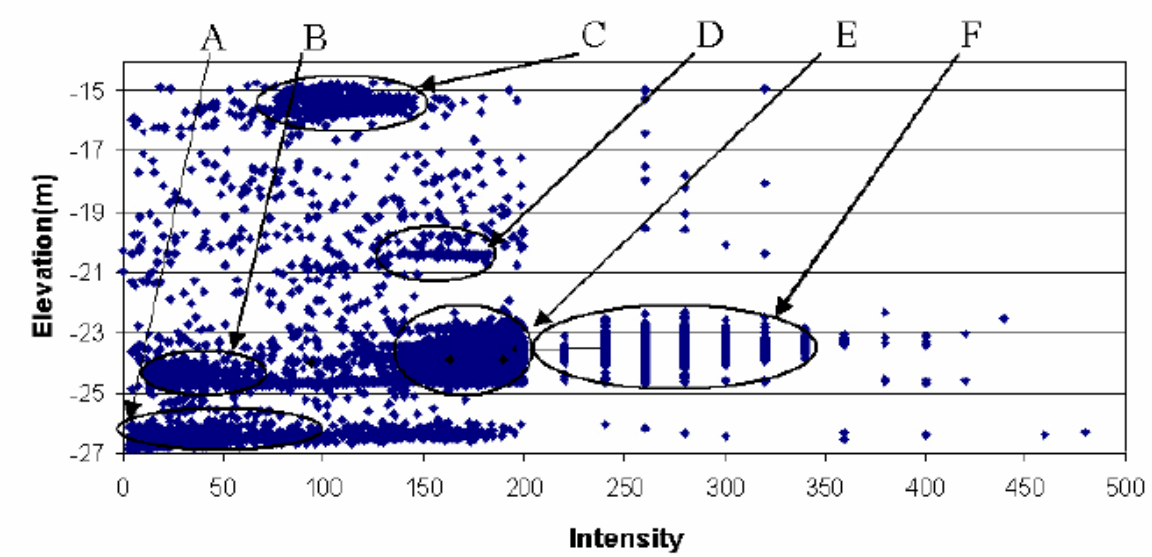

Figure A.6.3. Correlation of the ALS height data to intensity data. Figure adapted from Park et al. (2002).

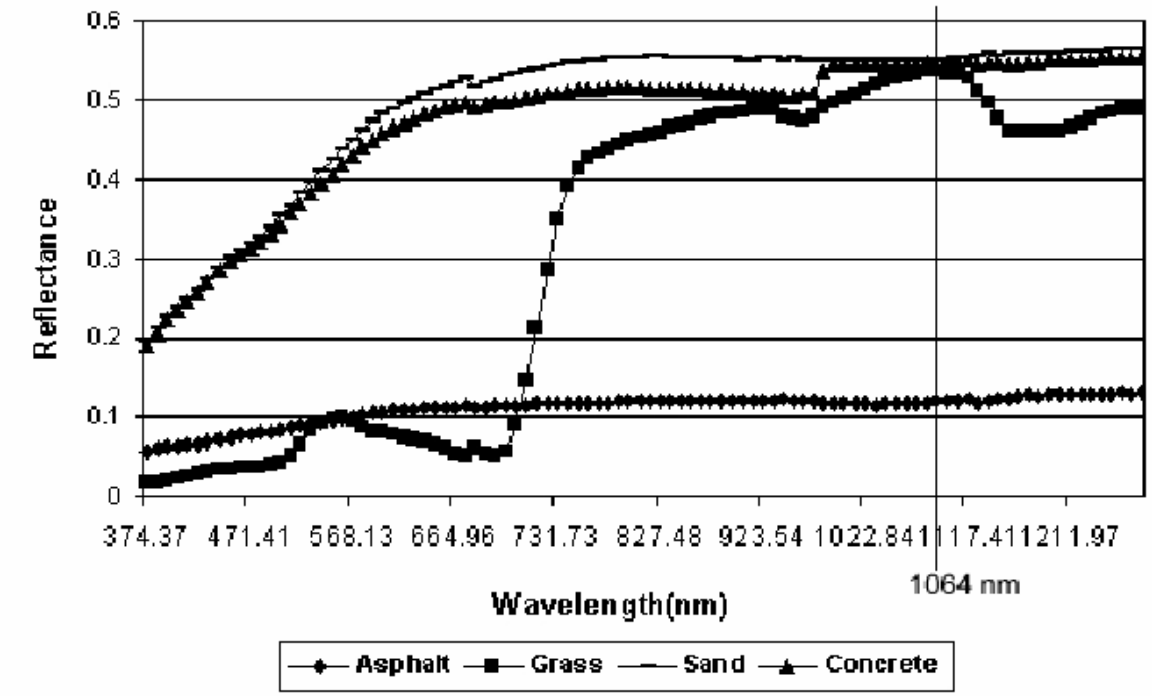

Figure A.6.4. Correlation between reflectance and wavelength of the AVIRIS hyperspectral data. Figure adapted from Park et al. (2002).

The reflectivity of a target for a given wavelength also influences the maximum range. Thus, manufacturers and system providers' specifications for the maximum range should always specify type of target reflectivity (Wehr and Lohr, 1999).

A.6.3 References

Baltsavias, E.P., 1999, "Airborne Laser Scanning: Basic Relations and Formulas," *ISPRS Journal of Photogrammetry & Remote Sensing*, vol. 54, pp. 199-241.

Park, J.Y., 2002. Data fusion techniques for object space classification using airborne laser data and airborne digital photographs. PhD dissertation. University of Florida, Gainesville, FL.

Wehr, A. and U. Lohr, 1999, "Airborne Laser Scanning: An Introduction and Overview," *ISPRS Journal of Photogrammetry & Remote Sensing*, Vol. 54, pp. 68-82.

APPENDIX B: Riparian vegetation classification from airborne laser scanning data with an emphasis on cottonwood trees

A. Farid [a], D. Rautenkranz [b], D.C. Goodrich [c], S.E. Marsh [b], S. Sorooshian [d]

[a] Department of Hydrology and Water Resources, University of Arizona, Tucson, AZ 85721, USA

[b] Arizona Remote Sensing Center, Office of Arid Land Studies, University of Arizona, Tucson, AZ, USA

[c] USDA-ARS-SWRC, Southwest Watershed Research Center, Tucson, AZ, USA

[d] Department of Civil and Environmental Engineering, University of California, Irvine, CA, USA

Abstract

The high point density of airborne laser mapping systems enables achieving a detailed description of geographic objects and of the terrain. Growing experience indicates, however, that extracting useful information directly from the data can be difficult. In this study, small-footprint lidar data were used to differentiate between young, mature, and old cottonwood trees in the San Pedro River Basin near Benson, Arizona, USA. The lidar data were acquired in June 2003, using Optech's 1233 ALTM (Optech Incorporated, Toronto, Canada), during flyovers conducted at an altitude of 750 m. The lidar data was

pre-processed to create a two-band image of the study site: a high accuracy canopy altitude model band and a near-infrared intensity band. These lidar-derived images provided the basis for supervised classification of cottonwood age categories, using a maximum likelihood algorithm. The results of classification illustrate the potential of airborne lidar data to differentiate age classes of cottonwood trees for riparian areas quickly and accurately.

B.1 Introduction

In the mapping sciences, the ultimate goal is to completely describe the object space with regard to the type and location of the individual objects within it, and to represent this understanding in an iconic form as a map. Two approaches are widely used. When high planimetric accuracy or elevation data are required, maps are produced using photogrammetric techniques. For small-scale or land-cover mapping projects, automated segmentation and classification algorithms are generally applied to passive spectral data in order to produce classification maps.

Other technologies have begun to compete with photogrammetry. The rapid evolution of two active sensing technologies, lidar (**li**ght **d**etecting **a**nd **r**anging) and SAR (Synthetic Aperture Radar), have made it possible to directly produce three-dimensional data, and simultaneously to generate two-dimensional images of the intensity of the return signal.

Lidar has emerged in recent years as a leading technology for the extraction of information about physical surfaces. The ever-increasing point density of current airborne systems allows a detailed description of the surveyed surfaces to be achieved and provides a wealth of information on physical objects and the terrain.

Previous work has used lidar data in two principal ways, by classifying the data 1) as terrain and non-terrain points, and 2) as features such as trees or buildings. Examples of the first approach are Kraus and Pfeifer's work (1998), using an iterative linear prediction scheme for removing vegetation points in forested areas, and the utilization of gradient-based techniques by Vosselman (2000) to separate building points from terrain points. Using the second approach, Axelsson (1999) presented algorithms for filtering and

classification of data points into terrain, buildings, and electrical power lines using multiple returns of lidar data as well as the intensity return. Maas (1999) applied height texture for segmentation of lidar data. Song et al. (2002) focused on assessing separation of different land cover types such as trees, grass, roads, and roofs, based on interpolated intensity data, using three different interpolation techniques. Filin (2004) proposed a surface clustering technique for identifying regions in lidar data that exhibit homogeneity in a certain feature space, using attributes of position, tangent plane, and relative height difference for every point. The surfaces were categorized as high vegetation, low vegetation, smooth surfaces, and planar surfaces. Most of these previous studies involving classification of lidar data have focused on the use of unsupervised algorithms on a small number of classes, resulting in generalized classifications.

This research represents the first evaluation of the use of lidar data for age discrimination of riparian vegetation. We employed a supervised classification technique, the maximum likelihood algorithm, for differentiating age classes of cottonwood trees by using small-footprint lidar data for riparian areas. Riparian cottonwood trees use water in proportion to their age (Schaeffer et al., 2000), and are especially large users of water in flood plains along rivers in semi-arid environments. More accurate quantification of riparian water use is required to manage basin water resources to maintain the economic, social, and ecological viability of these areas and ensure water for the growing human population in the basin. Cottonwoods of different ages cannot be distinguished by multi-spectral methods. However, older cottonwoods exhibit a canopy that is more crowned in shape than the younger trees, thus differences in tree shape as a function of tree age led us to

investigate the use of lidar data to identify and classify cottonwoods of different age classes.

B.2 Study area

The study was conducted along a reach of the San Pedro River (Escalante study site; 31º 51´N, 110º 13´W; 1110m elevation) within the San Pedro Riparian National Conservation Area (SPRNCA) in southeastern Arizona, USA (Figure B.1). The study site is 1.2 km long north to south and 1.4 km wide east to west and is relatively flat. The overstory is dominated by riparian forest vegetation, consisting of cottonwood (*Populus fremontii*) and mesquite (*Prosopis velutina*) as dominant and sub-dominant overstory species, respectively. The study area is populated by young-to-old dense cottonwood stands. Patches of cottonwood riparian forest are located along the stream channel. The understory consists mainly of a perennial bunchgrass (*Sporobolus wrightii*), creosote (*Larrea tridentata*), and saltcedar (*Tamarix chinensis*).

B.3 Methods

The Optech ALTM 1233 (Optech Incorporated, Toronto, Canada) was used to survey the study site on June 6, 2003. Characteristics of the ALTM 1233 include a scanning frequency of 28 Hz, a scan angle of ± 20º, a collection mode of first and last returns, and intensity of returns from a 1064 nm laser. The ALTM 1233 was mounted on an aircraft operated by the University of Florida flying at 750 m above the ground at a velocity of 60 m/s. The aircraft and ALTM 1233 configuration resulted in a cross-track point spacing of 0.9 m, a forward point spacing of 2.1 m, and a footprint size of approximately 15 cm. The density of lidar point measurements is approximately 2-4 points/m². The entire study area was covered by 4 parallel flight-lines with 50% overlapping flight-lines, which generated approximately 2 million laser returns. The data was pre-processed into first and last returns. The attributes of any given laser return not only include x, y, and z coordinate data, but also an intensity return value.

The point data in first-return hits were interpolated using a kriging technique to produce a Canopy Altitude Model (CAM) with a 0.5 m pixel grid. Additionally, the intensity return data and its xy coordinates for both first and last hits were interpolated to the same 0.5 m regular grid corresponding to the CAM, thereby creating a near-infrared intensity image. Figure B.2 illustrates the CAM and the corresponding intensity image for the study site.

We performed a supervised classification of the 2-band lidar image (altitude and intensity images) using the maximum likelihood algorithm. The maximum likelihood classifier assumes that the training sample data are normally distributed. Pixels are assigned to classes based on the probability of matching the training sample class signature (Jensen,

1996; Richards, 1999). Supervised classification is particularly applicable to a study site such as ours, in which there are a limited number of land cover types; the researchers are familiar with the area; the geographic extent is reasonably small; and, ground-truth data can be obtained.

Ground validation data were collected from July 2004 to March 2005. Three different ages of cottonwood trees were included in the field sampling: young cottonwoods (less than 15 years), mature cottonwoods (16 to 50 years), and old cottonwoods (greater than 50 years). Stem diameters at breast height (dbh) (diameter measured at 1.37 m above the ground) were measured with a diameter tape and recorded to the nearest mm to discriminate between young, mature, and old cottonwood patches, based on river-specific equations that relate dbh to tree age (Stromberg, 1998). Dbh values varied, from less than 25 cm for young cottonwoods, 25 to 90 cm for mature cottonwood stands, and greater than 90 cm for old cottonwoods.

We selected training sites representative of the main land cover types, from which class signatures were generated. Signatures were generated for different age classes of cottonwood trees, mesquite, saltcedar, dry stream channel, and open ground categories. Training sites were chosen by visual inspection of the lidar image, using expert knowledge of the study site, to identify a region of signal purity (pixel uniformity) for each category. Training sites for cottonwood are sets of trees visually selected in the image from the three age classes. Selection criteria for trees used for signature generation are (1) unambiguous identification in the lidar images, and (2) clear separation of signatures between classes. To validate the image classification, we performed an

accuracy assessment, in which actual land cover, as determined by field identification, was compared with classes for the corresponding areas assigned by the maximum likelihood classification. Two different methods were used for field ground-truth: 1) four differentially corrected GPS points were acquired at the corners of a square centered on each cottonwood, from which we identified each cottonwood on the classified image; and 2) for non-cottonwood classes (stream channel, open ground, saltcedar, and mesquite), we generated a random sample, 20 points for each class. Ground truth data was obtained at the GPS coordinates for each random point. We calculated the classification error matrix using these ground truth results as our reference data. Because there are low numbers of young and old cottonwoods, all field-identified young and old trees were used both in signature generation and in the accuracy assessment. Twenty of the 40 mature cottonwoods were used in signature generation. All 40 mature trees were used in the accuracy assessment. For the other categories there is no overlap in regions used for signature generation and for accuracy assessment. Users' and producers' accuracy and Cohen's kappa were computed. The users' accuracy indicates the probability that accurate prediction of actual land-cover can be made from the classified image. Cohen's kappa is a statistical measure of the proportionate decrease in classification error for the classified image, compared to the class assignments expected by a random classification process (Congalton and Green, 1999, p. 49).

B.4 Results and discussion

Our initial classification included: young, mature, and old cottonwood classes; mesquite; saltcedar; stream channel; and open ground. The objective of our study was to determine the feasibility of identifying cottonwood age classes from lidar data. The final classified image is shown in Figure B.3. Accuracy assessment indicated that 78% of the 2-band lidar image was correctly classified. The classification resulted in a Cohen's kappa of 0.73. If only cottonwood classes are considered, accuracy assessment gives a Cohen's kappa of 0.44 and an overall accuracy of 68%. The error matrix used for accuracy assessment is given in Table B.1. Accuracy assessment results are presented in Table B.2. Although the overall classification accuracy was reasonably good, it can be seen from Table B.1 that discrimination of young cottonwoods from mature cottonwoods failed for almost half the young trees (an error of omission). Overlap in height between young and mature cottonwoods may be a contributing factor in the confusion between young and mature cottonwoods. Another confounding factor is the absence of a significant difference in lidar mean intensity between young and mature trees (Farid et al., 2006). Leaves and branches of young and mature cottonwoods have almost the same color and brightness and have very similar surface reflectance in the near-infrared, giving rise to similar lidar intensity returns. All of the trees classified in the image as young cottonwoods corresponded to trees identified by fieldwork as young cottonwoods (no error of commission). We failed to achieve accurate separation of mature from old cottonwoods in the image for approximately one-third of the mature trees because of overlap between the crowns of mature and old cottonwoods. 73% of mature cottonwoods

identified as such by fieldwork were classified as mature in the image (producer's accuracy). Successful separation of old from young and mature cottonwoods was facilitated by the strong differences in crown shape. Old cottonwoods have conical and flat-topped crowns, whereas young cottonwoods have narrow and upright crowns. The crowns of these old cottonwoods are isolated from each other, and also there is a large difference between the elevations of each tree crown and the surrounding understory vegetation, allowing the maximum likelihood algorithm to classify them more accurately. One tree (of a total of nine field-identified old cottonwoods) was misclassified as a mature tree.

Of the non-cottonwood classes, saltcedar proved the most difficult to classify correctly. Only 55% of saltcedar in the field was classified as such in the image (producer's accuracy). The rest were classified as either mesquite (3 of 20 trees) or as open ground (6 of 20 trees). The confusion between saltcedar trees and open ground may result from saltcedar with sparse foliage, allowing penetration through the canopy to the ground by lidar pulses. It might also be expected that this could occur in the case of young cottonwood and mesquite. Overall, we did not find this to be a factor for cottonwoods.

A major factor in the classification of non-cottonwoods as cottonwoods, especially as mature cottonwoods, is the topography of the study area. Methods used in this study did not sufficiently remove all topographic effects. For example, the assignment of a road northwest of the stream channel to the mature cottonwood class was caused by elevation change between the stream channel and the area to the northwest. The riparian area is noticeably lower than the area of the main road, such that the canopy tops of the old

cottonwoods along the stream channel are at the same height as the main road surface (diagonal green line in the upper right corner). In future work, correction for topographic effects might be accomplished by including a digital elevation model based on ground returns as a third image band in the analysis.

B.5 Conclusions

This research employed a supervised classification technique, the maximum likelihood algorithm, for differentiating age classes of cottonwood trees in a riparian area using small-footprint airborne lidar data.

We performed a maximum likelihood classification of the 2-band lidar image (altitude and intensity images), resulting in seven land-cover classes: young, mature, and old cottonwoods, mesquite, saltcedar, dry stream channel, and open ground.

To validate the image classification, we performed an accuracy assessment, in which actual land-cover, as determined by field identification, was compared with classes for the corresponding areas assigned by the maximum likelihood classification. The overall classification accuracy was 78%; and the overall Kappa statistic value of classification was 0.73.

Accuracy assessment of the classified land-cover map illustrates that lidar data contains information of value for image analysis. Old and mature cottonwoods were well determined on the classified image. Young cottonwoods were, for the most part, correctly classified, although some image areas actually corresponding to mesquite or mature cottonwood were incorrectly identified as young cottonwoods.

Overall, classification results illustrate the potential of airborne lidar data to differentiate age classes of cottonwood trees for riparian areas quickly and quantitatively. Thus, identifying cottonwoods in the riparian forest and, more importantly, differentiating cottonwood age classes using lidar provides an important contribution to precision forest inventory and automated data processing for riparian forestry applications.

Future research should consider fusing high spatial resolution multi or hyperspectral data and lidar data to improve classification results for species identification in riparian areas.

B.6 References

Axelsson, P., 1999. Processing of laser scanner data-algorithms and applications. ISPRS Journal of Photogrammetry and Remote Sensing, 54, 138-147.

Congalton, R.G., Green, K., 1999. Assessing the Accuracy of Remotely Sensed Data: Principles and Practices. Lewis Publishers, 45-53.

Farid, A., Goodrich, D.C., Sorooshian, S., 2006. Using airborne lidar to discern age classes of cottonwood trees in a riparian area. Western Journal of Applied Forestry. In press.

Filin, S., 2004. Surface classification from airborne laser scanning data. Computers & Geosciences, 30, 1033-1041.

Jensen, J.R., 1996. Introductory Digital Image Processing: A Remote Sensing Perspective. Second Edition, Prentice Hall, Upper Saddle River, NJ. Pp. 229-231.

Kraus, K., Pfeifer, N., 1998. Determination of terrain models in wooded areas with airborne laser scanner data. ISPRS Journal of Photogrammetry and Remote Sensing, 53, 193-203.

Maas, H.G., 1999. The potential of height texture measures for the segmentation of airborne laser scanner data. Fourth International Airborne Remote Sensing Conference and Exhibition, Ontario, Canada.

Richards, J.A., 1999. Remote Sensing Digital Image Analysis. Springer Verlag, Berlin. 240 p.

Schaeffer, S.M., Williams, D.G., Goodrich, D.C., 2000. Transpiration of cottonwood/willow forest estimated from sap flux. Agric. For. Meteorol., 105, 257-270.

Song, J.H., Han, S.H., Yu, K.Y., Kim, Y.II, 2002. A study on using lidar intensity data for land cover classification. ISPRS Commission III Symposium, Graz, Austria.

Stromberg, J.C., 1998. Dynamics of Fremont cottonwood (*Populus fremontii*) and saltcedar (*Tamarix chinensis*) populations along the San Pedro River, Arizona. Journal of Arid Environments, 40, 133-155.

Vosselman, G., 2000. Slope based filtering of laser altimetry data. International Archives of Photogrammetry and Remote Sensing, XXXIII, Amsterdam, Netherlands.

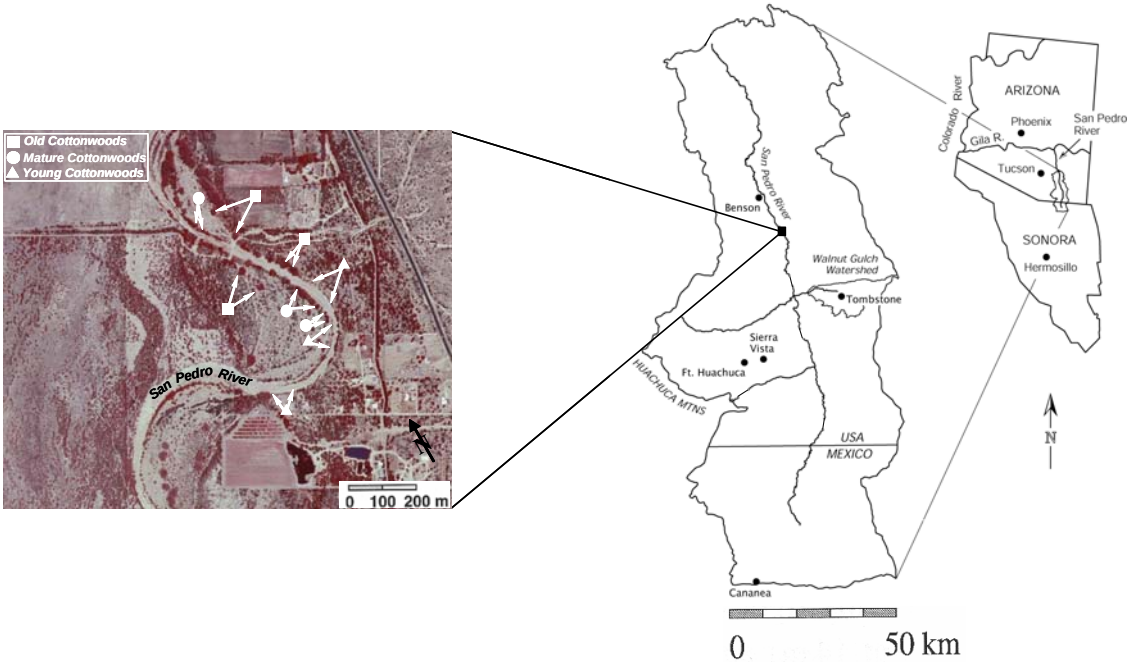

Figure B.1. Location map and color infrared aerial photograph of the Escalante study site in the San Pedro River Basin, Arizona.

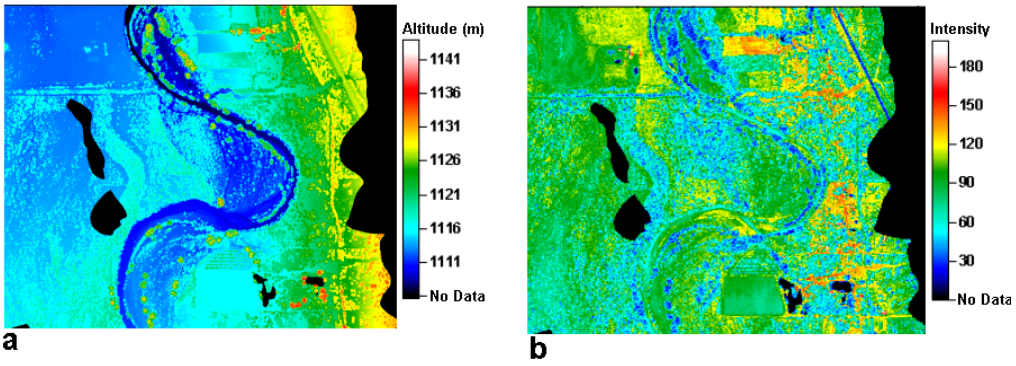

Figure B.2. Spatial patterns of (a) canopy altitude model and (b) near-infrared (1064 nm) intensity for the study site.

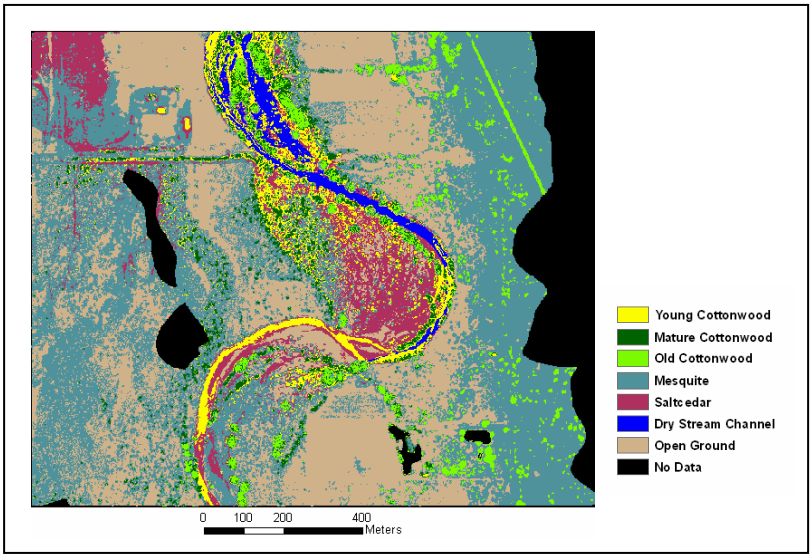

Figure B.3. Classified lidar image, showing three cottonwood age classes, mesquite, saltcedar, dry stream channel, and open ground.

Table B.1 Error matrix for maximum likelihood classification of the 2-band lidar image

	Reference Data							
Classified Data	Old cottonwood	Mature cottonwood	Young cottonwood	Mesquite	Saltcedar	Dry stream channel	Open ground	Row Total
Old cottonwood	8	11	2	0	0	0	0	21
Mature cottonwood	1	29	7	0	0	0	0	37
Young cottonwood	0	0	7	0	0	0	0	7
Mesquite	0	0	1	57	3	0	1	62
Saltcedar	0	0	0	1	11	0	2	14
Dry stream channel	0	0	0	0	0	16	1	17
Open ground	0	0	0	0	6	4	16	26
Column Total	9	40	17	58	20	20	20	184

Table B.2 Accuracy assessment result for maximum likelihood classification of the 2 band lidar image

Class Name	Reference Totals	Classified Totals	Number Correct	Producers Accuracy (%)	Users Accuracy (%)
Old cottonwood	9	21	8	89	38
Mature cottonwood	40	37	29	73	78
Young cottonwood	17	7	7	41	100
Mesquite	58	62	57	98	92
Saltcedar	20	14	11	55	79
Dry stream channel	20	17	16	80	94
Open ground	20	26	16	80	62
Total	184	184	144		
Overall classification accuracy = 78%					
Overall kappa statistic = 0.73					

B.7 Appendix I: Classification using an expert system approach

Lidar image interpretation produces a high-level description of a three-dimensional environment from which the lidar data were taken. Through interpretation, we try to understand the lidar image by identifying important features or objects and analyzing them in the context of the scene (Kopparapu and Desai, 2001). In this way, a human analyst moves easily from lidar data to information in decision processing. While working on an image, they may take into consideration other data, such as that from available thematic maps, personal field experience, and common sense. The objective of an image interpretation system is to make the computer do the same task. Many researchers have sought to develop automated systems which replicate the human process. One obvious approach to this effort is to generate a number of decision rules which mimic the human logical processes. A system of rules designed for a specific purpose is often called an expert system. The simplest and perhaps most common expert system is through the generation of a set of production rules. These rules are implemented as a succession of IF/THEN statements. In this section, we explore the use of an expert system for lidar data to differentiate age classes of cottonwood trees in the San Pedro River Basin.

B.7.1 Rule-based classification

In traditional methods of land cover classification, the primary determinants of classification detail can be achieved by the spectral and spatial resolution of the imagery. If additional data from different sources can be fused with a given combination of

spectral and spatial information, it might be possible to achieve either greater classification detail or greater classification accuracy (Lawrence and Wright, 2001) or to produce a higher level of data abstraction. This goal is important because it addresses the central task of moving from data to information.

In many cases, the use of ancillary data in addition to spectral data can lead to greater class distinctions (Strahler et al., 1978; Hutchinson, 1982; Trotter, 1991; Jensen, 1996). Combining different data types derived from lidar for cottonwood tree classification can increase its accuracy and precision.

We investigated the supervised classification technique in the previous chapter. In this section, we will use one decision-level data fusion method to differentiate age classes of cottonwood trees. There are several decision-level methods in which an expert system can be implemented for classification. The simplest way, and perhaps the most common, is through the generation of a set of production rules. These rules are implemented as a succession of IF/THEN statements. Figure B.7.1 shows the processing diagram that is applied for one decision-level rule-based classification for differentiating age classes of cottonwood trees from different data types derived from lidar measurements in this research.

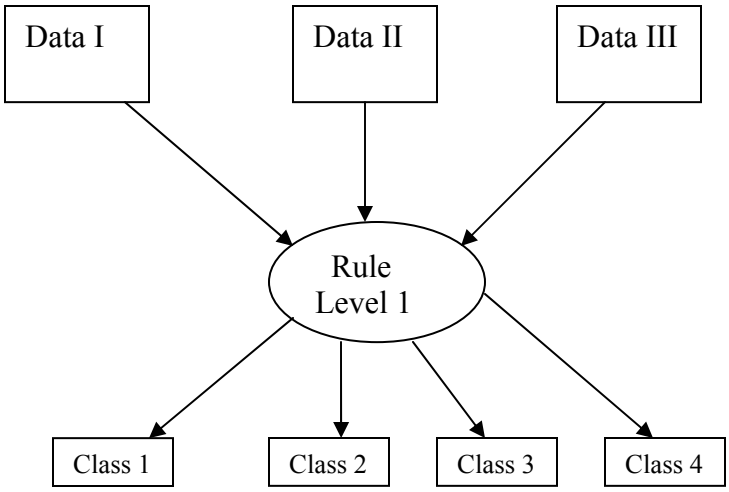

Figure B.7.1. The diagram of rule-based lidar data for differentiating age classes of cottonwoods.

B.7.2 Methods

The Optech ALTM 1233 (Optech Incorporated, Toronto, Canada) was used to survey the study site on June 6, 2003. Characteristics of the ALTM 1233 include a pulse rate of 33 kHz, a scanning frequency of 28 Hz, a scan angle of ± 20º, a collection mode of first and last returns, and intensity of returns from a 1064 nm laser. The ALTM 1233 was mounted on a University of Florida plane flying at 750 m above the ground at a velocity of 60 m/s. The aircraft and ALTM 1233 configuration resulted in a cross track point spacing of 0.9 m, a forward point spacing of 2.1 m, and a footprint size of approximately 15 cm. The density of lidar point measurements is approximately 2-4 points/m²; as a result, the entire study area was covered by 4 parallel flight lines. For the entire research area, 50% overlapping flight lines were used to ensure complete coverage, which generated approximately 2 million laser returns. The lidar data were processed and

classified using the Optech REALM 3.0.3d software. Two data layers were produced from the classification: last-return and vegetation first-return. The standard data format initially supplied comprised the first and last returns in separate ASCII files.

Ground validation data were collected from July to October 2003. Three different ages of cottonwood trees were included in the field sampling: young cottonwoods (less than 15 years), mature cottonwoods (16 to 50 years), and old cottonwoods (greater than 50 years). Stem diameters at breast height (dbh) (diameter measured at 1.37 m above the ground) were measured with a diameter tape and recorded to the nearest mm to discriminate between young, mature, and old cottonwood patches, based on river-specific equations that relate dbh to tree age (Stromberg, 1998). Dbh values varied, from less than 25 cm for young cottonwoods, 25 to 90 cm for mature cottonwood stands, and greater than 90 cm for old cottonwoods. Four differentially corrected GPS points were performed at the corners of a square centered on each cottonwood, from which we identified each cottonwood on the lidar image, then three sets of data estimated for each identified tree area from lidar measurement, which were used to made rule-based classification. The following data were used:

1) Tree height data; 2) Mean intensity value of return laser pulses from the canopy surface; and 3) Derived Leaf Area Index (LAI) from field-lidar measurements.

To derive any type of tree height data, a ground reference level must be established. The point data in ground-classified hits were kriged to produce a Digital Elevation Model (DEM) with a 0.5 m pixel grid. The point data in vegetation-classified hits were interpolated to a regular grid that corresponded to the DEM, thereby creating a canopy

altitude model. The canopy altitude model has a grid size of 0.5 m. Figure B.7.2 shows the terrain and overlaid canopy altitude model for the study site. The top of the tree was assumed to be the tallest point in the tree's canopy altitude model. The base of the tree was taken to be the point on the DEM beneath the top of the tree. Tree height was calculated by subtracting of the elevations of the bottom from the top of the tree.

In the rules of level-1 rule-based classification based on tree height, cottonwood trees having an elevation higher than 20 m in the height were classified as old cottonwoods, mature trees were classified in height value from 14 to 20 m, and young cottonwoods were below a height value 14 m.

The near infrared intensity image from airborne lidar was helpful for classifying cottonwoods. In the intensity distribution for each canopy surface the mean value of this distribution was calculated for each cottonwood tree. In the rules of level-1 classification, based on intensity, cottonwoods having less than intensity value 50 were classified as old trees, mature trees were classified in intensity value from 50 to 80, and for young cottonwood trees intensity value was selected from 80 to 100. These thresholds are based on Farid et al.'s experience (2006) suggested for height and intensity.

In addition, four metrics (canopy height, height of median energy, ground return ratio, and canopy return ratio) were derived by synthetically constructing a large footprint lidar waveform from the airborne small-footprint lidar data. These four metrics were incorporated into a stepwise regression procedure to predict field-derived LAI for different age classes of cottonwoods. These parameters will be explained in detail in the next chapter.

In the rules of level-1 rule-based classification based on LAI, cottonwoods having less than LAI value 2.1 were classified as old trees, mature trees were classified in LAI value from 2.1 to 2.7, and for young cottonwood trees the LAI value was selected from 2.7 to 3.3. LAI is related to the return intensity. At lidar wavelength, young cottonwoods exhibit a different reflectance than older ones because of their different LAI (Schaeffer et al., 2000). Also, we selected LAI thresholds for classification based on the differences between different age classes of cottonwoods for the growing season, which is shown in Figure B.7.3.

After combining these three data sets by using a rule-based classification algorithm, the level-1 classification rule created four classes: old, mature, and young cottonwood trees. The fourth class will be 'no defined objects', not belonging to any age class of cottonwood trees, i.e., possibly another form of vegetation. Table B.7-1 shows the rules for the level-1 classification.

Table B.7-1 Rules of Level-1 classification for cottonwood trees

IF ((TREE_HEIGHT > 20.0 M) AND (INTENSITY < 50.0) AND (LAI < 2.1))

THEN

LIDAR_CLASS = OLD COTTONWOODS

ELSE

IF ((14.0 M < TREE_HEIGHT < 20.0 M) AND (50.0 < INTENSITY < 80.0) AND (2.1 < LAI < 2.7))

THEN

LIDAR_CLASS = MATURE COTTONWOODS

ELSE

IF ((TREE_HEIGHT < 14.0 M) AND (80.0 < INTENSITY < 100.0) AND (2.7 < LAI < 3.3))

THEN

LIDAR_CLASS = YOUNG COTTONWOODS

ELSE

LIDAR_CLASS = NO DEFINED OBJECTS

ENDIF

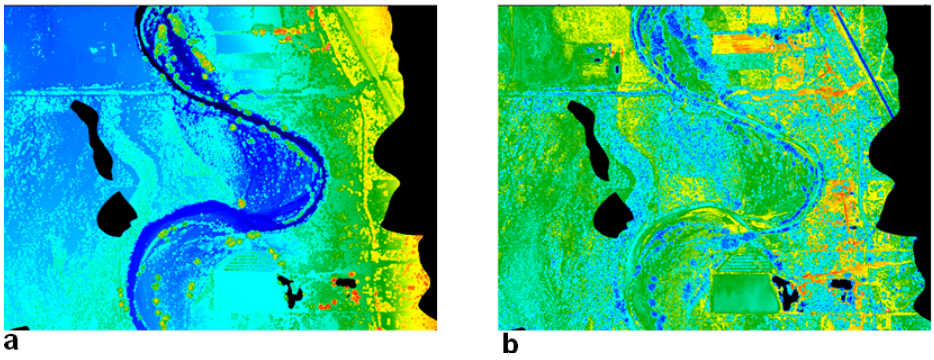

Figure B.7.2. Spatial patterns of (a) canopy altitude model and (b) near infrared intensity for the study site.

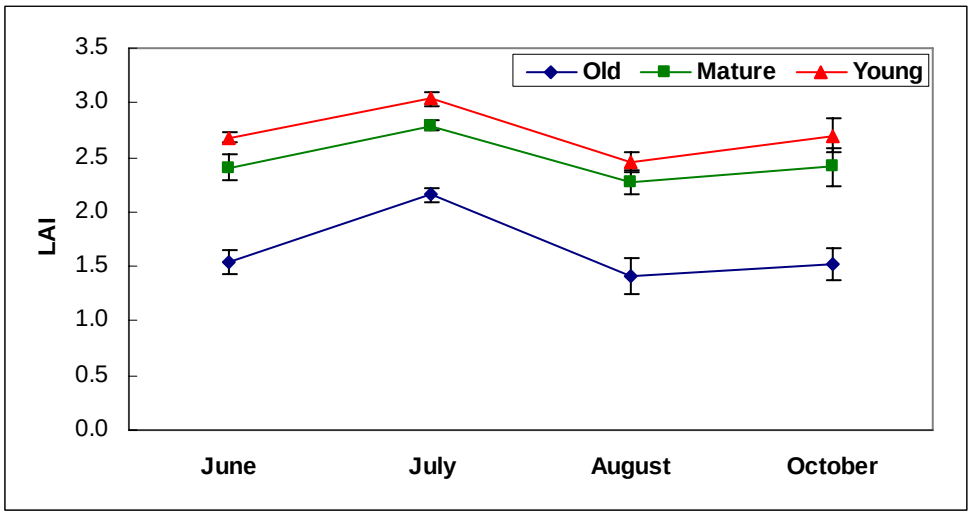

Figure B.7.3. Mean LAI (leaf area m^2 ground area m^{-2}) for different age classes of cottonwoods for the growing season at the Escalante site. Error bars represent the standard error of the mean (S.E.).

B.7.3 Results

The objective of this section was to determine the feasibility of identifying cottonwood age classes from rule-based classification. We generated three rules to produce level-1 classification for differentiating age classes of cottonwood trees from lidar data. Our initial classification included: young, mature, and old cottonwood classes, and no defined objects. Accuracy assessment indicated that 76% of lidar data were correctly classified. The classification resulted in a Cohen's kappa of 0.60. The error matrix used for accuracy assessment is given in Table B.7-2. Accuracy assessment results are presented in Table B.7-3. Although the overall classification accuracy was reasonably good, it can be seen from Table B.7-2 that discrimination of mature cottonwoods from old cottonwoods failed for almost one-third of the mature trees (an error of omission). Overlap in height between mature and old cottonwoods may be a contributing factor in the confusion between mature and old cottonwoods. 73% of mature cottonwoods identified as such by fieldwork were classified as mature in rule-based classification (producer's accuracy). Successful separation of old from young and mature cottonwoods was facilitated by the strong differences in lidar-derived LAI value, because old cottonwoods have conical and flat-topped crowns, whereas young cottonwoods have narrow and upright crowns. Another confounding factor is a significant difference in lidar mean intensity between young and old trees (Farid et al., 2006). We failed to achieve accurate separation of young from mature cottonwoods in classification for one-forth of the young trees because leaves and branches of young and mature cottonwoods have

almost the same color and brightness and have similar surface reflectance in the near-infrared, giving rise to similar lidar intensity returns.

Table B.7-2 Confusion matrix of rule-based classification

	Reference Data			
Classified Data	Old cottonwood	Mature cottonwood	Young cottonwood	Row Total
Old cottonwood	9	11	0	20
Mature cottonwood	0	29	5	34
Young cottonwood	0	0	12	12
Column Total	9	40	17	66

Table B.7-3 Accuracy assessment result for Rule-based classification

Class Name	Reference Totals	Classified Totals	Number Correct	Producers Accuracy (%)	Users Accuracy (%)
Old cottonwood	9	20	9	100	45
Mature cottonwood	40	34	29	73	85
Young cottonwood	17	12	12	71	100
Total	66	66	50		
Overall classification accuracy = 76%					
Overall kappa statistic = 0.60					

B.7.4 Discussion

Many classification methods are available for image processing in a remote sensing area, and no single classification solution always performs best. In this section, we applied the expert system—production rule—to classify age classes of cottonwood trees using three different lidar data types.

Production rules are easy to make and apply, but the key problem in the application of this approach to classification of different age classes of cottonwoods is how to make reasonable rules. Since this technique totally depends on the rules that can be created by users or operators, the initial data set should be carefully analyzed to find applicable rules. It may take another step to understand the data set to be used, and to analyze the geometric characteristics of the study area. Every rule is suitable for specific data sets and study areas.

B.7.5 References

Farid, A., Goodrich, D.C., Sorooshian, S., 2006. Using airborne lidar to discern age classes of cottonwood trees in a riparian area. Western Journal of Applied Forestry. In press.

Hutchinson, C.F., 1982, "Techniques for combining Landsat and ancillary data for digital classification improvement," *Photogrammetric Engineering & Remote Sensing,* Vol. 48, pp. 123-130.

Jensen, J.R., 1996, *Introductory Digital Image Processing: A Remote Sensing Perspective,* Second Edition, Prentice Hall, Upper Saddle River, New Jersey, p. 316.

Kopparapu, S.K., and U.B. Desai, 2001, *Bayesian Approach to Image Interpretation*, Kluwer Academic Publishers, Boston, U.S.A.

Lawrence, R.L. and A. Wright, 2001, "Rule-Based Classification System Using Classification and Regression Tree (CART) Analysis," *Photogrammetric Engineering & Remote Sensing*, Vol. 67, No. 10, pp. 1137-1142.

Schaeffer, S.M., Williams, D.G., Goodrich, D.C., 2000. Transpiration of cottonwood/willow forest estimated from sap flux. *Agric. For. Meteorol.*, 105, 257-270.

Strahler, A.H., T.L. Logan, and N.A. Bryant, 1978, "Improving forest cover classification accuracy from Landsat by incorporating topographic information," *Proceedings of 12th International Symposium on Remote Sensing of Environment*, 20-26 April, Manila, Philippines, pp. 927-942.

Stromberg, J.C., 1998. Dynamics of Fremont cottonwood (*Populus fremontii*) and saltcedar (*Tamarix chinensis*) populations along the San Pedro River, Arizona. *Journal of Arid Environments*, 40, 133-155.

Trotter, C.M., 1991, "Remotely-sensed data as an information source for geographical information system in natural resource management: A review," *International Journal of Geographic Information System*, 5:225-239.

APPENDIX C: Using airborne lidar to predict leaf area index in cottonwood trees and refine riparian water use estimates

A. Farid [a,*], D.C. Goodrich [b], R. Bryant [b], S. Sorooshian [c]

[a] Department of Hydrology and Water Resources, University of Arizona, Tucson, AZ 85721, USA

[b] USDA-ARS-SWRC, Southwest Watershed Research Center, Tucson, AZ, USA

[c] Department of Civil and Environmental Engineering, University of California, Irvine, CA, USA

Abstract

Quantification of riparian forest structure is important for developing a better understanding of how riparian forest ecosystems function. Additionally, estimation of riparian forest structural attributes, such as the Leaf Area Index (LAI), is an important step in identifying the amount of water use in riparian forest areas. In this study, small-footprint lidar data were used to estimate biophysical properties of young, mature, and old cottonwood trees in the Upper San Pedro River Basin, Arizona, USA. The lidar data were acquired in June 2003, during flyovers conducted at an altitude of 750 m. Canopy height, maximum laser height, and mean laser height were derived for the cottonwood trees from the data. Linear regression models were used to develop equations relating lidar height metrics with corresponding field-measured LAI for each age class of cottonwoods. The lidar height metrics are well correlated with field-measured LAI. In

addition, four metrics (tree height, height of median energy, ground return ratio, and canopy return ratio) were derived by synthetically constructing a large footprint lidar waveform from small-footprint lidar data which were compared it to ground-based high-resolution Intelligent Laser Ranging and Imaging System (ILRIS) scanner images. These four metrics were incorporated into a stepwise regression procedure to predict field-derived LAI for different age classes of cottonwoods. Metrics derived from the airborne lidar synthetic waveform are capable of estimating LAI, though in all cases logarithmic transformation of the dependent variable was necessary. Furthermore, this research applied the Penman-Monteith model to estimate transpiration of the cottonwood clusters using lidar-derived canopy metrics. These transpiration estimates compared very well to ground-based sap flux transpiration estimates indicating lidar-derived LAI can be used to improve riparian cottonwood water use estimates.

Keywords: Lidar; Leaf Area Index; Cottonwood; Riparian; San Pedro River Basin

* Corresponding author. Tel.: +1-520-891-0735; fax: +1-520-626-4479.
E-mail address: farid@hwr.arizona.edu (A. Farid).

C.1 Introduction

Vegetation patterns and associated canopy structure influence landscape functions such as water use, biomass production, and energy cycles. The properties of vegetation and canopy must be quantified in order to understand their roles in landscapes and before management plans can be developed for the purpose of conserving natural resources.

Vegetation patterns can be mapped from ground-based inventory techniques, or by using aerial photography or satellite imagery. If sampling is sufficiently dense, ground-based techniques alone can produce accurate results. However, determining the physical properties of canopy architecture and structure (i.e. height, leaf area index, timber volume) with conventional ground-based technology is difficult, labor intensive, costly, and usually very limited for assessing landscape scale characteristics. Resource managers are always interested in developing and utilizing alternative sources of information that are more cost effective or offer opportunities to manage resources more efficiently.

Recent progress in three-dimensional forest characterization at the stand level mainly includes digital stereophotogrammetry, synthetic aperture radar, and lidar (**li**ght **d**etecting **a**nd **r**anging). Lidar is a technique in which light at high frequencies, typically in the infrared wavelengths, is used to measure the range between a sensor and a target, based on the round trip travel time between source and target. Airborne Laser Scanning (ALS) is a measurement system in which pulses of light (most commonly produced by a laser) are emitted from an instrument mounted in an aircraft and directed to the ground in a scanning pattern. This method of recording the travel time of the returning pulse is referred to as pulse ranging (Wehr and Lohr, 1999). The type of information collected

from this returning pulse distinguishes two broad categories of lidar sensors: discrete-return (small footprint) lidar devices and full-waveform (large footprint) recording devices. Discrete-return systems typically allow for one (e.g., first or last), two (e.g., first and last), or a few (e.g., five) returns to be recorded for each pulse during flight. Conversely, a full-waveform lidar system senses and records the amount of energy returned to the sensor for a series of equal time intervals. The number of recording intervals determines the level of detail present in a laser footprint. For forested environments, the result is a waveform indicative of the forest structure (i.e., from the top of the canopy, through the crown volume and understory layer, and finally to the ground surface). The footprint for most discrete-return systems is on the order of 0.2 to 0.9 m. For full-waveform systems, the footprint size may vary from 8 m to 70 m (Means et al., 1999).

Theoretical studies model full-waveform characteristics for simple, unvegetated terrain (Gardner, 1992), and for one-dimensional surfaces (Abshire et al., 1994). Additionally, Blair and Hofton (1999) demonstrated that vertical distribution of the discrete-return data is closely related to the full-waveforms recorded by waveform-recording devices when certain conditions are met. The most important being a high density of samples collected using a very small footprint (on the order of 25 cm).

The foundations of lidar forestry measurements lie with photogrammetric techniques developed to assess tree height, canopy density, forest volume, and biomass. Airborne laser measurements were used in place of photogrammetric measurements to estimate forest heights and canopy density (Nelson et al., 1984) and forest volume or biomass

(Maclean and Krabill, 1986; Nelson et al., 1988a; 1988b). For instance, Nelson et al. (1988b) predicted the volume and biomass of southern pine (*Pinus taeda, P. elliotti, P. echinata, and P. palustris)* forests using several estimates of canopy height and cover from small-footprint lidar, explaining between 53% and 65% of the variance in field measurements of these variables.

Research efforts have investigated the estimation of forest stand characteristics with scanning lasers with either a relatively large laser footprint (Harding et al., 1994; Weishampel et al., 1997; Blair et al., 1999; Lefsky et al., 1999; Means et al., 1999; Drake et al., 2002) or a small footprint, but with only one laser return (Ritchie et al., 1993; Naesset, 1997a; 1997b; Magnussen and Boudewyn, 1998; Magnussen et al., 1999). For instance, Ritchie et al. (1993) used discrete-return lidar to study natural pine stands in Mississippi; Lefsky et al. (1999) used data from full-waveform lidar to derive canopy height and Leaf Area Index (LAI) in Douglas fir/western hemlock forests; Drake et al. (2002) estimated tropical forest structural attributes, such as aboveground biomass, using a full-waveform lidar recording device. Small-footprint lidars are available commercially and research results on their potential for forestry applications are very promising. Despite these research efforts, practical applications of small-footprint lidar have not progressed as rapidly, primarily because of the current cost of lidar data. The height of a forest stand is a crucial forest inventory attribute for calculating timber volume, site potential, and LAI. Lim et al. (2003) derived various laser height metrics from small footprint lidar data and determined how well they estimated various forest biophysical properties such as LAI for tolerant hardwood forests in Canada.

The primary purpose of this research was to use a small-footprint lidar to derive various height metrics (maximum laser height, mean laser height, and canopy height) and model full-waveform characteristics in cottonwood trees in the San Pedro Riparian National Conservation Area (SPRNCA) in southeastern Arizona, USA. The SPRNCA is a globally important migratory bird route. Its cottonwood riparian forest supports a great diversity of species and is widely recognized as a regionally and globally important ecosystem (World Rivers Review, 1997). Additionally, lidar studies published at this point have shown success in several forest types with large-footprint lidar, but applications of small-footprint lidar to forestry have not progressed as far (Means, 2000), being limited mainly to measuring even-aged coniferous stands. Thus, the performance of lidar in cottonwood riparian forests remains untested and any related analytical and processing issues are yet to be identified.

The main objective of this study was to estimate LAI from various laser height metrics and synthetic large footprint lidar waveform for different age classes of cottonwood trees. Additionally, this study applied the Penman-Monteith model (Monteith and Unsworth, 1990) to estimate cottonwood transpiration using lidar-derived LAI, compared with transpiration measured by sap flow. Riparian cottonwood trees use water in proportion to their age and canopy shape (Schaeffer et al., 2000), and are especially large users of water in flood plains along rivers in semi-arid environments. More accurate quantification of riparian water use is required to manage basin water resources to maintain the economic, social, and ecological viability of these areas and ensure water for a growing human population in the basin. Cottonwoods of different age cannot be

distinguished by multi-spectral methods. However, the older cottonwoods exhibit a canopy that is more crowned in shape than the younger trees, thus differences in tree shape as a function of tree age led us to investigate the use of lidar to identify cottonwoods of different age classes and estimate LAI, which these parameters directly impact water use. The specific objectives of this study were:

(1) Model a laser altimeter return waveform as the sum of reflections within a laser small footprint and compare the results with ground-based Intelligent Laser Ranging and Imaging System (ILRIS) scanner images in cottonwood trees.

(2) Derive various laser height metrics (maximum laser height, mean laser height, and canopy height) from the small footprint lidar data and determine how well they can estimate LAI for different age classes of cottonwoods.

(3) Derive four metrics (canopy height, height of median energy, ground return ratio, and canopy return ratio) from synthetic lidar full-waveform. These four metrics are incorporated into a stepwise regression procedure to predict field-derived LAI for different age classes of cottonwood trees.

(4) Apply the Penman-Monteith model to estimate transpiration of the cottonwood clusters using lidar-derived LAI and compare the results with transpiration measured by sap flow techniques.

C.2 Study sites

The study sites are located on the floodplain of the San Pedro River within the SPRNCA in southeastern Arizona, USA. The Escalante study site (31º 51´N, 110º 13´W;

1110m elevation) is about 1.2 km long north to south and 1.4 km wide east to west and is relatively flat. The overstory is dominated by riparian forest vegetation, consisting of cottonwood (*Populus fremontii*) and mesquite (*Prosopis velutina*) as dominant and sub-dominant overstory species, respectively. This study area is populated by young-to-old dense cottonwood stands with patches of cottonwood riparian forest located along the stream channel. The understory consists mainly of a perennial bunchgrass (*Sporobolus wrightii*), creosote (*Larrea tridentata*), and saltcedar (*Tamarix chinensis*).

Additionally, a cluster of cottonwood trees was selected at two additional sites with contrasting groundwater depth levels. The Boquillas study site (31º 69´N, 110º 18´W; 1180m elevation) is located along an intermittent reach of the river where the groundwater depth ranged from 3.1 to 3.9 m. In contrast, the Lewis Springs study site (31º 33´N, 110º 07´W; 1250m elevation) is located along a perennially flowing reach of the San Pedro River where the groundwater depth ranged from 1.1 to 1.8 m. The cottonwood trees in the sap flow clusters at both intermittent and perennial stream sites were very similar in age and size characteristics.

C.3 Data acquisition

C.3.1 Ground inventory data

Ground validation data were collected from April 2003 to October 2004. Three different ages of cottonwood trees were included in the field sampling – young cottonwoods (less than 15 years), mature cottonwoods (16 to 50 years), and old cottonwoods (greater than 50 years) (Fig. C.1). Stem diameters at breast height (dbh)

(diameter measured at 1.37 m above the ground) were measured with a diameter tape and recorded to the nearest mm to discriminate between young, mature, and old cottonwood patches, based on river-specific equations that relate dbh to tree age (Stromberg, 1998). Dbh values varied, from less than 25 cm for young cottonwoods, 25 to 90 cm for mature cottonwood stands, and greater than 90 cm for old cottonwoods.

A total of 41 cottonwood trees were used to determine LAI. Of the 41 cottonwoods, 9 old, 15 mature, and 17 young isolated trees were selected that were at least 6 m apart. A differential global positioning system (DGPS) was used to determine the location of each individual tree within sub-meter planimetric accuracy (Trimble 5700 GPS). We measured 4 points around each tree at the edge of the tree canopy. In addition, all tree locations were determined using 60-second static measurements with a 12-channel GPS receiver. The GPS antenna height varied between 1.8 m and 3.6 m, with an average height of 2.5 m. All measurements were collected during the leaf-off season. The lack of canopy foliage and the raised antenna in the old cottonwood stands reduced the error effects of forest canopies on GPS measurements. These trees were identified in the lidar dataset by matching field DGPS locations with the georeferenced lidar data.

The LAI was measured using a plant canopy analyzer (LAI 2000, LiCor, Lincoln, NE) in June 2003 for different age classes of cottonwoods. LAI readings were taken from the four cardinal directions around the base of each cottonwood tree by one sensor with a 90º view cap. The sensor was aligned along the canopy of the tree, as well as across the canopy. Measurements were made near sunset.

In 2006, Gazal et al. measured sap flow of four cottonwood trees within a cluster at each of the two study sites (Boquillas and Lewis Springs), using constant heat flow Granier-type probes (TDP-30 and TDP-80, Dynamax Inc., Houston, Texas). The system measures the temperature difference between two probes inserted radially in the xylem, one constantly heated and the other unheated. Sap flow was measured continuously from April 5 to November 9, 2003 using a datalogger (CR10x datalogger, Campbell Scientific Inc., Logan, Utah). Cottonwood cluster transpiration was calculated based on individual tree sap flow, total sapwood area and crown area of the cluster (Wullschleger, 1998). Additionally, air temperature, relative humidity, solar radiation, wind speed and air pressure were measured at nearby meteorological towers located 3 km from the Boquillas intermittent stream site and 0.3 km from the Lewis Springs perennial stream site (Scott et al., 2000). For both perennial and intermittent stream sites, the measurements were recorded every 15 and 30 min, respectively. Stand transpiration was estimated for the period 1-11 June 2003 (DOY: 152-162), which is corresponded to lidar surveyed time.

C.3.2 Lidar datasets

The Optech ALTM 1233 (Optech Incorporated, Toronto, Ont.) was used to survey the study site on June 6, 2003. Characteristics of the ALTM 1233 include a scanning frequency of 28 Hz, a scan angle of ± 20º, a collection mode of first and last returns, and intensity of returns from a 1064 nm laser. The ALTM 1233 was mounted on a University of Florida plane flying at 750 m above the ground at a velocity of 60 m/s. The aircraft and ALTM 1233 configuration resulted in a cross track point spacing of 0.9 m, a forward

point spacing of 2.1 m, and a footprint size of approximately 15 cm in diameter. The average ground swath width was 546 m and the entire study area was covered by 4 parallel flight lines. For the entire research area, 50% overlapping flight lines were used to ensure complete coverage, which generated approximately 2 million laser returns. The lidar data were processed and classified using the Optech REALM 3.0.3d software. Three data layers were produced from the classification: (1) ground last-return, (2) vegetation last-return and (3) vegetation first-return. The ground last return data layer was a robust representation of the terrain. For this study, vegetation last and vegetation first data layers were merged into a single vegetation class. The attributes of any given laser return not only include x, y, and z coordinate data but also an intensity return value (Farid et al., 2006).

C.3.2.1 Ground based laser scanner

The ground based laser scanner acquired for the study site on June 2004, was the Intelligent Laser Ranging and Imaging System-Three-Dimensional (ILRIS-3D) manufactured by Optech (Optech Incorporated, Toronto, Ont.), with a vertical accuracy of 0.3 cm. The laser scanner fires a focused laser at ground targets and measures the target position based on laser travel time to the target and back to the sensor. The hit size is 1.5 cm in diameter at 50 meters from the scanner, which is the approximate distance used in this study (the laser beam width changes slightly with distance). The laser scanner collects x, y, and z relative coordinates for every 1.5 cm hit scanned for a complete three

dimensional image of the object. Distance between hits (resolution) was on average 0.2 cm. The resolution changes with distance between the target and the scanner.

Capturing an entire cottonwood tree canopy required two scans on opposite sides the tree. If three sub-meter accuracy GPS points can be located within each scanned image, the images can easily be merged. We placed three large cardboard boxes in the foreground of each cottonwood tree that was to be scanned and then secured a piece of rebar into the ground at the corner of each box. Fig. C.2 shows the boxes in the foreground of one old cottonwood tree as an example (two scans on opposite sides the tree). These points on the ground were then georeferenced with a differential global positioning system (DGPS) at a later date. The corners of the boxes where the rebar was located allowed us to locate the georeferenced points in the scanned image. Then the x, y, and z coordinates of the images were given UTM values and sea level altitude values in meters. Unfortunately, due to our remote location which is covered by dense vegetation and the stream channel bank, only one scanned tree had georeferenced points with enough accuracy for the images to be merged accurately into a full canopy. The other trees had to be manually merged. Manually merging is a tedious process and only works if at least three common points can be located in each image that is to be merged. This limitation reduced the number of trees with fully scanned canopies to five. Therefore, of the 24 old and mature cottonwoods, 3 old and 2 mature cottonwood trees were selected. No young trees were selected because their locations were neighbored by dense vegetation, such as mesquite and saltcedar; additionally the river bank obstructed the laser scanning beams.

C.4 Analysis

This analysis will include a combination of both ground-based and airborne lidar data from 2003 and 2004.

C.4.1 Modeling a return waveform and comparing with ground based laser scanner

Our model for a medium-large footprint laser altimeter return waveform is formulated under the assumption that the shape of any waveform represents the vertical distribution of intercepted surfaces within an individual footprint. The waveform beams bounce off layers of foliage and the ground, usually generating 25 m diameter footprints. We chose the average crown width of an old cottonwood tree for a synthetic waveform footprint as a starting point. The modeled large-footprint return waveform is composed of the sum of the small-footprint pulses reflected from different elements in the footprint. Each reflection has the spatial intensity characteristic that its intensity is normally-distributed over a finite vertical and horizontal distance. The sum of the small-footprint reflections is convolved with a Gaussian approximation to generate the synthetic waveform. Therefore, we sum up a series of Gaussian pulses that vertically stacked the elevations produced by the small-footprint elevation data to create a modeled large-footprint return waveform. Fig. C.3a contains the three-dimensional distribution of small-footprint lidar data from within a 26 m footprint centered on a tree approximately 30 m tall. Fig. C.3b illustrates the distribution of these points as a function of height. Blair and Hofton (1999) demonstrated that vertical distribution of the small-footprint lidar data is closely related to the full-waveforms recorded by waveform-recording devices in tropical forests in Costa Rica. However, modeling of large-footprint return waveform in cottonwood

riparian forests remains untested and any related analytical and processing issues are yet to be identified. Also, in this study, the similarity between each modeled waveform and the return waveform from the ILRIS scanner was assessed using Pearson correlation, ρ, given by $\rho = S_{xy} / \sqrt{S_{xx} S_{yy}}$, where S_{xx} , S_{yy} and S_{xy} are the variances and shared variance of the ILRIS and synthetic waveforms. The comparison between modeled waveform and the return waveform from the ILRIS scanner proved that small-footprint airborne lidar data is able to model large-footprint return waveform in cottonwood trees quickly and quantitatively. Furthermore, LAI will be derived from the modeled large-footprint return waveforms for different age classes of cottonwood trees in a riparian corridor. The waveform comparison utilized 2004 airborne lidar and 2004 ground-based ILRIS data.

Figure C.4 plots five synthetic waveforms and corresponding ILRIS return waveforms. The results of comparison of the modeled waveform and the return waveform from ILRIS for old cottonwood trees are presented in Fig. C.4a-c. In this case, the highest ρ was 0.73 between the modeled and ILRIS waveforms. Fig. C.4d-e contains the waveforms comparing modeled and ILRIS for mature cottonwoods. The highest ρ value increased from 0.73 to 0.75 when mature cottonwoods were considered. Simple, single modal waveforms are typically returned from flat, unvegetated ground surfaces (Figs. C.4a and C.4e). The modeled and ILRIS waveforms from vegetated regions were multi-modal, each mode representing a vertically-distinct, consolidated layer within the canopy. Overall, the ground and airborne-based waveforms had a good degree of correlation. Although the modeled and ILRIS waveforms identify reflecting layers at the same elevations, the relative strengths of reflections from those layers varied; for instance, the

modeled and ILRIS waveforms both detected a reflecting surface at ~18 m elevation, but the reflection was much stronger when measured by ILRIS, possibly a result of different tree cover conditions at the time of the airborne and ILRIS surveys. The systematic difference noted between modeled and ILRIS waveforms was the consistently-higher amplitude of the canopy response in the ILRIS return waveform (e.g. Fig. C.4a). This difference is due to the first-return only nature of the ILRIS system, and a different view angle configuration between the airborne and ILRIS sensors. Also, a large gap through the canopy along the beam path may result in reduction of the amplitude of the canopy response in the modeled return waveform using the airborne system. Furthermore, the ILRIS system presents difficulties in detecting the uppermost portion of old cottonwood tree canopies because of the conical and flat-topped nature of the tree crown. However, the top portion of the crown may not be of sufficient area to register as a significant reflecting surface and therefore may not be detected well. Finally, the majority of modeled and ILRIS wave shapes have similar vertical structure in cottonwood trees.

C.4.2 Estimation of LAI from lidar data

C.4.2.1 The relationship between LAI and various laser height metrics

For each cottonwood tree, three laser height metrics were derived by all small-footprint lidar returns from the cottonwood canopy surface: (1) canopy height (h_{canopy}), (2) maximum laser height (Lz_{max}), and (3) mean laser height (Lz_{mean}). To derive any type of tree height measurement, a ground reference level must be established. The point data in ground-classified hits were kriged to produce a Digital Elevation Model (DEM) with a

0.5 m pixel grid. The point data in vegetation-classified hits were interpolated to a regular grid that corresponded to the DEM, thereby creating a canopy altitude model. The canopy altitude model has a grid size of 0.5 m. Fig. C.5 shows the terrain and overlaid canopy altitude model for the study site. The local maximum technique was used to discriminate cottonwoods in the canopy altitude model (Farid et al., 2006). It operates with two shapes of the search window, specifically a square $n \times n$ window and a circular window that is more appropriate for identifying tree crowns. Variable window sizes were used by Wulder et al. (2000) for the extraction of tree locations and estimation of basal area from high spatial resolution imagery for stands of Douglas fir and western red cedar. The top of the tree was assumed to be the tallest point in the tree's canopy altitude model. The base of the tree was taken to be the point on the DEM beneath the top of the tree. Canopy height (h_{canopy}) was calculated by subtracting of the elevations of the bottom from the top of the tree.

Additionally, the derivation of two other laser height metrics is straightforward. The derivations of these two laser height metrics were formulated as Equations C-1 and C-2.

Maximum laser height (m) $$Lz_{max} = \max(\text{all\_}z_{hits}\text{\_tree}) \quad \text{(C-1)}$$

Mean laser height (m) $$Lz_{mean} = \frac{\sum_{i=1}^{n} tree\_z_{hit(i)}}{n} \quad \text{(C-2)}$$

Fig. C.6a-c contains the scatterplots comparing field-measured LAI and lidar-derived canopy height for each type of cottonwood tree. In this case, the coefficient of determination for field LAI versus lidar canopy heights were 0.77, 0.75, and 0.63 for young, mature, and old, respectively. As noted above, the lidar system presents

difficulties in detecting the uppermost portion of old cottonwood tree canopies because of the conical nature of the tree crown and the small area of the top portion of the crown. In addition, determining the exact elevation of the ground surface poses difficulties for both old and mature cottonwoods because the understory is dense enough to substantially occlude the ground surface. The r^2 increased from 0.63 to 0.77 when young cottonwoods were considered. The actual ground terrain detected by lidar for young trees is more accurate and precise than those estimates for old and mature trees because the area beneath the young trees is predominantly bare soil. The scatterplots comparing field-measured LAI and maximum laser height for each age class of cottonwood trees are presented in Fig. C.6d-f. The coefficient of determination for field LAI versus maximum laser heights were 0.74, 0.73, and 0.67 for young, mature, and old, respectively. The lowest r^2 value was obtained for old cottonwoods for the reasons stated above.

The scatterplots comparing field-measured LAI and mean laser height for each age class of cottonwoods are shown in Fig. C.6g-i. Results from regressing LAI and mean laser height on all age classes of cottonwoods did not produce r^2 values greater than 0.80. Lz_{mean} is affected by canopy cover as demonstrated when Lz_{mean} was used to estimate LAI, where the mean laser height of an old cottonwood with high canopy cover was found to be dominated by the high number of laser returns from the canopy surface. The lowest r^2 value was obtained for young cottonwoods due to the presence of the gaps in young canopies which permitted a number of the laser pulses to penetrate the canopy, generating lower values for canopy cover. As a result the Lz_{mean} value is problematic in a regression model.

C.4.2.2 Estimation of LAI from synthetic lidar full-waveforms

Four metrics were derived by synthetically constructing a large footprint lidar waveform (see Fig. C.7) from the airborne small-footprint lidar data for different age classes of cottonwoods. Lidar canopy height (LHT) was calculated by identifying: (1) the location within the waveform when the first Gaussian pulse increases above a median energy level/threshold (the canopy top), and (2) the center of the last Gaussian pulse (the ground return), and then calculating the distance between these locations. Second, the height of median energy (HOME) was calculated by finding the median of the entire waveform. The location of the median energy is then referenced to the center of the last Gaussian pulse to derive a height. The HOME metric is, therefore, predicted to be sensitive to changes in both the vertical arrangement of canopy elements and the degree of canopy openness (Drake et al., 2002). Third, a simple ground return ratio (GRND) was calculated by taking the number of hits in the last Gaussian peak divided by the sum of all other numbers of hits (total hits minus last Gaussian peak hits) (see Fig. C.7). Thus, GRND provides an approximation of the degree of canopy closure (Drake et al., 2002; Means et al., 1999). Finally, the canopy return ratio (CRND) was calculated by taking the number of hits in the location within the waveform when the first Gaussian pulse increases above a median energy level/threshold (the canopy top), divided by the sum of all other numbers of hits. CRND provides an approximation of the degree of canopy cover.

These four metrics were incorporated into a stepwise regression procedure to predict field-derived LAI for different age classes of cottonwoods. During this process,

transformations of dependent and independent variables (including square, square root, and logarithmic) were also explored (Table C.1). Metrics from the lidar waveform are able to estimate LAI for different age classes of cottonwood trees, though in all cases logarithmic transformation of the dependent variable was necessary. In this case, the coefficient of determination for field LAI versus lidar metrics were 0.76, 0.78, and 0.84 for young, mature, and old, respectively. Meanwhile, the RMSE for all age classes is low. The weaker relationship between field LAI and lidar metrics in young trees could be affected by two factors. First, the level of variability in old tree structure at the scale of a waveform is higher than for a young one. A second contributing factor is the presence of gaps in young canopies, which allowed a number of the laser pulses to penetrate the canopy, generating lower values for CRND.

Also, in areas with densely packed canopy materials such as old canopies, fewer lidar pulses will reach the ground, thereby increasing HOME. Conversely, in more open or disturbed areas (e.g., a young tree canopy), more lidar pulses will reach the ground, reducing HOME. Additionally, the height metrics (e.g., LHT and HOME) are the most sensitive, and increase with increasing cottonwood tree age and basal area. The LHT is perhaps the metric with the strongest potential for estimating riparian forest structural characteristics. The LHT metric is influenced by the highest detectable canopy surface within a footprint.

Furthermore, the slightly weaker relationship between LAI and lidar metrics among young, mature, and old-growth stands is caused by the lack of significant differences in LAI between different age classes of cottonwoods that have been measured in the field.

Overall, the ability of a synthetic large footprint lidar to accurately predict LAI for different age classes of cottonwoods is very good.

C.4.3 Estimation of cottonwood transpiration from lidar data

In this section, we present the lidar-predicted versus sap flow measured cottonwood transpirations at two contrasting riparian sites in order to more accurately estimate cottonwood water use. Along the San Pedro River, Gazal et al. (2006) quantified cottonwood transpiration using sap flow measurements for a cluster of trees located on a perennial section of the river and another located along a reach with intermittent stream flow. Hydrologically, these sites differed in the depth and seasonal fluctuation of the water table. For trees instrumented with sap flow probes, sap flow rate per tree (J_s) was scaled based on the sapwood area that covers the position of the two thermocouples per probe (Gazal et al., 2006). J_s from the north and south side of each thermocouple position was averaged and multiplied by the sapwood area corresponding to the depth of the thermocouple in the sapwood (j_s). j_s from the two thermocouple positions was then added and the sum was divided by the total sapwood area of the tree ($\overline{J}_s$). $\overline{J}_s$ from the instrumented trees in the cluster was averaged and multiplied by the total sapwood area of the entire cluster to get the total water use of the stand (Gazal et al., 2006). Total water use of the entire cottonwood cluster was divided by projected canopy area (m^2) to determine ground-area based transpiration, E (mm/day). The projected canopy area of the clusters was estimated digitally using lidar canopy altitude model images.

The Penman-Monteith (P-M) model (Monteith and Unsworth, 1990) was selected to estimate cottonwood transpiration using lidar-derived LAI for June 1 through June 11, 2003 (DOY: 152-162). This model allows the calculation of evaporation from meteorological variables and resistances which are related to the stomatal and aerodynamic characteristics of the tree, and has the form

$$E = \frac{1}{\lambda}\left[\frac{\Delta A + \rho_a c_p D / r_a}{\Delta + \gamma(1 + r_c / r_a)}\right] \qquad \text{(mm/day)} \qquad \text{(C-3)}$$

where Δ is the slope of the saturation vapor pressure/temperature curve (kPa^{o}C^{-1}), ρ_a the density of moist air (kg m^{-3}), c_p = 1.013 (kJkg^{-1}^{o}C^{-1}) the specific heat capacity of dry air under constant pressure, D the vapor pressure deficit (kPa), γ the psychrometric constant (kPa^{o}C^{-1}), r_c the bulk canopy resistance (s m^{-1}), r_a the aerodynamic resistance (s m^{-1}), λ the latent heat of vaporization of water (MJkg^{-1}), and A the available energy (MJm^{-2}day^{-1}). Parameters such as Δ, ρ_a, γ and D were calculated from air temperature, relative humidity, and air pressure measured from nearby meteorological stations. The available energy to the canopy is given by

$$A = S\downarrow(1-\alpha) + L_{net} - S_t \qquad \text{(C-4)}$$

Where S is the incoming solar radiation (MJm^{-2}day^{-1}), α the canopy albedo, L_{net} the net long-wave radiation (MJm^{-2}day^{-1}), and S_t the temporary storage of energy into the tree itself (trunk and limbs) and the energy used in the photosynthesis process (MJm^{-2}day^{-1}). Canopy albedo was estimated to be 0.18, a value which has been measured over

broadleaf oak trees (Bras, 1990). S_t was estimated to be 5% of the incoming solar radiation based on work by Moore and Fisch (1986) who found that S_t ranged between 0 and 10% of the net radiation available to a tropical forest. The net long-wave radiation contribution to the available energy was calculated from a formula provided by Shuttleworth (1993, p. 4.7).

The aerodynamic resistance (r_a) is the sum of the turbulent resistance between the canopy and the atmosphere from turbulent eddies and the boundary layer resistance (Thom, 1975). Due to the relatively open nature of the cottonwood canopy, the turbulent canopy resistance is assumed negligible in comparison to the boundary layer resistance (Goodrich et al., 2000). Hence r_a is assumed to equal the boundary layer resistance (r_b). To estimate the boundary layer resistance, the model proposed by Choudhury and Monteith (1988) was used:

$$r_b = \frac{1}{(LAI)(b)} \frac{\alpha_{att}}{(1-\exp(-\frac{1}{2}\alpha_{att}))} \sqrt{\frac{\omega}{U}} \qquad \text{(C-5)}$$

In this equation, *LAI* is the canopy projected leaf area index (the same as leaf area index) derived from synthetic large footprint lidar. The quantity *b* was set equal to 0.0067 m $s^{-1/2}$. It is a scaling coefficient for leaf boundary layer resistance (Magnani et al., 1998). α_{att} is an attenuation coefficient for wind speed inside the canopy, ω = 0.05 m is a typical leaf width, and *U* the wind speed outside the canopy (measured at 10 m above the ground). The value for the wind attenuation coefficient, $\alpha_{att,}$ was set equal to 3 following Magnani et al. (1998).

The only remaining quantity required to compute cottonwood transpiration is the bulk canopy resistance (r_c). The canopy resistance is related to individual leaf stomatal resistance (r_s) by the following expression (Goodrich et al., 2000):

$$r_c = \frac{r_s}{2LAI} \tag{C-6}$$

r_s was estimated by Gazal et al. (2006) at both sites. Meanwhile, four metrics (canopy height, height of median energy, ground return ratio, and canopy return ratio) were derived from synthetic large footprint lidar for a cottonwood cluster at each of the two study sites (intermittent and perennial). These four metrics were incorporated into a stepwise regression equation to predict lidar-derived LAI (Table C.1). The lidar-derived LAI at the perennial was 3.48 and at intermittent stream site was 2.78. These values were constant throughout the study time period.

Daily total lidar-predicted transpiration of the cottonwood cluster at the perennial stream site was higher than that at the intermittent stream site throughout the study time period (Fig. C.8). Total lidar-predicted ET at the intermittent stream site was 23 mm and 55 mm at the perennial stream site. This is also consistent with Schaeffer et al. (2000) who found that riparian water use was directly correlated to LAI. Depth to groundwater (d_{gw}) at the intermittent stream site was higher than at the perennial stream site. At the intermittent stream site, d_{gw} increased from 3.1 m during the early part of the spring season to 3.9 m during the peak of the drought period (Gazal et al., 2006). At the perennial stream site, d_{gw} had a gradual but much smaller decline during the pre-monsoon drought. The depth at the beginning of the spring season was 1.5 m and increased to only 1.8 m at the peak of

the drought period (0.5 m less than at the intermittent site; Gazal et al., 2006). Thus, greater depths to groundwater corresponded with lower rates of lidar-predicted LAI and transpiration.

Additionally, r_s at the intermittent stream site was greater than at the perennial stream site with maximum r_s attained at the peak of the pre-monsoon drought period (Gazal et al., 2006). Leaf defoliation also caused r_s to increase. Hence, at the intermittent stream site, increase in r_s caused large reductions in lidar-predicted transpiration that may be associated with the loss of hydraulic conductivity that also facilitated a reduction in stomatal conductance.

Lidar-predicted transpiration of the cottonwood cluster at two stream sites was 2-5% more than their sap flow measurements (Fig. C.9). The differences in LAI between the lidar-derived and sap flow measured transpiration (Gazal et al., 2006) accounts for most of the differences in the magnitude of ET. Lidar-derived LAI was greater than sap flow measured at two stream sites. Hence, greater LAI values corresponded with higher rates of cottonwood transpiration at two contrasting riparian sites. Additionally, the differences in the projected canopy area of the clusters between lidar and aerial photograph (Schaeffer et al., 2000) estimates caused reductions in sap flow measured transpiration at the two stream sites.

Overall, canopy structure, atmospheric demand, and depth to groundwater played significant roles in the fluctuations in transpiration of cottonwood trees in this riparian ecosystem.

C.5 Conclusions

We have shown that one can synthesize the vertical structure information for cottonwood trees in a medium-large footprint laser altimeter return waveform using a small-footprint elevation data set. The similarity between modeled waveform and return waveform from ILRIS scanner was assessed using the Pearson correlation statistic. Overall, the waveforms had a good degree of correlation. Although the modeled and ILRIS waveforms identify reflecting layers at the same elevations, the relative strengths of reflections from those layers varied. In addition, cottonwood tree-age changes are likely mirrored in the shape or vertical geolocation of the waveform.

For each cottonwood tree, three laser height metrics were derived by all small-footprint lidar returns from cottonwood canopy surface. The h_{canopy} and Lz_{max} laser height metrics have been demonstrated as capable of estimating LAI for different age classes of cottonwoods. Additionally, four metrics were derived from the modeled large-footprint return waveforms for different age classes of cottonwood trees in a riparian corridor. These four metrics were incorporated into a stepwise regression procedure to predict field-derived LAI. The metrics from the lidar waveform were able to estimate LAI for different age classes of cottonwood trees, though in all cases logarithmic transformation of the dependent variable was necessary. Furthermore, the slightly weaker relationship between LAI and lidar metrics among young, mature, and old-growth stands is caused by the lack of large differences in LAI between different age classes of cottonwoods that have been measured in field.

Lidar and meteorological based estimates of cottonwood transpiration versus sap flow measured cottonwood at perennial and intermittent riparian sites were also made. Lidar-met-based transpiration estimates of the cottonwood cluster at the two stream sites was 2-5% greater than their sap flow measurements over an eleven day period centered on the lidar flight. The differences in LAI between the lidar-derived and sap flow measured transpiration accounts for most of the differences in the magnitude of ET. Additionally, the differences in the projected canopy area of the clusters between lidar and aerial photograph estimates caused reductions in sap flow measured transpiration at two stream sites. Overall, canopy structure, atmospheric demand, and depth to groundwater played significant roles in the fluctuations in transpiration of cottonwood trees in this riparian ecosystem.

Future research will apply the Penman-Monteith model to estimate cottonwood transpiration using lidar-derived canopy metrics for the whole riparian corridor.

Acknowledgements

This study is based upon work supported by SAHRA (Sustainability of semi-Arid Hydrology and Riparian Areas) under the STC Program of the National Science Foundation, Agreement No. EAR-9876800. We are indebted to the following people who assisted us in various aspects of this work: Michael Sartori and William Cable. In addition, we wish to acknowledge the staff at the USDA-ARS Southwest Watershed Research Center, Tucson, Arizona.

C.6 References

Abshire, J.B., McGarry, J.F., Pacini, L.K., Blair, J.B., Elman, G.C., 1994. Laser Altimetry Simulator, Version 3.0 User's Guide, NASA Technical Memorandum 104588, NASA/GSFC, Greenbelt, MD, 70 p.

Blair, J.B., Hofton, M.A., 1999. Modeling laser altimeter return waveforms over complex vegetation using high-resolution elevation data. Geophysical Research Letters, 26, 2509-2512.

Blair, J.B., Rabine, D.L., Hofton, M.A., 1999. The Laser Vegetation Imaging Sensor (LVIS): a medium-altitude, digitization-only, airborne laser altimeter for mapping vegetation and topography. ISPRS Journal of Photogrammetry & Remote Sensing, 54, 115-122.

Bras, R., 1990. Hydrology. Addison-Wesley, Reading, MA, p. 44.

Choudhury, B.J., Monteith, J.L., 1988. A four-layer model for the heat budget of homogeneous land surfaces. Quarterly J. Royal Meteorol. Soc. 114, 373-398.

Drake, J.B., Dubayah, R.O., Clark, D.B., Knox, R.G., Blair, J.B., Hofton, M.A., Chazdon, R.L., Weishampel, J.F., Prince, S.D., 2002. Estimation of tropical forest structural characteristics using large-footprint lidar. Remote Sensing of Environment, 79, 305-319.

Farid, A., Rautenkranz, D., Goodrich, D.C., Marsh, S.E., Sorooshian, S., 2006. Riparian vegetation classification from airborne laser scanning data with an emphasis on cottonwood trees. Can. J. Remote Sensing, Vol. 32, No. 1, pp. 15-18.

Farid, A., Goodrich, D.C., Sorooshian, S., 2006. Using airborne lidar to discern age classes of cottonwood trees in a riparian area. Western Journal of Applied Forestry. In press.

Gardner, C.S., 1992. Ranging performance of satellite laser altimeters, IEEE Trans. Geo. Rem. Sens., 30, 1061-1072.

Gazal, R.M., Scott, R.S., Goodrich, D.C., Williams, D.G., 2006. Controls on transpiration in a desert riparian cottonwood forest. In press.

Goodrich, D.C., Scott, R., Qi, J., Goff, B., Unkrich, C.L., Moran, M.S., Williams, D., Schaeffer, S., Snyder, K., Macnish, R., Maddock, T., Pool, D., Chehbouni, A., Cooper, D.I., Eichinger, W.E., Shuttleworth, W.J., Kerr, Y., Marsett, R., Ni, W., 2000. Seasonal estimates of riparian evapotranspiration using remote and in-situ measurements. Agric. For. Meteorol., 105, 281-309.

Harding, D.J., Blair, J.B., Garvin, J.B., Lawrence, W.T., 1994. Laser altimetry waveform measurement of vegetation canopy structure. Proceedings of the International Remote Sensing Symposium, Pasadena, CA, pp. 1251 – 1253.

Lefsky, M.A., Cohen, W.B., Acker, S.A., Spies, T.A., Parker, G.G., Harding, D., 1999. Lidar remote sensing of biophysical properties and canopy structure of forest of Douglas-fir and western hemlock. Remote Sensing of Environment, 70, 339-361.

Lim, K., Treitz, P., Baldwin, K., Morrison, I., Green, J., 2003. Lidar remote sensing of biophysical properties of tolerant northern hardwood forests. Can. J. Remote Sensing, 29, 658-678.

Maclean, G.A., Krabill, W.B., 1986. Gross-merchantable timber volume estimation using an airborne LIDAR system. Can. J. Remote Sensing, 12, 7-18.

Magnani, F., Leonardi, S., Tognetti, R., Grace, J., Borghetti, M., 1998. Modelling the surface conductance of a broadleaf canopy: effects of partial decoupling from the atmosphere. Plant, Cell Environ. 21, 867-879.

Magnussen, S., Boudewyn, P., 1998. Derivations of stand heights from airborne laser scanner data with canopy-based quantile estimators. Canadian Journal of Forestry Research, 28, 1016-1031.

Magnussen, S., Eggermont, P., LaRiccia, V.N., 1999. Recovering tree heights from airborne laser scanner data. Forest Science, 45, 407-422.

Means, J.E., Acker, S.A., Harding, D.J., Blair, J.B., Lefsky, M.A., Cohen, W.B., Harmon, M., McKee, W.A., 1999. Use of large-footprint scanning airborne lidar to estimate forest stand characteristics in the western Cascades of Oregon. Remote Sensing of Environment, 67, 298-308.

Means, J.E., 2000. Comparison of large-footprint and small-footprint lidar systems: design, capabilities, and uses, Proceedings: Second International Conference on Geospatial Information in Agriculture and Forestry, 10-12 January, Lake Buena Vista, Florida (ERIM International), 1:85-192.

Monteith, J.L., Unsworth, M.H., 1990. Principles of Environmental Physics. Edward Arnold, London.

Moore, C.J., Fisch, G., 1986. Estimating heat storage in Amazonian tropical forests. Agric. For. Meteorol. 38, 147-169.

Naesset, E., 1997a. Determination of mean tree height of forest stands using airborne laser scanner data. ISPRS Journal of Photogrammetry and Remote Sensing, 52: 49-56.

Naesset, E., 1997b. Estimating timber volume of forest stands using airborne laser scanner data. Remote Sensing of Environment, 61, 246-253.

Nelson, R.F., Krabill, W.B., Maclean, G.A., 1984. Determining forest canopy characteristics using airborne laser data. Remote Sensing of Environment, 15, 201-212.

Nelson, R.F., Swift, R., Krabill, W.B., 1988a. Using airborne lasers to estimate forest canopy and stand characteristics. Journal of Forestry, 86, 31-38.

Nelson, R.F., Krabill, W.B., Tonelli, J., 1988b. Estimating forest biomass and volume using airborne laser data. Remote Sensing of Environment, 24, 247-267.

Ritchie, J.C., Evans, D.L., Jacobs, D., Everitt, J.H., Weltz, M.A., 1993. Measuring canopy structure with an airborne laser altimeter. Transactions of the ASAE, Vol. 36, 1235-1238.

Schaeffer, S.M., Williams, D.G., Goodrich, D.C., 2000. Transpiration of cottonwood/willow forest estimated from sap flux. Agric. For. Meteorol., 105, 257-270.

Scott, R.L., Shuttleworth, W.J., Goodrich, D.C., Maddock ,T. III, 2000. The water use of two dominant vegetation communities in a semiarid riparian ecosystem. Agric. For. Met. 105:241-256.

Shuttleworth, W.J., 1993. Evaporation. In: Maidment, D.R. (Ed.), Handbook of Hydrology. McGraw-Hill, New York, pp. 4.1-4.53 (Chapter 4).

Stromberg, J.C., 1998. Dynamics of Fremont cottonwood (*Populus fremontii*) and saltcedar (*Tamarix chinensis*) populations along the San Pedro River, Arizona. Journal of Arid Environments, 40, 133-155.

Thom, A.S., 1975. Momentum, mass and heat exchange of plant communities. In: Monteith, J.L. (Ed.), Vegetation and the Atmosphere. Academic Press, New York, pp. 57-109.

Wehr, A., Lohr, U., 1999. Airborne laser scanning-an introduction and overview. ISPRS Journal of Photogrammetry and Remote Sensing, 54, 68-82.

Weishampel, J.F., Harding, D.J., Boutet, J.C. Jr., Drake, J.B., 1997. Analysis of laser altimeter waveforms for forested ecosystems of central Florida. In Proceedings of the SPIE Conference on Advances in Laser Remote Sensing for Terrestrial and Oceanographic Applications, Vol. 3059, 184-189.

World Rivers Review, 1997. Biodiversity, North America. World Rivers Review, News Briefs, Vol. 12, No. 1, February 1997. International Rivers Network. Internet document: http://www.irn.org/pubs/wrr/9701/briefs.html (last date accessed: 15 May 2004).

Wulder, M., Niemann, K.O., Goodenough, D.G., 2000. Local maximum filtering for the extraction of tree locations and basal area from high spatial resolution imagery. Remote Sensing of Environment, 73, 103-114.

Wullschleger, S.D., Meinzer, F.C., Vertessey, R.A., 1998. A review of whole-plant water use studies in trees. Tree Physiol. 18: 499-512.

Table C.1 Regression equations and statistics for relationship between LAI and lidar metrics for young, mature, and old-growth cottonwoods

Cottonwood age-class	Equation	R^2 *	RMSE	n
Young	log (LAI) = 0.27 + 0.01*LHT + 0.01*HOME - 0.01*GRND - 0.02*CRND	**0.76**	**0.02**	**17**
Mature	log (LAI) = 0.20 + 0.004*LHT + 0.02*HOME - 0.01*GRND + 0.01*CRND	**0.78**	**0.01**	**15**
Old	log (LAI) = -0.29 - 0.05*LHT + 0.16*HOME - 0.47*GRND - 0.83*CRND	**0.84**	**0.04**	**9**

*** All values significant (P<0.01).**

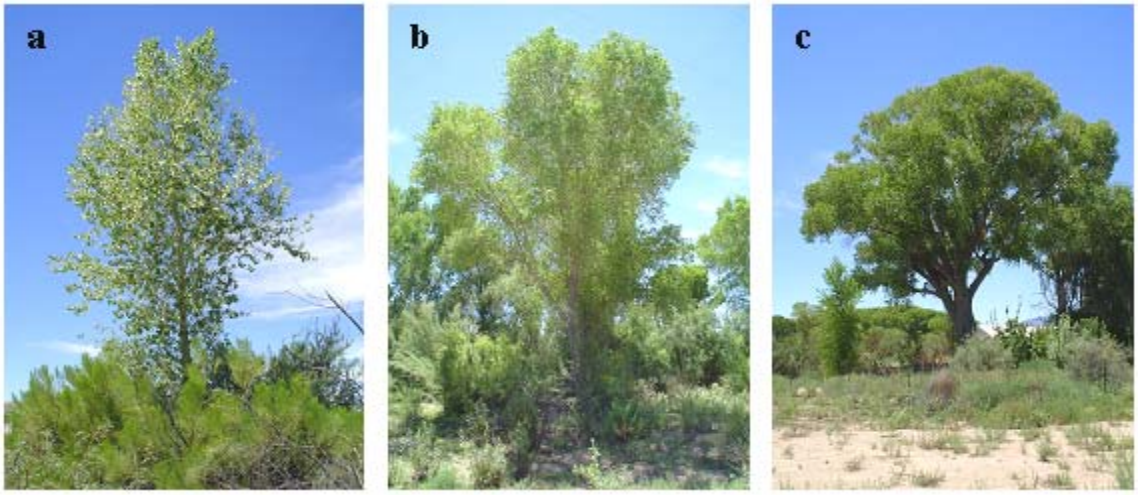

Figure C.1. Photos depicting (**a**) young, (**b**) mature, and (**c**) old cottonwood trees. Figure adapted from Farid et al. (2006), with permission from the Society of American Foresters.

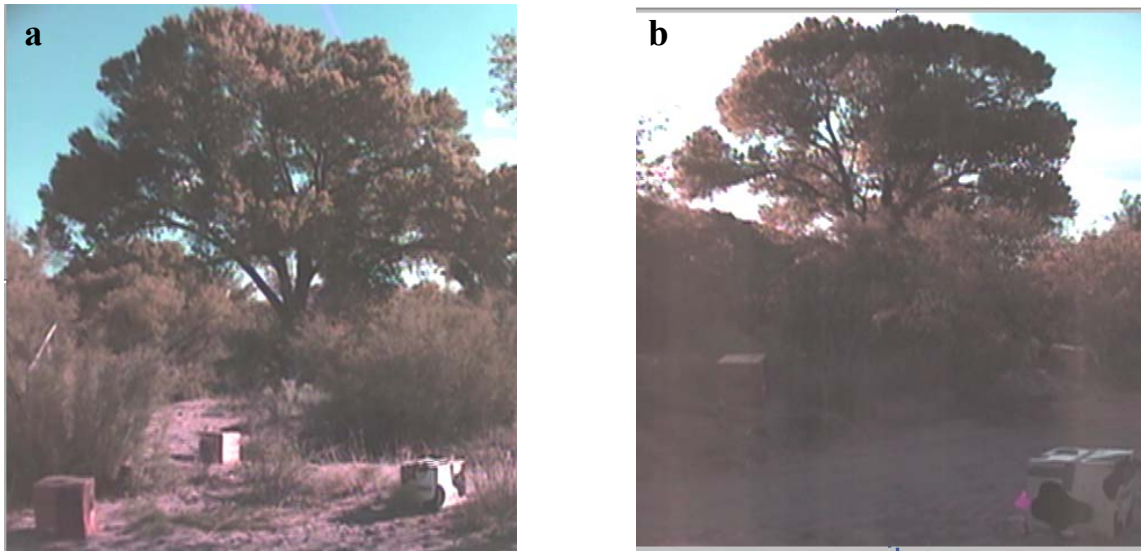

Figure C.2. Cardboard boxes in the (**a**) foreground and (**b**) back part of one of the old cottonwood trees (two scans on opposite sides the tree).

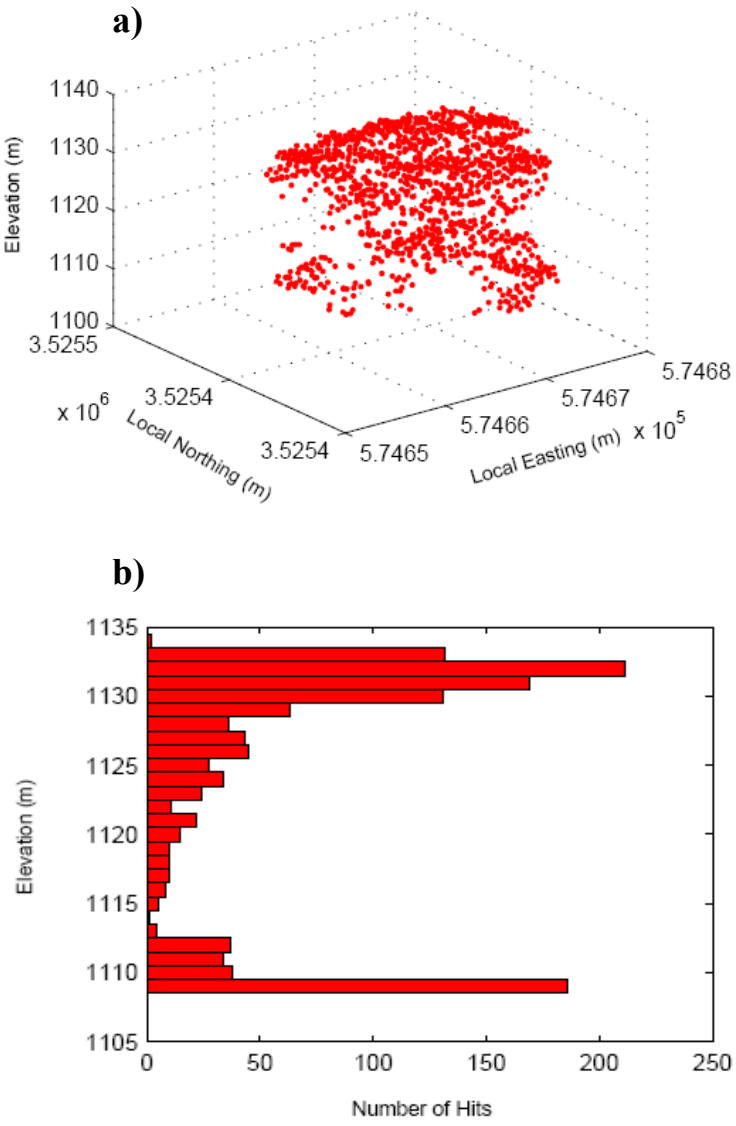

Figure C.3. Illustration of the potential for creating synthetic lidar waveforms from small-footprint lidar data. Section **a** shows the three-dimensional distribution of small-footprint lidar data from within a 22 m × 26 m footprint. Section **b** shows the vertical distribution of these returns.

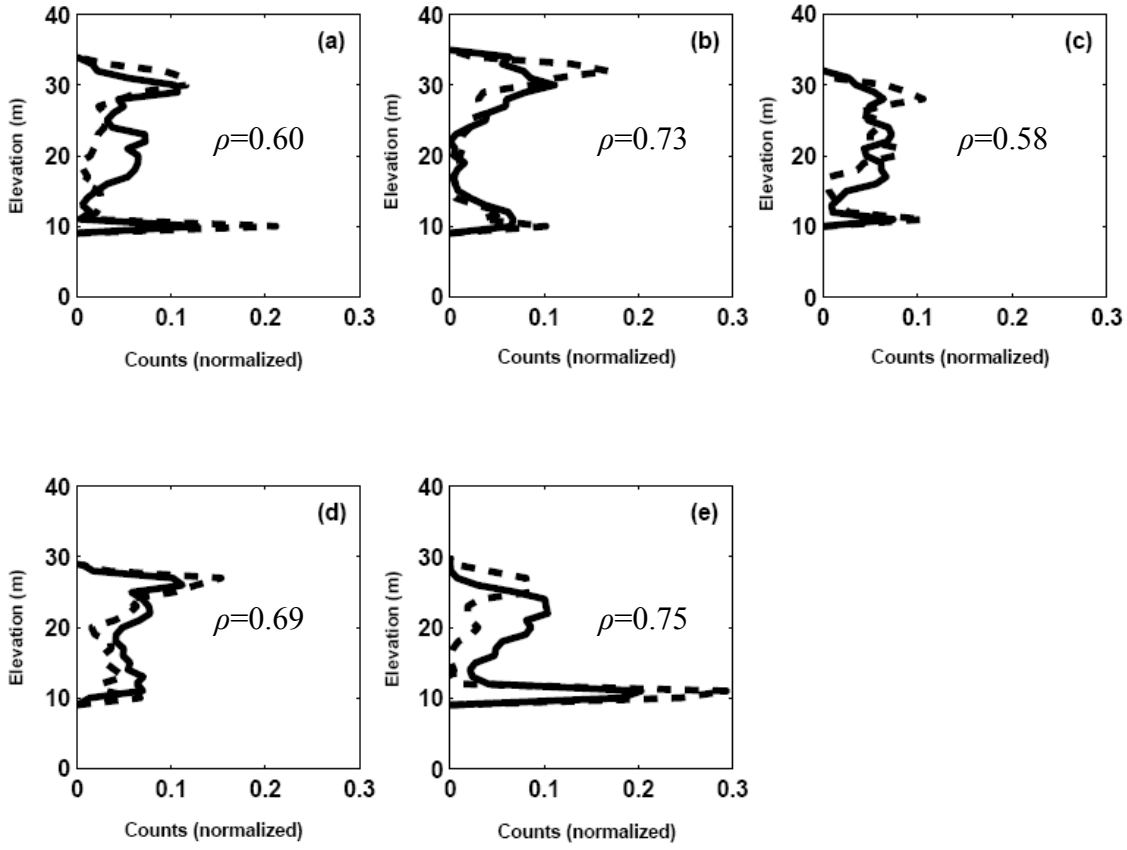

Figure C.4. ILRIS (solid line) and modeled (dashed line) waveforms for (a-c) old and (d-e) mature cottonwood trees. ρ is the Pearson correlation coefficient.

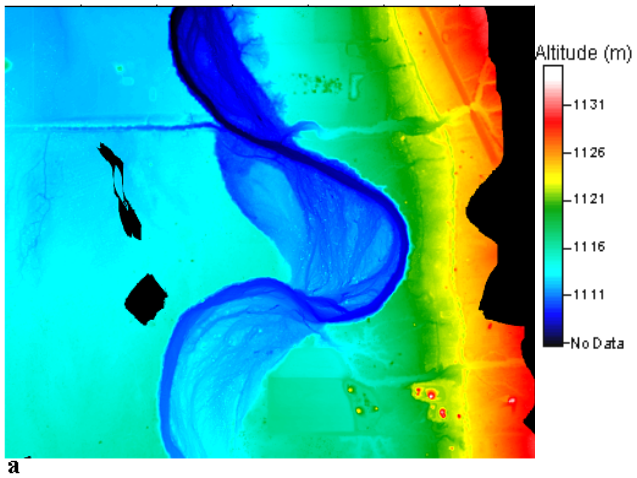

a

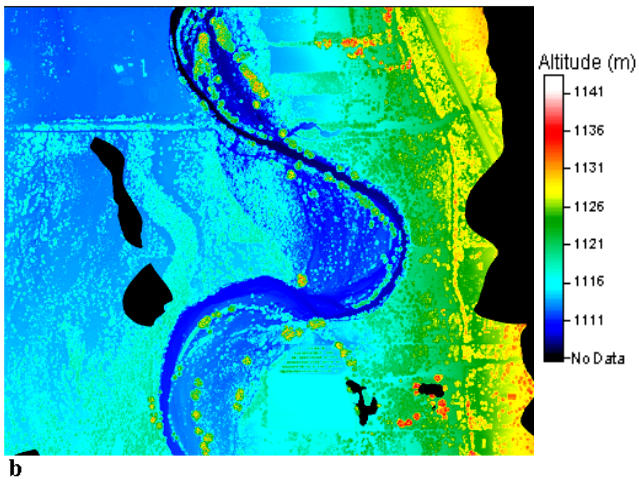

b

Figure C.5. Spatial pattern of DEMs (**a**) bare ground model and (**b**) canopy altitude model for the study site.

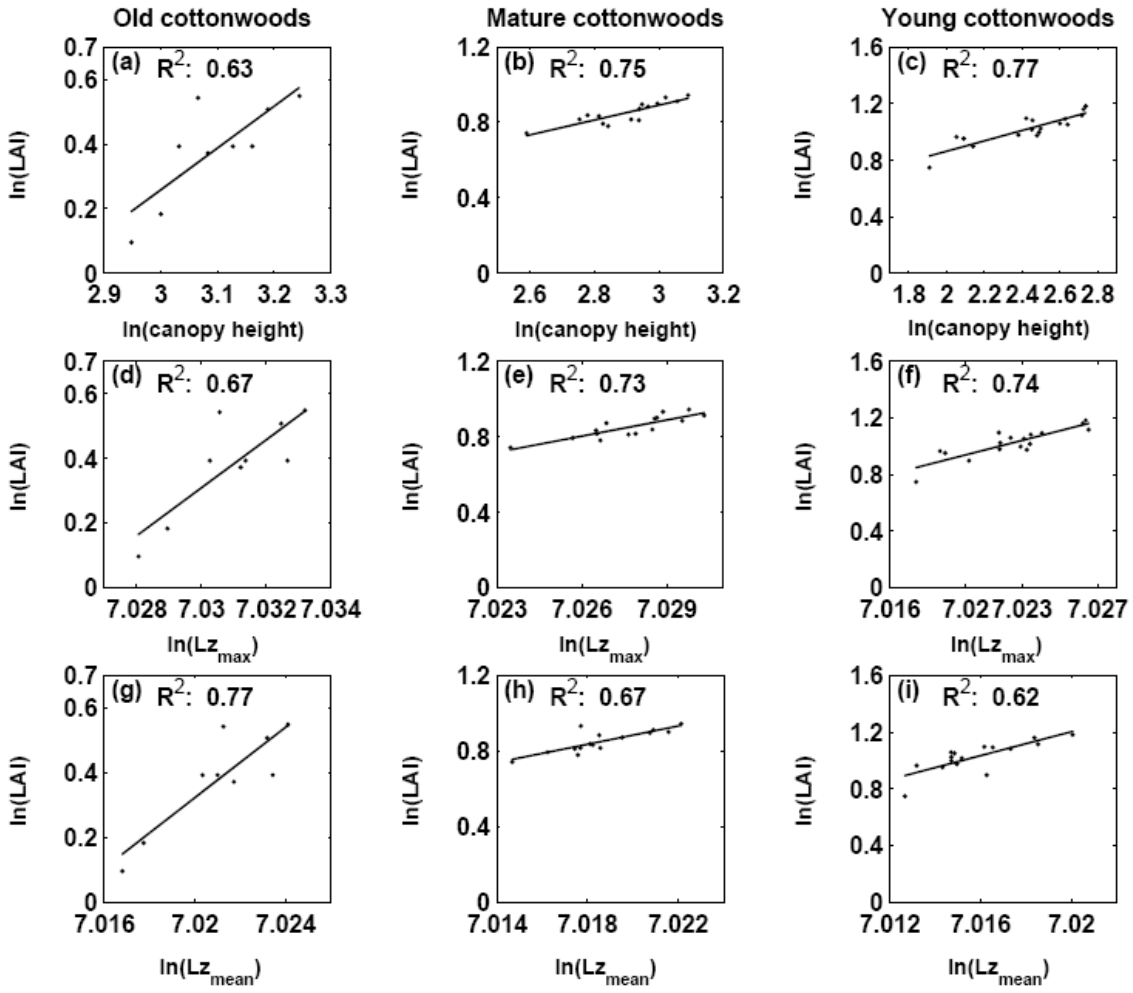

Figure C.6. Linear least-squares fit between LAI and (a-c) canopy height, (d-f) Lz_{max}, and (g-i) Lz_{mean} for each type of cottonwood tree on the study region.

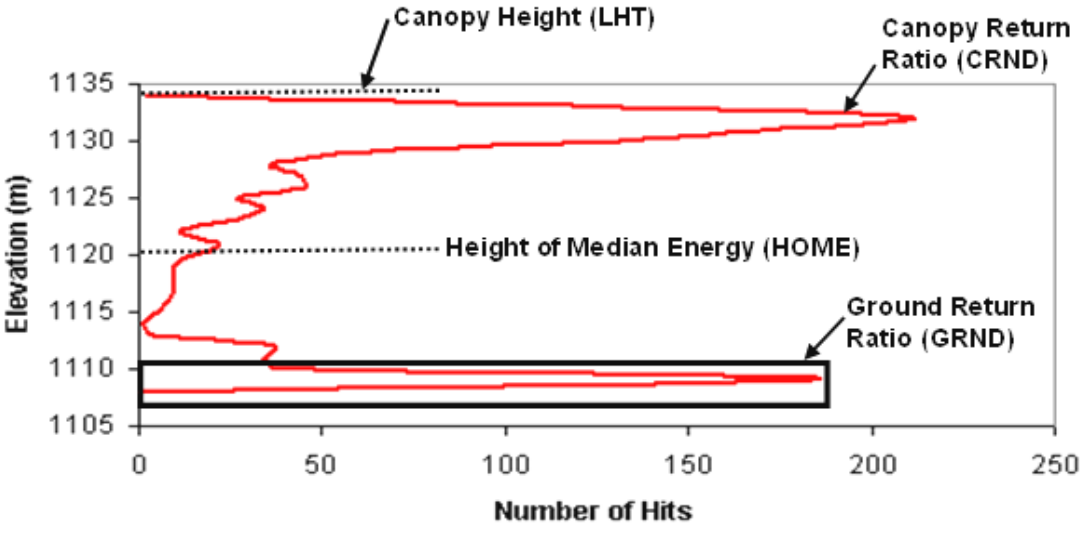

Figure C.7. Metrics derived from synthetic large footprint lidar waveforms. See text for discussion. These metrics were then used to estimate LAI for different age classes of cottonwoods.

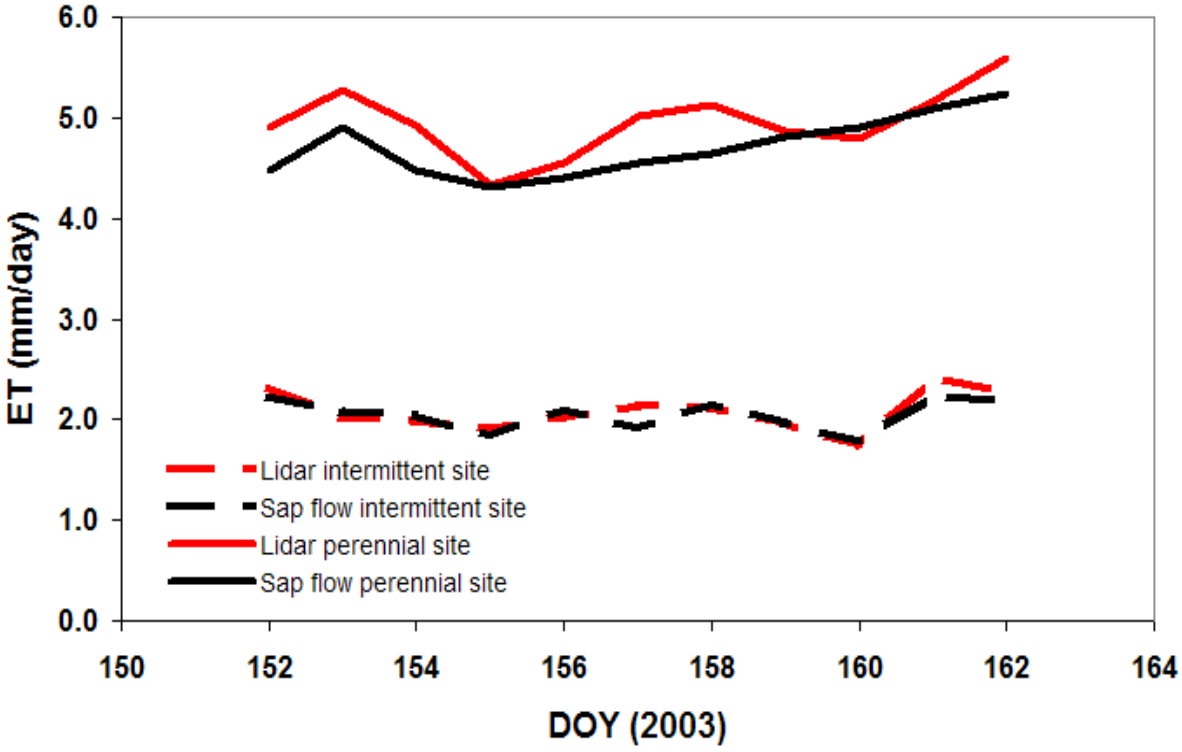

Figure C.8. Daily total lidar-predicted versus sap flow measured cottonwood transpirations at the intermittent and perennial stream sites.

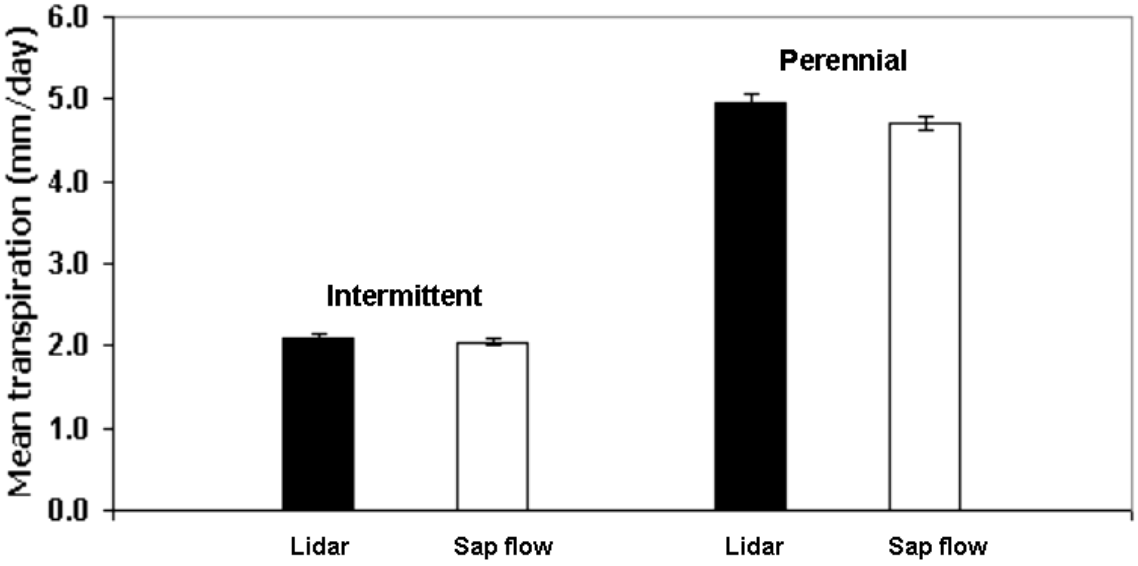

Figure C.9. The lidar-predicted versus sap flow measured cottonwood mean daily transpirations at the intermittent and perennial stream sites over an eleven day period centered on the lidar flight.